Gas Phase Reaction Kinetics of
Neutral Oxygen Species

Harold S. Johnston

University of California, Berkeley, California 94720
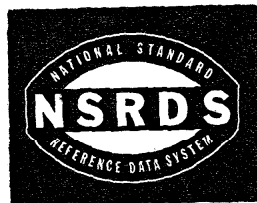
NSRDS-NBS 20
National Standard Reference Data Series —
National Bureau of Standards

Issued September 1968

Foreword

The National Standard Reference Data System is a Government-wide effort to provide for the technical community of the United States effective access to the quantitative data of physical science, critically evaluated and compiled for convenience, and readily accessible through a variety of distribution channels. The System was established in 1963 by action of the President's Office of Science and Technology and the Federal Council for Science and Technology.

The responsibility to administer the System was assigned to the National Bureau of Standards and an Office of Standard Reference Data was set up at the Bureau for this purpose. Since 1963, this Office has developed systematic plans for meeting high-priority needs for reliable reference data. It has undertaken to coordinate and integrate existing data evaluation and compilation activities (primarily those under sponsorship of Federal agencies) into a comprehensive program, supplementing and expanding technical coverage when necessary, establishing and maintaining standards for the output of the participating groups, and providing mechanisms for the dissemination of the output as required.

The System now comprises a complex of data centers and other activities, carried on in Government agencies, academic institutions, and nongovermental laboratories. The independent operational status of existing critical data projects is maintained and encouraged. Data centers that are components of the NSRDS produce compilations of critically evaluated data, critical reviews of the state of quantitative knowledge in specialized areas, and computations of useful functions derived from standard reference data. In addition, the centers and projects establish criteria for evaluation and compilation of data and make recommendations on needed modifications or extensions of experimental techniques.

Data publications of the NSRDS take a variety of physical forms, including books, pamphlets, loose-leaf sheets and computer tapes. While most of the compilations have been issued by the Government Printing Office, several have appeared in scientific journals. Under some circumstances, private publishing houses are regarded as appropriate primary dissemination mechanisms.

The technical scope of the NSRDS is indicated by the principal categories of data compilation projects now active or being planned: nuclear properties, atomic and molecular properties, solid state properties, thermodynamic and transport properties, chemical kinetics, colloid and surface properties, and mechanical properties.

An important aspect of the NSRDS is the advice and planning assistance which the National Research Council of the National Academy of Sciences-National Academy of Engineering provides. These services are organized under an overall Review Committee which considers the program as a whole and makes recommendations on policy, long-term planning, and international collaboration. Advisory Panels, each concerned with a single technical area, meet regularly to examine major portions of the program, assign relative priorities, and identify specific key problems in need of further attention. For selected specific topics, the Advisory Panels sponsor subpanels which make detailed studies of users' needs, the present state of knowledge, and existing data resources as a basis for recommending one or more data compilation activities. This assembly of advisory services contributes greatly to the guidance of NSRDS activities.

The NSRDS–NBS series of publications is intended primarily to include evaluated reference data and critical reviews of long-term interest to the scientific and technical community.

A. V. Astin, *Director.*

Preface

Now that chemical kinetics is approaching a certain level of maturity, with some of the field passing from frontline research to established applied science, its quantitative data should be tabulated in handbooks. Decisions must be made as to what to tabulate; suggestions have included: Empirical rate constants with defined order and regardless of mechanism, parameters of the Arrhenius equation or parameters of activated-complex theory, nothing but molecular transition probabilities or cross sections for identified changes of quantum states. The position taken in this review is that we should tabulate individual rate constants for elementary chemical reactions. I oppose basing handbooks on the other proposals listed above for the following reasons: Empirical rate data for an unanalyzed complex reaction are analogous to empirical thermodynamic data for an impure unanalyzed substance; the data may be useful for the case in hand but of no general interest. The bare reporting of parameters of the Arrhenius equation or activated-complex theory equation conceals the source of the numbers, the probable error, the relationship to other investigations. In tables of data of this sort one entry may represent an average of several hundred observed points as obtained by a dozen different investigators over a wide temperature range, and another entry may be a wild guess by an amateur in the field or the unsupported prediction of a crude theory. A refusal to tabulate any kinetic data except fundamental, quantum-state transitions is analogous to a refusal to tabulate any thermodynamic data until they are obtained by statistical mechanics from molecular parameters.

The idea of elementary chemical reactions, as opposed to complex reactions on the one hand and elementary chemical-physical reactions or elementary physical reactions on the other hand, is the main topic of section 1. A detailed discussion of each of three complex reaction systems (decomposition of O_2, decomposition of O_3, and isotopic exchange between oxygen species) is the subject matter of the next three sections. The fifth section gives a discussion of a theoretical problem raised by these data. The strictly handbook elements of this report are given by the tables, summarized further in tables 15, 17, and 28 and in section 6. Nonkineticists are inclined to expect greater precision from kinetic data than is really there; as a step toward correcting this misapprehension, all data are presented in figures, where the experimental scatter and range of observations are readily seen.

Acknowledgment

Contents

Gas Phase Reaction Kinetics of Neutral Oxygen Species

Harold S. Johnston

The available data for reactions among neutral oxygen species, oxygen atoms, oxygen molecules and ozone, have been reviewed. Selected data have been reanalyzed and used to establish values for the rates of these reactions:

$$O_2 + M \rightarrow O + O + M \text{——— } (M = O_2, Ar)$$
$$O + O + M \rightarrow O_2 + M \text{——— } (M = O_2)$$
$$O_3 + M \rightarrow O + O_2 + M \text{——— } (M = O_2, O_3, He, Ar, N_2, CO_2)$$
$$O + O_2 + M \rightarrow O_3 + M \text{———}(M = O_2, O_3, He, Ar, N_2, CO_2)$$
$$O + O_3 \rightarrow O_2 + O_2$$
$$O + O_2 \rightarrow O + O_2 \text{ (isotopic exchange)}$$
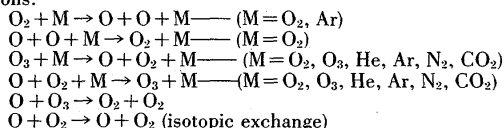
Key words: Chemical kinetics, dissociation, isotopic exchange, oxygen atom, oxygen molecule, ozone, recombination, review.

1. Complex Processes and Elementary Reactions

1.1. Neutral Oxygen Species

Neutral oxygen species are oxygen atoms, O, oxygen molecules, O_2, and ozone, O_3. However, each of these species has relatively long-lived electronic or vibrational states, which in one sense of the word constitute separate species. The electronic states of atomic oxygen include $O(^3P)$, $O(^1D)$, and $O(^1S)$. The first few electronic states of molecular oxygen are $O_2(^3\Sigma_g^-)$, $O_2(^1\Delta_g)$, $O_2(^1\Sigma_g^+)$, $O_2(^3\Sigma_u^+)$, and $O_2(^3\Sigma_u^-)$. The ground electronic state of ozone is expressed as $O_3(^1A)$. Certain spectroscopic constants of O, O_2, and O_3 are given in tables 1, 2, and 3.

In this review, reactions will be classified as in the author's book, *Gas Phase Reaction Rate Theory* [59] [1]: Complex chemical systems, elementary physical reactions, elementary chemical-physical reactions, and elementary chemical reactions. For definitions of these cases, the reader is referred to

the book; examples of each case of importance to this review are presented below.

1.2. Complex Chemical Systems

A laboratory operation that carries out a chemical reaction is typically "complex" in that it involves a number of elementary chemical steps. Certain experimental methods and chemical reactions involving neutral oxygen species are given here.

TABLE 1. *Properties of the first few electronic states of oxygen atoms* [19, 55, 57]

Atomic states	Energy relative to lowest state		ΔH_0°
	kcal/mole	*eV*	*kcal/mole*
$O(^3P)$	0	0	59.2
$O(^1D)$	45.4	1.967	104.6
$O(^1S)$	96.6	4.188	155.8

TABLE 2. *Properties of first few electronic states of oxygen molecules*

Molecular state	Relative energy (T_0)	Bond length	Vibrational frequency	D_0°	Dissociation products .
	kcal/mole	Å	cm^{-1}	*kcal/mole*	
$O_2(^3\Sigma_g^-)$	0	1.207	1580	118.3	$^3P + {}^3P$
$O_2(^1\Delta_g)$	22.5	1.216	1509	95.7	$^3P + {}^3P$
$O_2(^1\Sigma_g^+)$	37.5	1.227	1433	80.6	$^3P + {}^3P$
$O_2(^3\Sigma_u^+)$	102.1	1.42	819	15.1	$^3P + {}^3P$
$O_2(^3\Sigma_u^-)$	141.1	1.60	700	21.3	$^1D + {}^3P$

TABLE 3. *Molecular and thermodynamic properties of ozone* [57]

Moments of inertia, gram cm²
$I_x = 7.875 \times 10^{-40}$ $I_y = 62.844 \times 10^{-40}$ $I_z = 70.888 \times 10^{-40}$

Vibration frequencies, cm⁻¹
$\omega_1 = 705$ $\omega_2 = 1043$ $\omega_3 = 1110$

Thermodynamic properties
$\Delta_f H^{\circ}_{298} = 34.1$ kcal/mole $O_3(^1A) \rightarrow O_2(^3\Sigma_g^-) + O(^3P)$ $\Delta_r H^{\circ}_{298} = 25.46 \pm .4$ kcal/mole[a] $\Delta_r H^{\circ}_0 = 24.25 \pm .4$ kcal/mole[a]

[a] See discussion of error on p. 29.

a. Shock Tube Experiments [125, 62]

In a shock-tube experiment, a high-pressure gas is suddenly thrust into a low-pressure gas by breaking a plastic or a metal diaphragm. The low-pressure gas is compressed adiabatically and thereby heated (in a time much less than 1 μs) from room temperature to a much higher temperature, determined by pressure ratios between high- and low-pressure regions and by the thermodynamic properties of the gases. Temperature rises of hundreds or even thousands of degrees centigrade are obtainable this way. The compressed gas has a steady, high-temperature state for a few milliseconds. The temperature can be calculated from observed shock-wave velocities. Kinetic processes are observed by fast recording of some appropriate property of the system, such as absorption of x rays by dense carrier gases (krypton), absorption of vacuum ultraviolet radiation by the molecule O_2, or absorption of ultraviolet by the molecule O_3. Ozone decomposes with a millisecond lifetime around 700 900 K, and it decomposes in times much shorter than 1μs to produce excess oxygen atoms above 1500 K. Oxygen molecules decompose at a rate convenient for shock tube study between 4000 and 8000 K, although rate measurements have been carried out as low as 3000 K and as high as 17,000 K.

At low temperatures, processes involving different sized energy jumps tend to occur at widely different rates; reactions with low-energy barriers occur much faster than reactions with high-energy barriers. At high temperatures, energy differences become relatively unimportant, and many processes occur simultaneously at comparable rates. The Boltzmann factor, $\exp(-\Delta E/RT)$, for an energy difference of one electron volt, or about 23 kcal/mole, is 10^{-17} at room temperature but only 0.1 at 5000 K. Considerations such as products with high density of states, or high multiplicity, or high entropy become as important as energy differences at high temperatures.

In shock-tube experiments, the short observation times and the limited number of monochromatic photons that can be put through narrow slits lead to an irreducible error from "shot noise" in the measuring light beam. Under a typical set of conditions, this error turns out to be about 1 percent in measurement of concentration and about 10 percent in measurement of rate (calculated from 10^{12} photons per second at 10 Å band pass, 10^{-6} second observation limit, 10 percent absorption of light by the chemical of interest, and square root of 9×10^5 is 1 percent). There are other random errors associated with shock tubes, such as irregularities in membrane rupture and errors associated with velocity measurements. There are possible systematic errors associated with shock tubes, such as boundary layer cooling with adiabatic expansion of shocked gas into a cooled boundary layer and nonideality of shocked gas especially for nonmonatomic gases. Errors in the interpretation of data arise when one thinks one is measuring the rate of a given chemical reaction but another process of about the same rate is interfering. For example, the vibration-translational relaxation time of O_2 becomes the same order of magnitude as the dissociation lifetime at about 8000 to 10,000 K. When all errors are considered in shock-tube work, rate constants have somewhat greater scatter (factor of two to four in a single measured rate constant) than gas-kinetic data obtained by conventional, "slow" methods. Thus comparable precision is to be expected between fast shock experiments and ordinary slow experiments only if the shock-tube points are 4 to 16 times as numerous. Whereas shock tube experiments are subject to systematic errors (as mentioned above), conventional gas kinetics is also susceptible to systematic errors, such as competing surface reactions and thermal gradients in the reacting gas. Provided the investigator with the shock tube takes a large number of data points, the shock tube can be equally as valid as any other method in producing quantitative kinetic data.

b. Thermal Decomposition of Ozone in Static Systems

The overall reaction (2 $O_3 = 3$ O_2) produces a pressure increase as it occurs. The extent of reaction can be found from the initial pressure and composition and from the pressure at any time.

Alternatively the extent of reaction can be calculated from pressure at any time and final pressure when all the ozone has decomposed. Ozone attacks mercury manometers, and its decomposition is catalyzed by most metals, so the problem of pressure measurement requires care in selection of method. Sulfuric acid manometers have been widely used for this purpose. Most measurements of the decomposition of ozone at temperatures between 300 and 500 K have been carried out in this way, although pressure measurements have been supplemented or replaced by other physical or chemical methods in some cases.

Data developed by this technique are reviewed in some detail in section 3 and will not be discussed in detail here.

c. Photolysis of Ozone

Ozone weakly absorbs red light [26] around 6000 Å to give the forbidden transition,

$$O_3 + h\nu \ (6000 \ \text{Å}) \rightarrow O_2(^3\Sigma_g^-) + O(^3P). \qquad (1-1)$$
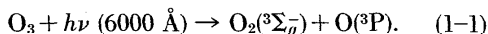
The upper limit to the observed quantum yield in wet or dry ozone is two:

$$O(^3P) + O_3 \xrightarrow{k_3} 2 \ O_2. \qquad (1-2)$$
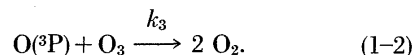
Quantum yields less than two are explained by competition from the back reaction,

$$O(^3P) + O_2 + M \xrightarrow{k_2} O_3 + M. \qquad (1-3)$$
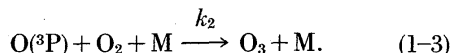
Studies of this system give quantitative values of the rate constant ratio, k_2/k_3, and the mechanism will be analyzed in detail in the chapter on ozone.

Ozone strongly absorbs ultraviolet radiation to produce singlet oxygen molecules and singlet oxygen atoms [91, 15, 52]

$$O_3 + h\nu \ (\lambda \leqslant 3130 \ \text{Å}) \rightarrow O_2(^1\Delta_g) + O(^1D),$$
$$(1-4)$$

$$O_3 + h\nu \ (\lambda \leqslant 2680 \ \text{Å}) \rightarrow O_2(^1\Sigma_g^+ \ \text{or} \ ^1\Delta_g)$$
$$+ O(^1D). \qquad (1-5)$$
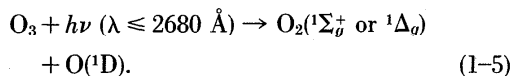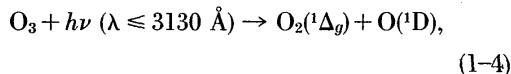
Although ground-state triplet oxygen atoms do not react with water vapor, singlet oxygen atoms rapidly react with water vapor [92], to produce hydroxyl radicals, which have been directly observed by the method of flash spectroscopy

$$O(^1D) + H_2O \rightarrow 2HO. \qquad (1-6)$$

Hydroxyl radicals catalyze the decomposition of ozone in a chain reaction:[2]

$$\left. \begin{array}{l} HO + O_3 \rightarrow HO_2 + O_2 \\ HO_2 + O_3 \rightarrow HO + 2 \ O_2 \end{array} \right\} \text{Chain} \qquad (1-7)$$

$$\text{net} \ \ 2 \ O_3 \rightarrow 3 \ O_2.$$
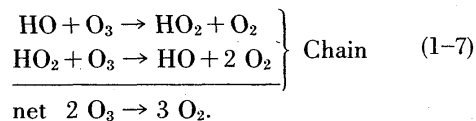
When ozone is photolyzed by ultraviolet radiation in the presence of water vapor, quantum yields greater than 100 are readily observed. Dry ozone photolyzed at 2537 Å has been observed by Norrish and Wayne [91] to give quantum yields up to 16, and this high quantum yield is explained in terms of a "thermal chain" carried by excited vibrational states of the product oxygen molecule:

$$\left. \begin{array}{l} O(^1D) + O_3 \rightarrow O_2 + O_2^* \ (\text{high} \ v) \\ O_2^*(v > 17) + O_3 \rightarrow 2 \ O_2 + O(^1D) \end{array} \right\} \text{Chain} \qquad (1-8)$$

$$\text{net} \qquad 2 \ O_3 \rightarrow 3 \ O_2.$$
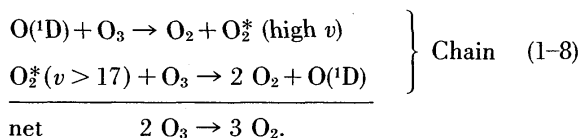
At 2537 Å the primary decomposition of ozone produces O_2 in excited electronic state or states ($^1\Sigma_g^+$ or $^1\Delta_g$), which also decomposes ozone [5, 70, 82, 85, 91]:

$$O_2(^1\Sigma_g^+ \ \text{or} \ ^1\Delta_g) + O_3 \rightarrow 2 \ O_2 + O. \qquad (1-9)$$
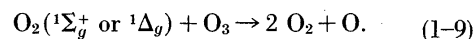
With added inert gases, N_2 or CO_2, the quantum yield is reduced,

$$O_3 + h\nu \rightarrow O_2(^1\Sigma_g^+ \ \text{or} \ ^1\Delta_g) + O(^1D) \qquad (1-10)$$

$$O(^1D) + N_2 \rightarrow O(^3P) + N_2. \qquad (1-11)$$
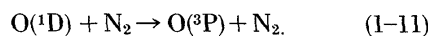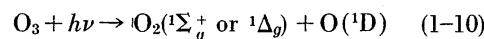
With added oxygen molecules the quantum yield of dry ozone decomposition approaches zero, because of the great speed of the reaction:

$$O(^1D) + O_2 + M \rightarrow O_3 + M. \qquad (1-12)$$
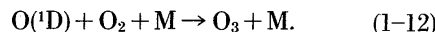
This complicated mechanism of the photolysis of ozone by ultraviolet light is fairly well understood on a qualitative basis, but there are relatively few data that give quantitative estimates of rate constants.

---

[2] The reaction (a), $HO + O_3 \rightarrow HO_2 + O_2$, is known not to be very fast, and the reaction (b), $HO_2 + O_3 \rightarrow HO + 2 \ O_2$, is expected to be even slower [64]. At high radical concentration, such as that produced by flash photolysis or microwave discharge, the fast [64] radical-radical termination reaction (c), $HO + HO_2 \rightarrow H_2O + O_2$, would quench this chain reaction. However, in photochemical reactions at moderate light intensity, such as direct sunlight or steady arc lamps, a long chain reaction is possible. The chain length is given by $k_a[O_a]/k_c[HO_a]$. The value of k_c is about 10^{-11} cm^3/particle-s. At 30 mm of O_3 and light absorption rate of 10^{13} photons/cm^3-s, the steady-state concentration of HO_2 is about 10^{12} per cm^3. The chain length, under these conditions, exceeds unity as k_a exceeds 10^{-17} cm^3/particle-s. The existence of long chains in ozone photolysis implies a rate constant of about 10^{-16} or larger for k_a.

3

d. Electrical Discharges

In typical, recent, quantitative studies, oxygen flows rapidly through an electrical discharge (usually a microwave cavity) and through long observation tubes. In some cases other substances are added to oxygen before the electrical discharge, and in some cases other gases are mixed with the flowing gas stream after it passed through the discharge. Oxygen atom concentration as a function of position in the steady-flow tube gives oxygen atom concentration as a function of time. The oxygen atom concentration can be measured by a number of physical and chemical methods [67, 72].

In the limit of absolutely pure oxygen, few or no oxygen atoms are produced in an electric discharge, but 10 to 20 percent of excited $O_2(^1\Delta_g)$ molecules are formed. Addition of traces of N_2, N_2O, NO, H_2, or H_2O markedly catalyze the formation of oxygen atoms. The measured catalytic efficiency of trace gases is as follows:

Added gas	O Atoms produced per molecule of added gas	
	Ref. [21]	Ref. [68]
N_2	80–100	80–90
N_2O		80–90
NO		40–45
H_2	150–195	160–120
H_2O	90–130	
He		$\leqslant 0.2$
Ar		$\leqslant 0.2$
CO_2		$\leqslant 0.2$

$$(1-13)$$

Kaufman [68a] believes the effect must be due to large changes in surface recombination efficiency within the active discharge region.

On the other hand, when argon is a carrier gas in great excess over oxygen, there is a fairly clean production of oxygen atoms, presumably by collision of O_2 with electronically excited Ar.

In a number of cases $O_2(^1\Delta_g)$ and $O_2(^1\Sigma_g^+)$ react with notably different rates than does $O_2(^3\Sigma_g^-)$. The unsuspected presence of large concentrations of metastable O_2 species and also the effects of impurities in these systems caused systematic errors in the observed rate constants for a number of studies. All studies of oxygen atoms produced from electrical discharges in oxygen should be examined very critically. Since the bond dissociation energy of ozone is approximately equal to the electronic excitation energy of $O_2(^1\Delta_g)$ and $O_2(^1\Sigma_g^+)$, the study of ozone kinetics is particularly sensitive to the presence of electronically excited oxygen molecules. Virtually all studies of ozone kinetics in electrical discharges before 1964 are not suitable for quantitative values of rate constants.

e. Surface Reactions of Oxygen Atoms and of Ozone

The overall recombination of oxygen atoms on a surface,

$$O + O + W \rightarrow O_2 + W, \qquad (1-14)$$
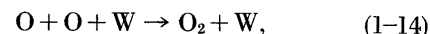
occurs by way of two successive collisions, with one atom being more or less loosely held by the surface until the other arrives. The subject was reviewed in detail by Kaufman [67]. Results are expressed in terms of the coefficient, γ, the fraction of collisions of oxygen atoms with the surface that leads to recombination. Results are not very reproducible. A given investigator may find variations of up to a factor of five for a given surface, and different investigators may differ by a factor of 10^2 or more. A sample of the internally consistent room-temperature results of Linnett [76] and co-workers is as follows:

Surface	γ
Ag	0.24.
other metals	0.003 to 0.17.
halides	around 10^{-3}.
Pyrex	$(3.1–4.5) \times 10^{-5}$.
silica	$(0.7–1.6) \times 10^{-4}$.
other oxides	10^{-4} to 10^{-2}.

$$(1-15)$$

On glass or silica the recombination coefficient, γ, increases slowly with an increase in temperature.

The thermal decomposition of ozone ($2\,O_3 = 3\,O_2$) is extremely sensitive to surface catalysts. Perman and Greaves [96] studied the effect of various solid substances placed at the bottom of a 350 ml flask, and Axworthy [3] reinterpreted the data in terms of actual rate relative to homogeneous rate of decomposition of ozone. Results are as follows:

T °C	Solid surface	Rate/homogeneous rate
100	clay pipe	2.6 to 244.
100	CuO powder	6.5 to 110.
100	Platinum black	5.0 to 6.6.
100	Platinum foil	1.0.
100	Nickel foil	1.1 to 1.3.
60	PbO_2 powder	21 to 25.
40	CuO powder	4.2×10^3 to 9.5×10^4.
40	MgO powder	2.5×10^5 to 4.3×10^6.
40	MnO_2	9.7×10^4 to 4.8×10^6.
15	MnO_2	2.9×10^6 to 2.2×10^8.

$$(1-16)$$

f. Production of Oxygen Atoms by Other Methods

Photolysis (17) of NO_2 between 3000 and 4000 Å gives NO plus $O(^3P)$. The mercury sensitized photolysis of N_2O also gives ^3P oxygen atoms and the relatively unreactive N_2. Photolysis [84] of CO_2 in the vacuum ultraviolet gives $O(^1D)$ and CO. Photolysis of O_2 in the vacuum ultraviolet gives $O(^1D) + O(^3P)$.

A special method of preparing oxygen atoms in large yields in a flow reactor and in an environment free of molecular oxygen is to dissociate N_2 to atoms in an electric discharge and then titrate the nitrogen atoms with nitric oxide [90]:

$$N + NO \rightarrow N_2 + O. \qquad (1-17)$$
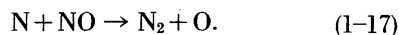
The thermal decomposition of ozone in a shock tube is an excellent method of producing a large excess of ground state oxygen atoms [125, 71]. The thermal decomposition of ozone at low pressure in a fast-flow system is a clean source of $O(^3P)$, whose reactions have been studied by fast mixing with other gases [70].

g. Isotopic Exchange

The isotopic composition (masses 16 and 18, usually) of O_2 and O_3 can be determined by high-resolution mass spectrometers; and the rate of isotopic exchange between $O_2 + O_2$, $O_2 + O_3$, and $O_3 + O_3$ has been studied, although these reactions are slow except under special circumstances.

1.3. Elementary Physical Reactions

An elementary physical reaction is a process that changes the quantum state, but not the structure, of a molecule. Important examples in this review are translational-vibrational energy transfer:

$$\underbrace{O_2(v) + M}_{\text{relative velocity 1}} \rightarrow \underbrace{O_2(v') + M}_{\text{relative velocity 2}}, \qquad (1-18)$$

$$\underbrace{O_3(v_1, v_2, v_3) + M}_{\text{relative velocity 1}} \rightarrow \underbrace{O_3(v_1', v_2'', v_3'') + M}_{\text{relative velocity 2}}. \qquad (1-19)$$
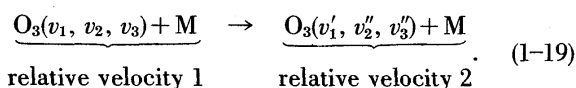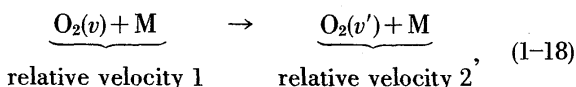
Also translational-electronic energy transfer is important in these systems:

$$\underbrace{O_2(^1\Delta_g) + M}_{\text{relative velocity 1}} \rightarrow \underbrace{O_2(^3\Sigma_g^-) + M}_{\text{relative velocity 2}}, \qquad (1-20)$$

$$\underbrace{O(^1D) + M}_{\text{relative velocity 1}} \rightarrow \underbrace{O(^3P) + M}_{\text{relative velocity 2}}. \qquad (1-21)$$
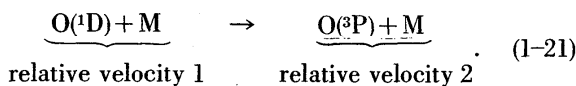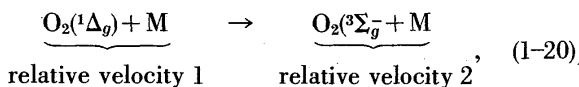
Absorption and emission of radiation often represent elementary physical reactions:

$$O_2(^3\Sigma_g^-) + h\nu \rightarrow O_2(^1\Delta_g), \qquad (1-22)$$

$$O_3(v_1, v_2, v_3) + h\nu \rightarrow O_3(v_1, v_2, v_3'). \qquad (1-23)$$
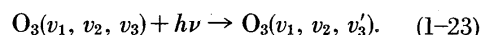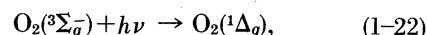
1.4. Elementary Chemical-Physical Reactions

In any chemical reaction the set of atoms that constitute the products are arranged in a different structure from the same set of atoms that were the reactants; the change in *structure* as opposed to a mere change in quantum number inside a given structure is the essence of a chemical process. The *ideal* elementary chemical-physical reaction is a chemical reaction that occurs as a result of a single collision in which the quantum state (translational, rotational, vibrational, and electronic) of every reactant and product is known, for example,

$$\underbrace{O(^3P) + O_3(^1A, v_1, v_2, v_3, J, K_a, K_b)}_{\text{relative velocity 1}}$$

$$\rightarrow \underbrace{O_2(^3\Sigma_g^-, v, J) + O_2(^1\Delta_g, v, J)}_{\text{relative velocity 2}}. \qquad (1-24)$$
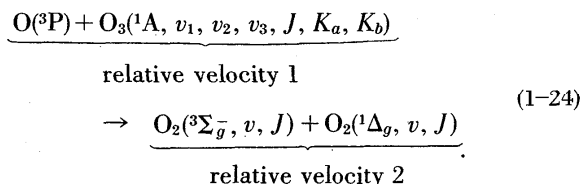
Although every reactive collision is an elementary chemical-physical reaction, so far, no laboratory experiment has been so well controlled that all states of all reactants and products were known when a rate was measured. (In principle, a velocity-selected crossed molecular beam with field-selected internal states of reactants and products could be used to observe and measure the reaction cross section for an ideal elementary chemical physical reaction.) In the absence of methods of observing *ideal* chemical-physical processes, the definition of an elementary chemical-physical reaction is extended to include a chemical reaction that occurs in one collision where the change of quantum state of at least one sort of energy is known:

$$O_3 + h\nu \ (3000 \ \text{Å}) \rightarrow O_2(^1\Delta_g) + O(^1D)$$

$$O + O + M \rightarrow O_2(v = 19) + M \qquad (1-25)$$

$$O(^1D) + O_3(^1A) \rightarrow O_2(^1\Delta_g) + O_2(^1\Sigma_g^+).$$
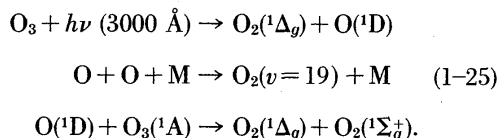
1.5. Elementary Chemical Reactions

a. Definition

A system undergoing no net chemical reaction and at thermal equilibrium with its surroundings will have a uniform temperature, and the molecules in the system will be distributed over translational and internal quantum states according to the Boltzmann distribution function. The molecules have an

5

equilibrium distribution over states. A system undergoing a chemical reaction may have a uniform translational temperature in equilibrium with surroundings, but the internal states of the molecule, especially electronic or vibrational, may be far from the equilibrium distribution characterized by the translational temperature. The unimolecular decomposition of a polyatomic molecule is a well-understood example of this effect:

$$O_3 + M \xrightarrow{a_i} O_{3_i}^* + M, \qquad (1\text{-}26)$$

$$O_{3_i}^* + M \xrightarrow{b_i} O_3 + M, \qquad (1\text{-}27)$$

$$O_{3_i}^* \xrightarrow{c_i} O_2 + O, \qquad (1\text{-}28)$$
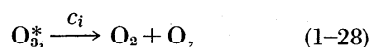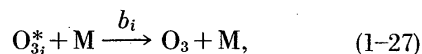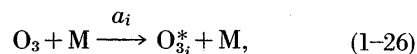
where the asterisk indicates vibrational energy in ozone greater than the critical energy for its dissociation. The steady-state concentration of vibrationally excited ozone in a particular energy level, i, is

$$\frac{[O_3^*]_i}{[O_3]} = \frac{a_i[M]}{b_i[M] + c_i} = (P_i)_{ss}. \qquad (1\text{-}29)$$

At sufficiently high pressure, deactivation b occurs very fast compared to decomposition c so that the actual distribution function approaches the equilibrium value, even though reaction is occurring:

$$\frac{[O_3^*]_i}{[O_3]} \cong \frac{a_i}{b_i} = (P_i)_{eq}. \qquad (1\text{-}30)$$

At low pressures, the unimolecular reaction, c_i, is so fast that deactivation, b_i, essentially never occurs; every molecule that reaches the critical level of energy eventually decomposes; the steady-state distribution function takes the limiting form:

$$\frac{[O_3^*]_i}{[O_3]} = \frac{a_i[M]}{c_i} = (P_i)_{ss}^o \qquad (1\ 31)$$

The equilibrium distribution function $(P_i)_{eq}$ is determined by one macroscopic variable, the temperature T. The steady-state distribution function $(P_i)_{ss}$ is determined by two macroscopic variables, temperature T and total effective gas concentration $[M]$. The two-parameter steady-state distribution function is as reproducible and well defined as the more familiar one-parameter equilibrium distribution function.

The definition of an elementary chemical reaction is the total effect of an elementary chemical-physical reaction where the *reactants* are distributed according to a steady distribution function, fixed by a small number of macroscopic variables (no restriction is made on the distribution of reaction products).

b. List of Cases Considered in this Review

The elementary chemical reactions of importance in this review are listed here for convenience of reference:

D. $O_2 + M \rightarrow O + O + M$

R. $O + O + M \rightarrow O_2 + M$

1. $O_3 + M \rightarrow O_2 + O + M$

2. $O + O_2 + M \rightarrow O_3 + M$ \qquad (1-32)

3. $O + O_3 \rightarrow 2\,O_2$

4. $2\,O_2 \rightarrow O + O_3$

5. $O + O_2 \rightarrow O_2 + O$ (exchange)

Rate constants are written with "lower case" k and subscripts: k_D, k_R, k_1, k_2, k_3, k_4, and k_5. Equilibrium constants are written with "upper case" K and subscripts: K_D, K_1, K_3 $(K_R = K_D^{-1}, K_2 = K_1^{-1}, K_4 = K_3^{-1})$.

The rate constant of an elementary reaction is *constant* throughout the course of reaction at one temperature, but it usually varies with temperature. In tables and figures we report observed rate constants and temperatures; and it is desirable to express these empirical data in an appropriate functional form. Most theories of elementary reaction rates indicate that the rate constant varies with temperature as $k \propto f(T) \exp(-E/RT)$, where $f(T)$ depends weakly on temperature and $\exp(-E/RT)$ is a strong function of temperature. Under limiting conditions, especially at high temperature, the weak $f(T)$ usually takes the form of T^m. Thus, the manner with which gas phase reaction-rate theory predicts the rate constant to vary with temperature may be expressed in an approximate general form as $BT^m \exp(-E/RT)$. In the theoretical models, the parameter E usually has the physical interpretation of an energy barrier, and the parameters B and m have physical interpretations. Chemical kinetic data usually possess so much experimental error and scatter that they are totally unable to support the three-parameter relation. A least-squares fit of the three-parameter relation to scattered experimental data usually gives physically ridiculous values to the parameters B, m, and E; and values of the parameters are quite unstable with respect to addition or removal of small blocks of data. Thus, experimental data are usually interpreted in terms of a two-parameter equation: (1) m is set to zero (Arrhenius equation), (2) E is set to zero, (3) m is assigned some theoretical value with B and E fitted to the data, (4) or E is assigned its theoretical value with B and m fitted to the data. As a part of this review, all rate constants were fitted by each of the following relations by the method of least squares:

$$k = A \exp(-E/RT), \qquad (1\text{-}33)$$

$$k = BT^m \exp(-E'/RT), \qquad (1\text{-}34)$$

$$k = CT^n, \qquad (1\text{-}35)$$

6

and in some cases either m or E' of eq (1–34) was assigned a theoretical value. The form of the final recommended equation differs for the various elementary reactions.

The activation energy is a measure of how the rate constants change with temperature:

$$E_A = -R \, \frac{d \ln k}{d(1/T)}. \qquad (1\text{–}36)$$

The activation energy for each of the equations for k given above is

$$E_A = E, \qquad (1\text{–}37)$$

$$E_A = E' + mRT, \qquad (1\text{–}38)$$

$$E_A = nRT. \qquad (1\text{–}39)$$

For the Arrhenius equation, the activation energy does not change with temperature; for the other two relations the activation energy is temperature dependent.

c. Side Reactions

Either the forward or the reverse reaction of each elementary reaction above can be imitated by complex, side reactions; and these reactions have been a major source of error in many would-be quantitative studies. Examples of complex mechanisms that imitate other chemical reactions are:

Reaction R $\quad O + O + M \rightarrow O_2 + M$
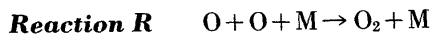
(1) Heterogeneous reactions on surfaces W:

$$O + W \rightarrow O \ldots W$$
$$\frac{O \ldots W + O \rightarrow O_2 + W}{\text{net } O + O \rightarrow O_2.} \qquad (1\text{–}40)$$
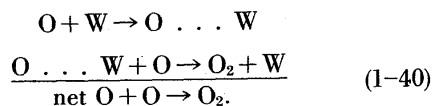
(2) Homogeneous catalysis by oxides of nitrogen:

$$\left. \begin{array}{l} O + NO + M \rightarrow NO_2 + M \\[2mm] O + NO_2 \rightarrow NO + O_2 \end{array} \right\} \text{ chain } \quad (1\text{–}41)$$

$$\text{net} \quad O + O + M \rightarrow O_2 + M.$$

(3) The ozone mechanism:

$$\left. \begin{array}{l} O + O_2 + M \rightarrow O_3 + M \\[2mm] O + O_3 \rightarrow 2 O_2 \end{array} \right\} \text{ chain } \quad (1\text{–}42)$$
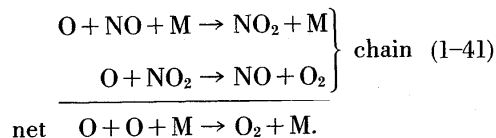
$$\text{net} \quad O + O + M \rightarrow O_2 + M.$$
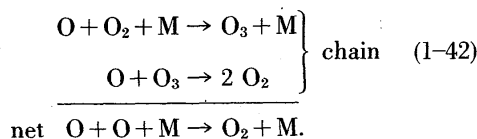
(4) Hydrogenous material giving H, HO, HO$_2$ free radicals (readily produced from some organic materials):

$$\left. \begin{array}{l} O + OH \rightarrow O_2 + H \\ H + O_2 + M \rightarrow HO_2 + M \\ O + HO_2 \rightarrow HO + O_2 \end{array} \right\} \text{ chain } \quad (1\text{–}43)$$

$$\text{net} \quad O + O \rightarrow O_2.$$
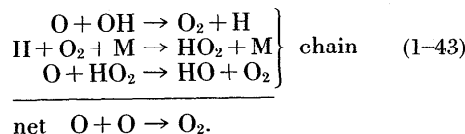
Decomposition of ozone $\quad 2\,O_3 = 3\,O_2$

(1) Heterogeneous decomposition of ozone (see section 1.2e above).
(2) Oxides of nitrogen produced from N$_2$ as impurity in ozonizer:

$$\left. \begin{array}{l} N_2O_5 \rightleftarrows NO_2 + NO_3 \\ NO_2 + O_3 \rightarrow NO_3 + O_2 \\ 2NO_3 \rightarrow 2NO_2 + O_2 \end{array} \right\} \text{ chain } \quad (1\text{–}44)$$

$$\text{net} \quad 2\,O_3 = 3\,O_2.$$
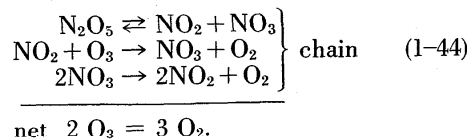
(3) Hydrogenous material giving H, HO, or HO$_2$ free radicals (readily produced from some organic materials):

$$\left. \begin{array}{l} H + O_2 + M \rightarrow HO_2 + M \\ HO + O_3 \rightarrow HO_2 + O_2 \\ HO_2 + O_3 \rightarrow HO + 2\,O_2 \end{array} \right\} \text{ chain } \quad (1\text{–}45)$$

$$\text{net} \quad 2\,O_3 = 3\,O_2.$$

(4) Excited states of O$_2$ and O:

$$O_2(^1\Sigma_g^+) + O_3 \rightarrow 2\,O_2 + O$$
$$O_2(^1\Delta_g) + O_3 \rightarrow 2\,O_2 + O \qquad (1\text{–}46)$$
$$O_2^* \text{ (vibrations)} + O_3 \rightarrow 2\,O_2 + O$$
$$O(^1D) + H_2O \rightarrow 2HO \text{ (followed by 1–45).}$$
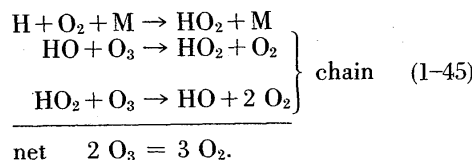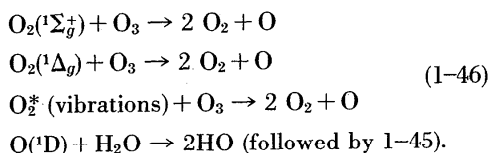
Reaction 2 $\quad O + O_2 + M \rightarrow O_3 + M$

(1) All side reactions that imitate reaction R and reaction R itself act to speed the removal of oxygen atoms. If the progress of reaction is followed in terms of disappearance of oxygen atoms, the observed rate is faster than that of reaction 2.
(2) All side reactions that destroy ozone (heterogeneous and homogeneous) make reaction 2 appear too slow if the reaction is followed in terms of formation of ozone.
(3) Homogeneous decomposition of ozone by excited states of O$_2$ (see above) both destroys O$_3$ and regenerates O. Thus reaction 2 appears to go too slowly.
(4) Hydrogen-containing free radicals regenerate O atoms to make reaction 2 appear too slow:

$$2HO \rightarrow H_2O + O. \qquad (1\text{–}47)$$
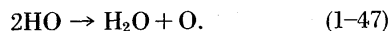
Reaction 3 $O + O_3 \rightarrow 2\,O_2$

(1) Hydrogen-containing free radicals:

$$\left.\begin{array}{l} O + HO \rightarrow O_2 + H \\[4pt] H + O_3 \rightarrow HO + O_2 \end{array}\right\} \text{chain} \quad (1\text{-}48)$$

net $O + O_3 \rightarrow 2\,O_2.$
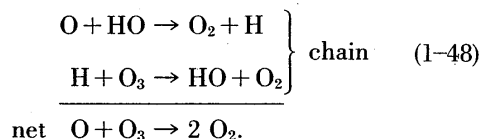
(2) Oxides of nitrogen (N_2O_5 in presence of ozone):

$$\left.\begin{array}{l} O + N_2O_5 \rightarrow O_2 + 2NO_2 \\ NO_2 + O_3 \rightarrow NO_3 + O_2 \\ NO_2 + NO_3 \rightarrow N_2O_5 \end{array}\right\} \text{chain} \quad (1\text{-}49)$$

net $O + O_3 = 2\,O_2.$
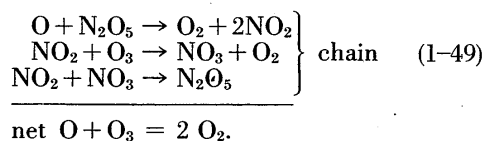
(3) Excited electronic states of O:

$$O(^1D) + O_3 \rightarrow 2\,O_2. \quad (1\text{-}50)$$
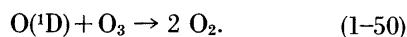
(4) All other processes listed above that remove O or decompose ozone would introduce error into a measured value of k_3. Almost all side reactions have the net effect of increasing the apparent rate of reaction 3.

1.6. Purpose of This Review

In section 1.2 above, we briefly discussed many different experimental systems where rates were measured involving some combination of O, O_2, and O_3. In all cases oxygen atoms are involved as reactants, products, or intermediates. In section 1.5 above we listed seven elementary chemical reactions of interest plus a substantial number of side reactions involving surfaces, hydrogen-containing free radicals, oxides of nitrogen and excited electronic species of O and O_2. Each elementary reaction involves oxygen atoms as either reactant or product. In principle every laboratory reaction involves all seven elementary reactions. Formally, the problem may be expressed in terms of a matrix of laboratory reactions and elementary reactions (see table below).

Experimental measurements give laboratory reactions as an unknown function of seven elementary reactions plus X elementary side reactions. What we desire may be formally expressed as the

Laboratory reactions	Elementary reactions							X side reactions
	D	R	1	2	3	4	5	
1. O_2, shock tube	1D	1R	11	12	13	14	15	1X
2. O_3, shock tube	2D	2R	21	22	23	24	25	2X
3. O_2, photolysis	3D	3R	31	32	33	34	35	3X
4. O_3, photolysis	4D	4R	41	42	43	44	45	4X
5. O_3, heated	5D	5R	51	52	53	54	55	5X
6. O_2, electrical discharge	6D	6R	61	62	63	64	65	6X
7. Photolysis of NO_2, N_2O, etc.	7D	7R	71	72	73	74	75	7X
8. Electrical discharge in N_2, etc.	8D	8R	81	82	83	84	85	8X
Y. Other studies	YD	YR	Y1	Y2	Y3	Y4	Y5	YX

inversion of these relations or the inversion of the matrix indicated above. We want to eliminate the effect of side reactions (either physically or by subtraction of their known effect), and evaluate the rate constants of the seven elementary reactions from observations of laboratory systems. By control of concentrations, temperature, light intensity, etc., we can set large numbers of entries in the matrix to zero. By combining two or more laboratory studies, we can sometimes evaluate two or more elementary reactions, formally analogous to reduction of a matrix to its irreducible blocks.

The object of this report is to go to the original literature and, insofar as possible, to reinterpret the published data of quantitative studies that contribute to the separation and evaluation of the seven elementary rate constants. The results of different investigators are combined. Isolated quantitative studies that do not lead to evaluation of the elementary rate constants are not utilized. Older studies (pre-1933) of ozone decomposition and early (pre-1964) studies involving electrical discharges in oxygen contain much larger experimental error (section 1.5c above) than recent studies, and usually these are omitted. Thus the object of this review is not to produce an exhaustive bibliography, nor to prepare exhaustive tables of observed data, but rather it is to get the best estimate of the seven elementary rate constants and to tabulate the quantitative experimental data used to get these best estimates.

2. Decomposition of Oxygen Molecules and Recombination of Oxygen Atoms

2.1. Decomposition of Molecular Oxygen

The equilibrium constants for the reaction

$$O_2 = O + O \quad (2\text{-}1)$$

$$K_D = [O]^2/[O_2], \text{ particles/cm}^3$$

has been taken from the JANAF tables [57], and are given between 100 and 6000 K in table 4.[3] Above 3000 K oxygen is significantly dissociated to atoms, and the rate of the thermal decomposition of oxygen,

---

[3] Table 4 and all subsequent numbered tables, as well as all figures, will be found at the end of the section in which they are first mentioned.

$$O_2 + M \xrightarrow{k_D} O + O + M \qquad (2\text{-}2)$$

$$-\frac{d[O_2]}{dt} = k_D[O_2][M], \text{ particles/cm}^3\text{-s},$$
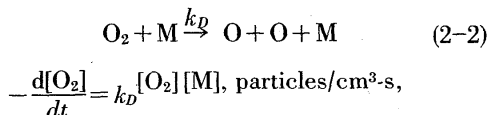
has been studied in shock tubes between 3000 and 17,000 K. Several investigators used argon as the shock-tube "fluid", with approximately 1 percent oxygen. Under these conditions the shock tube performs relatively closely to ideal theory, and the temperature of the gas can be accurately calculated from measured shock wave velocities. Other investigators used pure oxygen as the shocked gas, and in these cases there is ambiguity about the temperature-time relationship as translational energy is taken up by molecular vibrations, and the shock waves are more likely to give nonideal behavior. Limited studies have been made with krypton or xenon as foreign gas, M. This review gives especial emphasis to the extensive series of runs made with argon and with oxygen.

In the evaluation of rate constants from observed rates, it is usually necessary to consider the reverse reaction as well as the forward reaction:

$$O + O + M \xrightarrow{k_R} O_2 + M$$

$$-\frac{d[O_2]}{dt} = k_D[O_2][M] - k_R[O]^2[M]$$

$$= k_D[O_2][M] - (k_D/K_D)[O]^2[M]. \qquad (2\text{-}3)$$
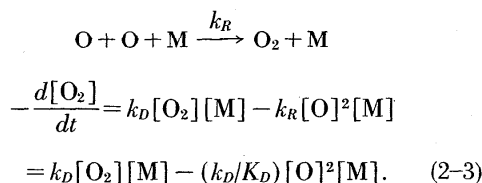
Some investigators published tables of rate constants k_D at each observed temperature, and these data are reproduced in tables 8 and 9. Other authors published only graphs showing data points in an Arrhenius plot of log k_D versus T^{-1}. In these cases we have read the points from the graphs and entered the data in tables 5, 6, and 7. In other cases the authors did not present the data as either tables or graphs, but rather they gave only the Arrhenius equation and temperature range. Such data are essentially lost, but table 10 summarizes the little information that is available from three such studies. We feel that authors should insist (to editors of journals) that both tables of data and graphs should be published for the rate constants of elementary chemical reactions.

For the decomposition of oxygen with excess argon as carrier gas, there are four sets of quantitative data, presented as tables 5, 6, 7, and 8, and all of the points of the four investigations are also given in figure 1A. The agreement between different studies and the scatter of points in each study is readily seen in figure 1. The data from each investigation were treated by the method of least squares for the two-parameter Arrhenius equation, (1-33), and by the three-parameter equation, (1-34). The parameters, E, m, and E', so obtained, are given for each of the four studies as the first four lines of table 11. The scatter of the points is so great that the data cannot support a three-

parameter, least-squares fit; the values of m and E' are in violent disagreement from one author to another and are physically absurd. The scatter of points is such that even the two parameters of the Arrhenius equation are given only with a large standard deviation, and reference [108] seems to have some systematic, temperature-dependent error. The data of all four studies were combined, and the least-squares parameters, E, m, and E', are given as the fifth entry in table 11. The last four entries in table 11 were obtained by use of all data except that for a given study. These last five entries show that even all the data taken together are not enough to establish a three-parameter relation, but the two parameters of the Arrhenius equation are fairly well established. The activation energy is about 105 kcal/mole, whereas the dissociation energy of oxygen is 118 kcal/mole. This computed activation energy is about the same whether all four sets of data are used or any three sets are employed. The curve shown in figure 1 was obtained in a way to be described later.

The data observed for the dissociation of pure oxygen are given in tables 9 and 10 and plotted in figure 1B. The line labeled k_4 in figure 1B is the reverse of the reaction obtained in the decomposition of ozone:

$$O_3 + O \xrightarrow{k_3} O_2 + O_2, \qquad (2\text{-}4)$$

$$O_2 + O_2 \xrightarrow{k_4} O_3 + O,$$
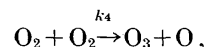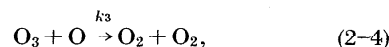
$$K_3 = k_3/k_4 \text{ and } k_4 = k_3/K_3.$$

From the observed value of k_3 (section 3) and the value of K_3 calculated from JANAF tables, the value of k_4 was found (table 26). It is clear from figure 1B that the decomposition of oxygen at high temperatures does not go by way of the ozone mechanism: k_4, k_1.

2.2. Recombination of Atomic Oxygen

The recombination of oxygen atoms has been studied in a variety of different ways. At room temperature a nonequilibrium excess of oxygen atoms has been formed by electrical discharges in oxygen, by reaction of nitrogen atoms with nitric oxide ($N + NO \rightarrow N_2 + O$), by ultraviolet photolysis of oxygen, and by other photochemical methods. At temperatures above 1000 K, large concentrations of oxygen atoms have been formed by the thermal decomposition of ozone ($O_3 + M \rightarrow O_2 + O + M$) in a shock tube. Also shock tubes have been used to dissociate O_2 at high temperatures, and then the shocked gas was cooled by expansion, and atom recombination was observed at a lower temperature. The data are given in table 12.

9
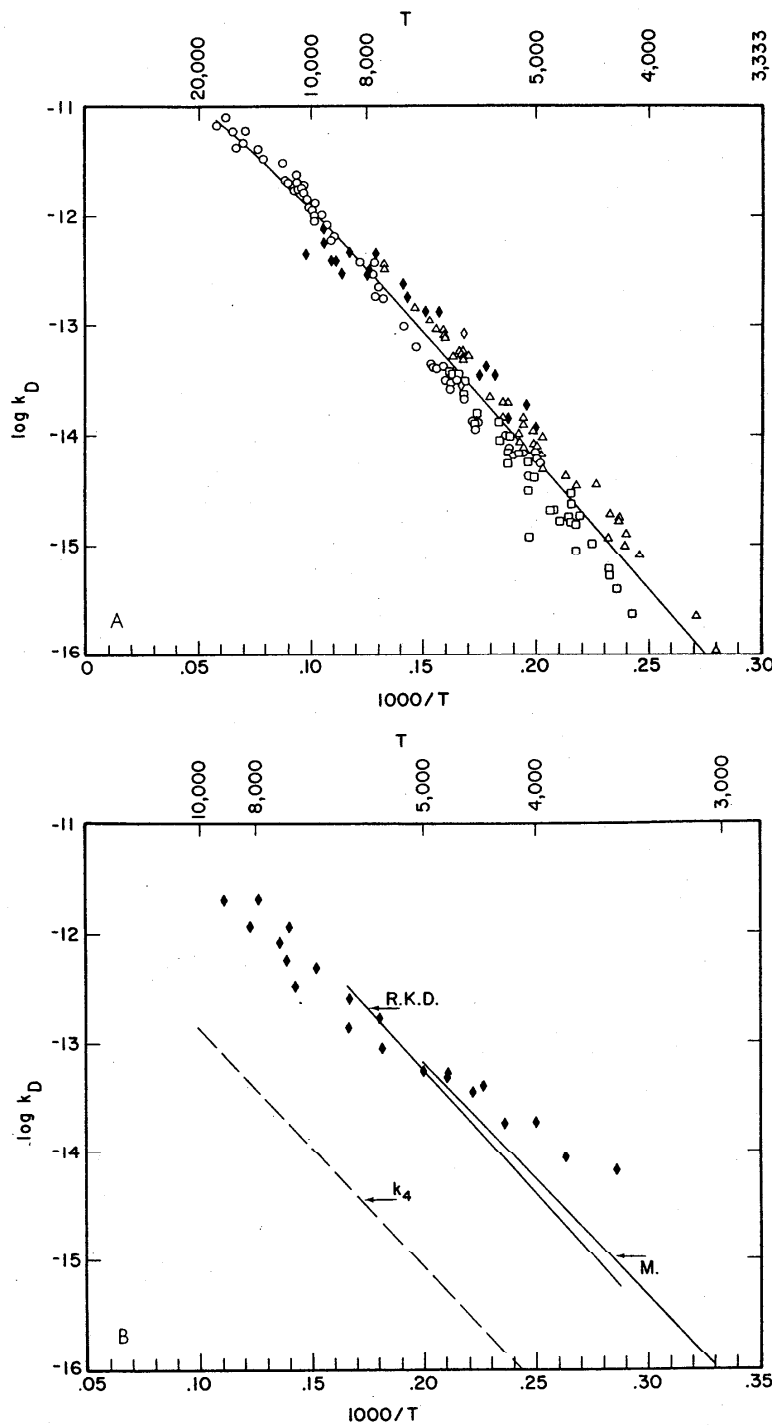
FIGURE 1. *Observed second-order rate constants* k_D ($cm^3/particle$-s) *for the thermal dissociation of oxygen.*

$$O_2 + M \rightarrow O + O + M$$
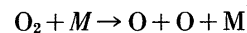
(A) M is Ar
  ○ Wray [125]
  ◆ Schexnayder and Evans [108]
  △ Camac and Vaughn [23]
  □ Anderson [1]
  Curve is calculated from
  $\log k_D = -5.37 - \log T - 25.95 \ (1000/T)$.
(B) M is O_2
  ◆ Schexnayder and Evans [108]
  Curve M: Function k_D as reported by Matthews [88]
  Curve R.K.D.: Function k_D as reported by Rink, Knight, and Duff [103].
  Curve k_4: Rate constant for the reaction $O_2 + O_2 \rightarrow O_3 + O$ as deduced from ozone kinetics (Table 28).

A considerable complication in the study of the recombination of oxygen atoms is the large number of alternate paths to reaction R, which give the same overall reaction (see section 1, 1.5c).

When oxygen atoms are produced by electrical or photochemical dissociation of O_2, there is always a large excess of O_2; and at low temperatures the ozone mechanism predominates. Except for reference [90], where O was produced from the titration of N and NO, all room temperature studies require corrections both for surface reactions and for the ozone mechanism. Such corrections have

10

been made (by the original authors except where noted otherwise) for the room-temperature rate constants entered in table 12.

The observed rate constants for recombination of oxygen atoms are listed in table 12 and plotted in figure 2. Certain parameters of the Arrhenius equation from the data are given in table 13, and also the data are treated by means of the two-parameter equation (1–35). The scatter in the data is so great that neither E nor n can be reliably obtained, although a value of about -1 is indicated for n from the argon data.

As an energy-transfer agent, O_2 is much more effective than argon, although various authors give widely different estimates of the relative efficiency (Camac and Vaughn 3; Schexnayder and Evans 9; and Wray 18). The relative efficiencies of various foreign gases for the dissociation and recombination of oxygen are given in table 14. The relative efficiency of O atoms to O_2 molecules is obtained by the authors' detailed interpretation of their data during the course of individual runs. The various authors are in considerable disagreement with each other concerning relative efficiency of M gases. However, there is a concensus that O_2 is about an order of magnitude more efficient than Ar, and O is about three times as efficient as O_2.

2.3. Equilibrium Constants and Rate Constants

It should be emphasized that tables 4 to 14 contain *observed* kinetics data. No use has been made of the relation between rate constants and equilibrium constants, which is valid at chemical equilibrium,

$$K_D = k_D/k_R, \qquad (2-5)$$

although the individual authors made minor use of this relation in correcting their observed dissociation rate for back reaction. At the short times and fast rates observed in a shock tube, several authors have questioned whether the above relation is applicable. In *Gas Phase Reaction Rate Theory*, we showed that a sufficient criterion for a rate constant having its equilibrium value is that *reactants* have an equilibrium distribution over states. The reactants for the recombination reaction are atoms, and the only important energy states are translational; translational energy states are equilibrated within a few collisions. The reactants for the dissociation are oxygen molecules, with translational, rotational, vibrational, and low-lying .electronic energy levels. Vibrational relaxation

FIGURE 2. *Observed third-order rate constants* k_R $(cm^6/particle^2\text{-}s)$ *for recombination of oxygen atoms.*

$$2O + M \rightarrow O_2 + M.$$
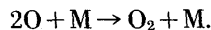
● M = Ar
◆ M = O_2 with corrections at room temperature for surface recombination of atoms and for contribution of ozone-mechanism $(O + O_2 + M \rightarrow O_3 + M, O_3 + O \rightarrow 2O_2)$.

11
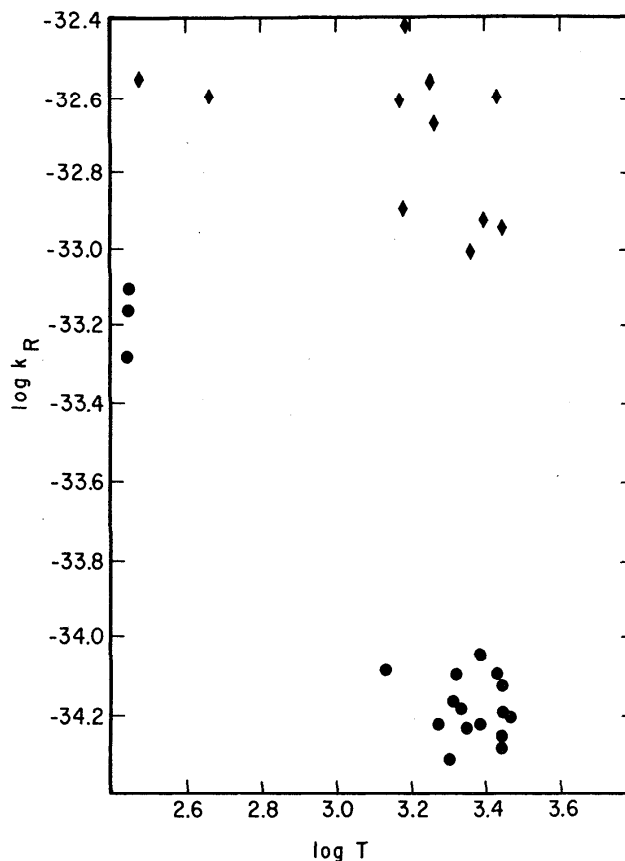
times have been measured and are about the same magnitude as dissociation times [125] above 8000 K, and thus, it is fairly certain that the reactant O_2 does *not* have an equilibrium distribution over vibrational states. With k_R having its equilibrium value (that is, the elementary physical and chemical-physical rate functions are averaged over an equilibrium distribution of states of O and of M) and with k_D being an average over the nonequilibrium distribution function, the relation $K = k_D/k_R$ is not expected to be literally true. But the question remains whether the departure of k_D from its equilibrium value is a small effect (1 percent or less) or a large effect (a factor of 10 or more).

As a test of the magnitude of this effect, k_D is calculated from $k_R \cdot K_D$. All the points where M is O_2 are plotted on figure 3, along with a bar showing the range of observed k_D. The high temperature k_R point by Wilson [123] (where a shock wave was cooled by expansion), and the high temperature points of Kiefer and Lutz [71] (where ozone was decomposed in a shock wave) join smoothly on the extenuation of the observed rate constants for decomposition. The low temperature rate constants for recombination give values of $k_D = k_R K_D$ that lie on the same curve as the observed function k_D. For the runs with argon and with oxygen, the other test of $K = k_D/k_R$ is given by figure 4, where k_R is calculated from k_D/K_D and plotted on the same graph with observed values of k_R. The scatter of the observed k_D in figure 3 is plus or minus a factor of two, and the scatter in values of k_R is even larger, about a factor of 5. Figures 3 and 4 show that the relation $K_D = k_D/k_R$ is obeyed within this (rather large) range of experimental scatter. Thus it is

concluded that the effect of nonequilibrium distribution of O_2 during reaction is smaller than experimental error, and full use of the relation $K_D = k_D/k_R$ should be made in the interpretation of data.

2.4. Recommended Values of Rate Factors

The observed activation energy from 3000 to 17,000 K is between 100 and 110 kcal/mole, table 11, whereas the dissociation energy is 118 kcal/mole. Although the Arrhenius equation $k = A \exp(-E/RT)$ is widely used in kinetics, theories of kinetics indicate that A is a weak function of temperature. Especially at high temperatures, simple theories of reaction rates indicate that the rate constant should have the form of eq (1–34), $k = BT^m \exp(-E'/RT)$. However, we have already shown that the data contain so much scatter that they cannot support a least-squares fit to a three-parameter relation. The procedure followed is that all data were examined together and judgment was used to pick the parameter m, and then the method of least squares was applied to all the data to fix B and E'. The arguments and methods used are discussed below.

The activation energy is a measure of how the rate constants change with temperature, eq (1–36). Any relation of activation energy to barrier height or other model follows from some theory, not from the definition of activation energy. If the rate constant has the form (1–34), the activation energy is $E = E' + mRT$ [eq. (1–38)]. If E' represents some
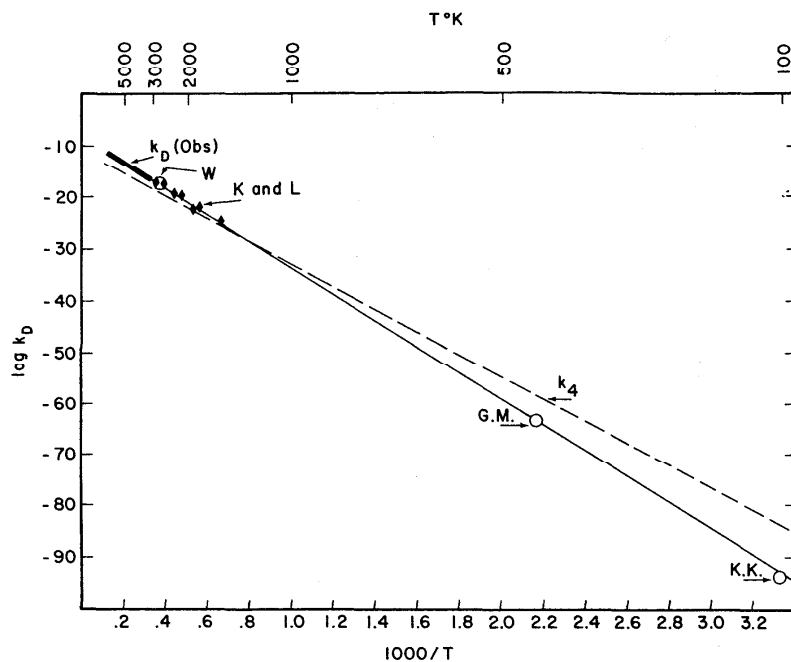
FIGURE 3. *Comparison of function fitted to observed dissociation rate constant, k_D, to that calculated from $k_D = k_R K_D$ where M is O_2. Range of k_D observed given by figure 1.*

W.   Wilson [123]
K.L.   Kiefer and Lutz [71]
G.M.   Golden and Myerson [48]
K.K.   Kaufman and Kelso [69]
Solid curve is calculated from log $k_D = -4.34 - \log T - 25.95 (1000/T)$. Dashed curve is k_4 from ozone kinetics $(O_2 + O_2 \rightarrow O_3 + O)$.
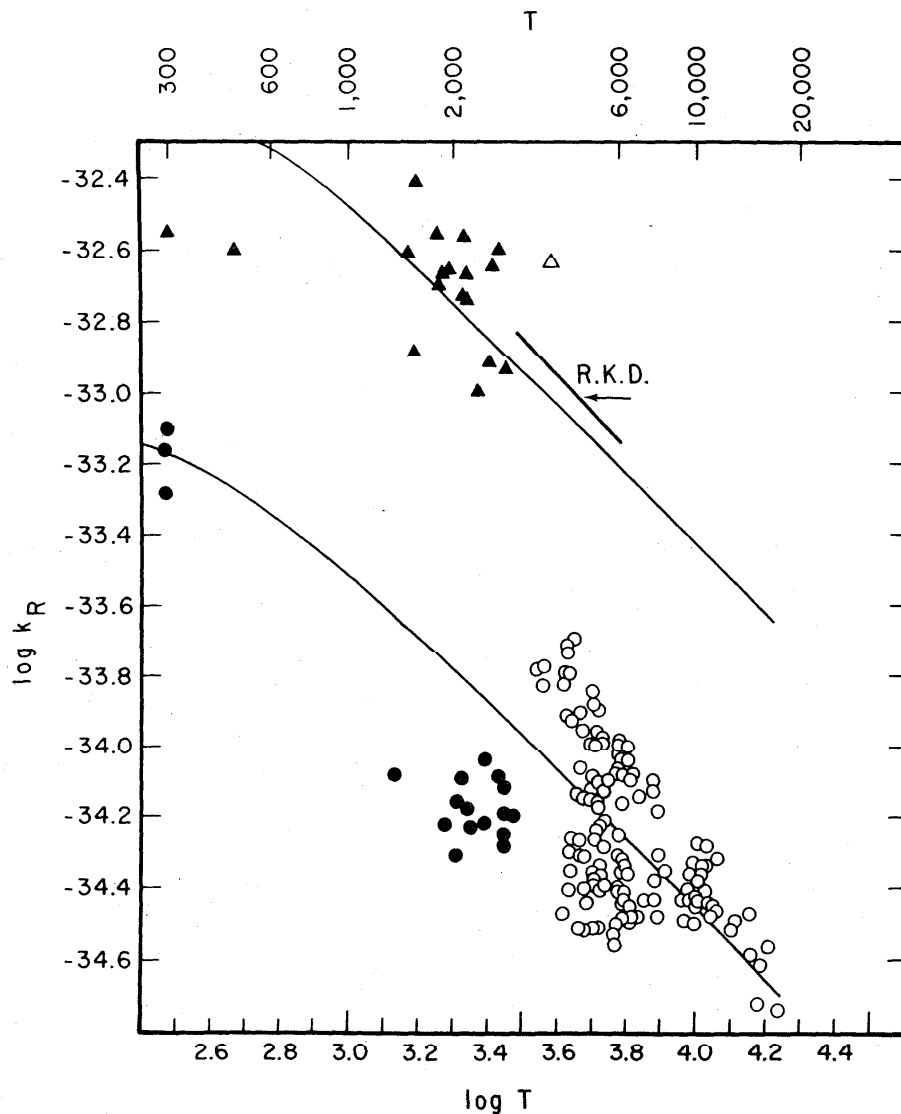
FIGURE 4. *Comparison of observed third-order rate constants* k_R *with values calculated from* $k_R = k_D/K_D$.

● M = Ar, k_R observed
○ M = Ar, $k_R = k_D/K_D$
▲ M = O_2, k_R observed
△ M = O_2, $k_R = k_D/K_D$

Line segment R.K.D. is range of data covered by Rink, Knight, and Duff [103]. Data by Schexnayder and Evans are not included. Curves are given by:

$$\log k_R(O_2) = -29.42 - \log T - 0.0745 \ (1000)/T$$
$$\log k_R \ (Ar) = -30.45 - \log T - 0.0745 \ (1000)/T$$

barrier height, the observed activation energy will be greater than the barrier height if m is positive or less than the barrier height if m is negative. In this case the observed activation energy is less than the bond dissociation energy, so m must be negative. The observed activation energy as a

13

function of temperature varies with m as follows (kcal/mole):

T	$-m=1/2$	$-m=1$	$-m=1.5$
0	118	118	118
3,000	115	112	109
5,000	113	108	103
10,000	108	98	88
15,000	103	88	73

$$(2\text{-}6)$$

The mid-range of observation is about 5,000 to 10,000 K; the observed activation energy ("all data," in table 11) is 105 ± 3 kcal/mole.[4] Thus m seems to be closer to -1 than to -0.5 or to -1.5.

Where argon is the catalyst, all data for observed k_D and for $k_D = k_R/K_D$ were combined and fitted to the three-parameter equation by least squares. The result was

$$\log b = -5.06$$
$$m = -1.085$$
$$E' = 118.06 \text{ kcal/mole.} \qquad (2\text{-}7)$$

Note that the indicated value of m is about minus one.

Inspection of figure 4 shows that the best slope through the points, plotted as $\log k$ versus $\log T$, is slightly less than one in magnitude, about -0.9.

With three lines of argument leading to a value of about minus one for the parameter m, it was decided to take minus one as its value, and the other terms B and E' are found from least squares and the data. The resulting recommended rate-constant functions for k_D are given in table 15. This function gives the curve plotted in figure 1.

The equilibrium constant K_D is given in table 4 and it is almost equally well approximated by the two parameter equation,

$$\log K_D = 25.0799 - 25.8745 \ (1000/T), \qquad (2\text{-}8)$$

as by the three-parameter equation,

---
[4] The estimated error is twice the standard deviation.

$$\log K_D = 25.4254 - 25.8959 \ (1000/T)$$
$$- 0.0977 \log T. \qquad (2\text{-}9)$$

The recombination rate constant is calculated from the function for k_D (table 15),

$$\log k_D(\text{Ar}) = -5.37 - 25.95 \ (1000/T)$$
$$- \log T, \qquad (2\text{-}10)$$

and the two-parameter equation for K_D to give

$$\log k_R(\text{Ar}) = -30.45 - \log T - 0.0745 \ (1000/T). \qquad (2\text{-}11)$$

This curve is plotted through the argon data in figure 4, and within experimental error the curve passes more or less through the center of the data at low and at high temperatures.

It was assumed that when M is O_2 the rate functions k_D and k_R have the same form as when M is Ar. The constant B was adjusted (leaving m and E' at the same values as for Ar) to give agreement with the O_2 data at high temperature, and the calculated curve for $k_D(O_2)$ is given in table 15 and plotted in figure 3. On this plot the agreement between observed data and fitted function seems quite satisfactory. However, the data for $k_R(O_2)$ present more of a problem. The function is taken as k_D/K_D, is written out in table 15, and is plotted with the data in figure 4. The agreement between the function $k_R(O_2)$ and the data above 1000 K is very good, but below 1000 K the experimental data, which have been heavily corrected for the ozone mechanism, lie far below the calculated curve. Figure 3 shows the ozone function $(O_2 + O_2 \xrightarrow{k_4} O_3 + O)$ over a wide range of temperature. Below 1000 K, the ozone mechanism (k_4) is faster than the direct decomposition (k_1); and as a usual thing the recombination by way of ozone will be faster than direct recombination. Thus, either the reported rate constants [69, 48] have been overly corrected for the ozone mechanism, or the $k_R(O_2)$ function behaves very much differently from the $k_R(\text{Ar})$ function below 1000 K. Table 15 gives recommended values for $k_D(\text{Ar})$ and $k_R(\text{Ar})$ between 300 and 15,000 K, but the corresponding functions for oxygen are recommended only between 1,000 and 8,000 K. These recommended values are also given in section 6.

TABLE 4. *Equilibrium constants from JANAF tables* [57] *for the reaction* $O_2 = O + O$ *(units of particles/cm^3)*

$$\log K_D = 2 \log K_p - RT + \log N_{Avog}.$$

T °K	1000/T	log K_D
100	10.000	− 233.594
200	5.000	− 104.421
300	3.333	− 61.281
400	2.500	− 39.682
500	2.000	− 26.713
600	1.667	− 18.060
700	1.429	− 11.879
800	1.250	− 7.241
900	1.111	− 3.631
1000	1.000	− 0.750
1200	0.8333	3.577
1400	.7143	6.674
1600	.6250	8.978
1800	.5556	10.776
2000	.5000	12.209
2200	.4545	13.381
2400	.4167	14.360
2600	.3846	15.179
2800	.3571	15.882
3000	.3333	16.489
3200	.3125	17.021
3400	.2941	17.488
3600	.2778	17.899
3800	.2632	18.272
4000	.2500	18.602
4200	.2381	18.902
4400	.2273	19.172
4600	.2174	19.419
4800	.2083	19.644
5000	.2000	19.853
5200	.1923	20.042
5400	.1852	20.217
5600	.1786	20.382
5800	.1724	20.532
6000	.1667	20.672

The equilibrium constant can be approximated by either of the following least-squares expressions:

$$\text{Log } K_D = 25.0799 - 25.8745 \ (1000/T)$$

$$\text{Log } K_D = 25.4254 - 25.8959 \ (1000/T) - 0.0977 \log T.$$

These expressions were obtained by fitting the JANAF data at 100° intervals over the range 100–6000K.

TABLE 5. *Observed rate constants* k_D *(cm^3/particle-s)* M = Ar

(Wray [125])

T	1000/T	log k
5076.	0.1970	− 14.400
5141.	.1945	− 14.190
5263.	.1900	− 14.200
5319.	.1880	− 14.120
5376.	.1860	− 14.020
5731.	.1745	− 13.900
5780.	.1730	− 13.960
5830.	.1715	− 13.890
5952.	.1680	− 13.680
6060.	.1650	− 13.510
6172.	.1620	− 13.600
6172.	.1620	− 13.550
6250.	.1600	− 13.520
6289.	.1590	− 13.390
6410.	.1560	− 13.410
6493.	.1540	− 13.400
6514.	.1535	− 13.380
6803.	.1470	− 13.210
7067.	.1415	− 13.020
7576.	.1320	− 12.770
7692.	.1300	− 12.660
7751.	.1290	− 12.740
7782.	.1285	− 12.430
7812.	.1280	− 12.540
8196.	.1220	− 12.430
9090.	.1100	− 12.200
9174.	.1090	− 12.230
9345.	.1070	− 12.090
9523.	.1050	− 12.000
9803.	.1020	− 11.890
9842.	.1016	− 12.050
9852.	.1015	− 12.000
9901.	.1010	− 11.960
10101.	.0990	− 11.920
10152.	.0985	− 11.850
10256.	.0975	− 11.720
10309.	.0970	− 11.800
10416.	.0960	− 11.740
10638.	.0940	− 11.760
10638.	.0940	− 11.700
10695.	.0935	− 11.620
10752.	.0930	− 11.770
11050.	.0905	− 11.740
11111.	.0900	− 11.700
11299.	.0885	− 11.680

15

TABLE 5. *Observed rate constants* k_D *(cm³/particles)* M= Ar — Continued

(Wray [125])

T	1000/T	log k
11363.	.0880	−11.510
12658.	.0790	−11.480
13157.	.0760	−11.380
14184.	.0705	−11.220
14285.	.0700	−11.320
15037.	.0665	−11.370
15384.	.0650	−11.220
16129.	.0620	−11.090
17241.	.0580	−11.170

Data read from graph; O_2 mostly 0.5 or 2 percent with 7 points at 4 percent; U.V. absorption.

TABLE 6. *Observed rate constants* k_D *(cm³/particles)*. M = Ar

(Camac and Vaughan [23])

T	1000/T	log k
3450.	0.2900	−16.210
3460.	.2889	−16.180
3565.	.2800	−16.000
3695.	.2705	−15.670
4070.	.2455	−15.100
4170.	.2398	−14.920
4180.	.2390	−15.020
4225.	.2367	−14.780
4230.	.2365	−14.760
4300.	.2325	−14.730
4310.	.2320	−14.850
4425.	.2260	−14.460
4580.	.2180	−14.470
4690.	.2130	−14.390
4930.	.2030	−14.020

TABLE 6. *Observed rate constants* k_D *(cm³/particles)* M= Ar — Continued

(Camac and Vaughan [23])

T	1000/T	log k
4930.	.2030	−14.180
4930.	.2030	−14.330
4950.	.2020	−14.280
4980.	.2005	−14.110
5020.	.1995	−14.170
5020.	.1995	−14.090
5020.	.1995	−13.970
5140.	.1945	−14.120
5140.	.1945	−13.920
5140.	.1945	−13.850
5180.	.1930	−14.090
5195.	.1925	−14.000
5360.	.1865	−13.720
5390.	.1855	−13.710
5390.	.1855	−13.850
5570.	.1795	−13.660
5890.	.1700	−13.290
5940.	.1685	−13.310
5970.	.1675	−13.330
5970.	.1675	−13.250
6020.	.1660	−13.240
6030.	.1655	−13.280
6130.	.1630	−13.300
6270.	.1595	−13.090
6270.	.1595	−13.090
6290.	.1590	−13.040
6410.	.1560	−13.050
6540.	.1530	−12.960
6840.	.1462	−12.850
7520.	.1330	−12.490
7550.	.1325	−12.440

Data read from graph; O_2 from 0.25 to 1 percent; U.V. absorption.

TABLE 7. *Observed rate constants* k_D *(cm³/particles)* M = Ar.		
(Anderson [1])		
T	$1000/T$	$\log k$
4130.	0.2421	− 15.660
4250.	.2353	− 15.420
4300.	.2326	− 15.290
4300.	.2326	− 15.240
4450.	.2247	− 15.000
4560.	.2193	− 14.740
4590.	.2179	− 14.820
4600.	.2174	− 15.060
4650.	.2151	− 14.800
4650.	.2151	− 14.640
4650.	.2151	− 14.550
4670.	.2141	− 14.770
4750.	.2105	− 14.890
4810.	.2079	− 14.700
4850.	.2062	− 14.700
5010.	.1996	− 14.440
5090.	.1965	− 14.950
5090.	.1965	− 14.520
5090.	.1965	− 14.270
5150.	.1942	− 14.180
5320.	.1880	− 14.010
5340.	.1873	− 14.280
5340.	.1873	− 14.170
5440.	.1838	− 14.070
5440.	.1838	− 13.890
5750.	.1739	− 13.920
5750.	.1739	− 13.820
5950.	.1681	− 13.680
5950.	.1681	− 13.520
6050.	.1653	− 13.510
6100.	.1639	− 13.520
6200.	.1613	− 13.440

Data read from graph; O_2 from 2.8 to 8.3 percent; U.V. absorption.

TABLE 8. *Observed rate constants* k_D *(cm³/particles)* M = Ar (9/1 Ar/O₂) k *based on equivalent* Ar		
(Schexnayder and Evans [108])		
T	$1000/T$	$\log k$
5000.	0.200	[a] − 13.940
5095.	.196	− 13.740
5316.	.188	− 13.860
5500.	.182	[a] − 13.470
5603.	.178	− 13.390
5710.	.175	− 13.470
5960.	.168	− 13.080
6000.	.167	[a] − 13.560
6364.	.157	− 12.890
6629.	.151	− 12.880
7000.	.143	[a] − 12.760
7081.	.141	− 12.620
7762.	.129	− 12.350
7935.	.126	− 12.500
8000.	.125	[a] − 12.540
8540.	.117	− 12.340
8760.	.114	− 12.530
9000.	.111	[a] − 12.420
9188.	.109	− 12.410
9426.	.106	− 12.250
9428.	.106	− 12.110
10204.	.098	− 12.350

[a] Calculated from data by "method of isothermal line," which is an alternate method of evaluating rate constants from experimental data.

TABLE 9. *Observed rate constants* k_D $(cm^3/particle-s)$ $M = O_2$

(Schexnayder and Evans [108])

T	$1000/T$	$\log k$
3500.	0.286	[a] −14.170
3805.	.263	−14.050
4000.	.250	[a] −13.720
4238.	.236	−13.730
4412.	.227	−13.380
4500.	.222	[a] −13.440
4745.	.211	−13.270
4749.	.211	−13.260
5000.	.200	[a] −13.240
5500.	.182	[a] −13.030
5542.	.180	−12.760
5985.	.167	−12.580
6000.	.167	[a] −12.850
6553.	.153	−12.290
7000.	.143	[a] −12.460
7150.	.140	−11.920
7162.	.140	−12.230
7387.	.135	−12.060
7885.	.127	−11.670
8122.	.123	−11.920
8988.	.111	−11.680

[a] Calculated from data by "method of isothermal line," which is an alternate method of evaluating rate constants from experimental data.

TABLE 10. k_D *at extremes of fitted Arrhenius function* M *is* O_2

T	$1000/T$	$\log k_D$	References
3000	0.333	−16.03	Matthews [88].
5000	.200	−13.17	
3500	.286	−15.20	Rink, Knight, and
6000	.167	−12.47	Duff [103].
2800	.343	−16.93	Byron [22].[a]
5000	.200	−13.22	
2600	.385	−16.95	Generalov and
7000	.143	−11.71	Losev [43a].[b]

Data presented only as function, neither as graphs nor tables.

[a] Rates observed, but reported in a form such that rate constants cannot be recalculated. The results above are from a recalculation by Wray [125].

[b] Although this article contains data points, presented graphically, it became available to us too late to be included in the detailed study. Only the end points are included here.

TABLE 11. *Least squares parameters for the dissociation of oxygen in presence of excess argon*

References	No. of points	$T/1000$	Least-squares parameters E (kcal)	m	E' (kcal)
Wray [125]	54	5.1 − 17	114 ± 3[a]	−2.2	150 ± 18[a]
Anderson [1]	32	4.1 − 6.2	116 ± 11	3.6	80 ± 209
Camac and Vaughn [23]	46	3.5 − 7.6	106 ± 3	0.8	98 ± 27
Schexnayder and Evans [108]	22	5.0 − 10	78 ± 10	−10	220 ± 98
All data	154	3.5 − 17	105 ± 3	−0.2	108 ± 16
All except Wray	100	3.5 − 10	105 ± 5	−2.4	131 ± 35
All except Anderson	122	3.5 − 17	100 ± 3	−0.1	101 ± 13
All except C and V	108	4.1 − 17	111 ± 4	−1.7	136 ± 21
All except S and E	132	3.5 − 17	106 ± 3	0.3	102 ± 15

[a] Twice the standard deviation.

$$O_2 + M \xrightarrow{k_D} O + O + M$$
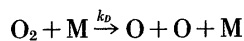
$$k = A \exp (-E/RT)$$
$$k = BT^m \exp (-E'/RT).$$

TABLE 12. *Observed data, recombination of oxygen atoms*

T	$1000/T$	M	$\log k$	$\log T$	T	$1000/T$	M	$\log k$	$\log T$
Wray [125]					Morgan and Schiff [90] — Continued				
1350	0.7407	Ar	-34.08	3.131			CO_2	-32.09	
1900	.5263		-34.22	3.279				-32.07	
2010	.4975		-34.31	3.303				-32.05	
2050	.4878		-34.16	3.312				-32.17	
2100	.4762		-34.09	3.323				-32.10	
2200	.4545		-34.18	3.343			SF_6	-32.07	
2250	.4444		-34.23	3.352				-32.10	
2450	.4082		-34.04	3.389				-32.10	
2450	.4082		-34.22	3.389				-32.17	
2700	.3704		-34.09	3.432	Kaufman and Kelso [69]				
2800	.3571		-34.12	3.447					
2800	.3571		-34.19	3.447	300	3.333	O_2	-32.55	2.478
2800	.3571		-34.25	3.447					
2800	.3571		-34.28	3.447	Golden and Myerson [48]				
2950	.3390		-34.20	3.470					
Reeves, Mannella, and Harteck [101]					460	2.173	O_2	-32.6	2.663
300	3.333	Ar	[a]-33.1	2.478	Wilson [123]				
Morgan and Schiff [90]					2700	0.3704	O_2	-32.60	3.432
293	3.412	Ar	-33.28	2.467	Kiefer and Lutz [71]				
293	3.413		-33.16	2.467					
293	3.413	N_2	-32.55		1486	0.6729	O_2[b]	-32.61	3.172
294	3.401		-32.55		1525	.6557		-32.89	3.183
294	3.401		-32.52		1545	.6472		-32.41	3.189
293	3.413		-32.55		1784	.5605		-32.56	3.252
293	3.413		-32.54		1843	.5426		-32.67	3.266
293	3.413		-32.57		2321	.4308		-33.00	3.366
294	3.401		-32.55		2511	.3982		-32.92	3.400
293	3.413	He	-33.06		2822	.3544		-32.94	3.450
			-33.26		1799	.5559	O_2[c]	-32.70	3.255
			-33.04		1919	.5211		-32.67	3.283
			-33.13		2107	.4746		-32.56	3.324
		N_2O	-32.42		2115	.4728		-32.73	3.326
			-32.46		2251	.4442		-32.74	3.352
			-32.45		2255	.4435		-32.67	3.353
			-32.47		2571	.3890		-32.65	3.410

[a] As recalculated (for surface reactions) by Morgan and Schiff.
[b] $O_2/Ar = 50/50$, but corrected to equivalent O_2.
[c] $O_2/Kr = 41/59$, but corrected to equivalent O_2.

TABLE 13. *Least-squares parameters for recombination of oxygen atoms*

References	No. of points	T	M	Least-squares parameters	
				E kcal	n
Kiefer and Lutz [71]....................	8	$1486-2822$	O_2 and Ar	-5.4	-1.4
	7	$1799-2571$	O_2 and Kr	0.52	0.12
	15	$1486-2822$	O_2	-3.6	-1.0
Wray [125].............................	15	$1350-2950$	Ar	-0.79	-0.17
All O_2 data [a]........................	18	$300-2822$	O_2	-0.30	-0.24
All Ar data [b].........................	18	$293-2950$	O_2	-1.54	-1.06

$k = A \exp(-E/RT)$ or $k = CT^n$.

[a] Refs [71, 69, 48, 123] (compare table 12).

[b] Refs [125, 90, 101] (compare table 12).

TABLE 14. *Relative efficiencies of various foreign gases for dissociation and recombination of oxygen*

$$\left(O_2 + M \overset{D}{\underset{R}{\rightleftarrows}} O + O + M\right)$$
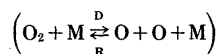
References	k	T	M/M'	k/k'
Camac and Vaughn [23]..................	k_D	$6000-7000$	Ar/O_2	$1/3$
		$5000-7500$	Ar/O	$1/25$
Schexnayder and Evans [108]...........	k_D	$5000-9000$	Ar/O_2	$1/9$
Wray [125]............................	k_D	5000	Ar/O_2	$1/18$
			Ar/O	$1/50$
Rink [102]............................	k_D	$3500-5000$	Ar/Kr	$1/2$
			Ar/Xe	$1/6$
Rink, Knight, and Duff [103].............	k_D	3500	O_2/O	$1/3$
			O_2/Xe	$3.4/1$
Morgan and Schiff [90]..................	k_R	293	Ar/N_2	$\leqslant 0.3$
			He/N_2	0.3
			N_2O/N_2	1.4
			CO_2/N_2	3.0
			SF_6/N_2	3.0
Morgan and Schiff [90] plus Kaufman and Kelso [69].	k_R	293	O_2/N_2	$1/1$

$$\log k_D(\text{Ar}) = -5.37 - \log T - 25.95 \ (1000/T)$$
$$\log k_D(\text{O}_2) = -4.34 - \log T - 25.95 \ (1000/T)$$
$$k_D(\text{Ar})/k_D(\text{O}_2) = 1/10.8$$
$$\log K = 25.08 - 25.8745 \ (1000/T)$$
$$\log k_R(\text{Ar}) = -30.45 - \log T - 0.0745 \ (1000/T)$$
$$\log k_R(\text{O}_2) = -29.42 - \log T - 0.0745 \ (1000/T)$$
$$k_D(\text{O}_2) = 4.57 \times 10^{-5} T^{-1} \exp(-118.7/RT) \ \text{cm}^3/ \text{particle-s}$$
$$k_R(\text{O}_2) = 3.80 \times 10^{-30} T^{-1} \exp(-0.34/RT) \ \text{cm}^6/ \text{particle}^2\text{-s}$$
$$k_R(\text{Ar})/k_R(\text{O}_2) = 1/10.8$$

These relations apply 300–15,000 for Ar as M
1000–8000 for O_2 as M.

3. Decomposition of Ozone

3.1. Mechanisms

a. Other Reviews

An early effort to make a quantitative study of the thermal decomposition of ozone was carried out by Jahn [56] in 1906. Between then and about 1930, several studies were made. In general, the authors encountered trends they could not explain and apparently erratic results, and they disagreed with one another. This situation was reviewed by Wulf and Tolman [128] in 1927 and by H. J. Schumacher [112] in 1930. The troubles were ascribed to impurities, and a series of investigations under Schumacher [113] made a major effort to eliminate impurities. The culmination of this effort was a study by Glissman and Schumacher [47]. The results had good precision, but there still were unexplained trends in the nonconstant second-order rate "constants". The real problem was that the investigators in the 1930's did not understand the nature of unimolecular reactions at the low-pressure limit. Here was a case where the experimentalist was unable to explain his data until the theory of the process was clarified.

The existence and nature of the low-pressure limit of unimolecular reactions [89] was established in the early 1950's, and the mechanism of the ozone decomposition was established by Benson and Axworthy [11] in 1957, largely by reinterpreting the data of Glissman and Schumacher. A detailed review of all the older data is to be found in Axworthy's Ph. D. thesis [3]. Another review covering data through 1959 is given by Campbell and Nudelman [24]. These authors reported that the only quantitative data in the literature before 1959 was that of Glissman and Schumacher. Between 1959 and 1967, several careful quantitative studies have made (see tables of data in this review), both on the direct decomposition of ozone and on related studies of oxygen atoms and molecules. In the literature a number of different mechanisms have been proposed and used. The so-called "Jahn mechanism," "unimolecular mechanism," and "bimolecular mechanism" are all special cases of the single mechanism as assembled by Benson and Axworthy [11]. The differential and integrated rate equations for each of the special "mechanisms" will be summarized in the following sections.

b. Jahn Mechanism

The overall reaction is

$$2O_3 = 3O_2. \tag{3-1}$$

The general definition of "the rate of reaction" then is

$$R = -\frac{1}{2}\frac{d[O_3]}{dt} = \frac{1}{3}\frac{d[O_2]}{dt}. \tag{3-2}$$

Jahn proposed that ozone is in thermal equilibrium with atomic and molecular oxygen, and the atomic oxygen irreversibly attacks ozone as a rate determining step:

$$O_3 \rightleftharpoons O_2 + O, \qquad K_1 = k_1/k_2 \tag{3-3}$$

$$O_3 + O \rightarrow O_2 + O_2, \ k_3. \tag{3-4}$$
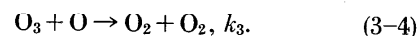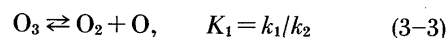
The rate expression from the mechanism is

$$-\frac{d[O_3]}{dt} = 2k_3[O_3][O]. \tag{3-5}$$

The concentration of atomic oxygen is given by the equilibrium constant,

$$K_1 = [O][O_2]/[O_3].\qquad (3\text{-}6)$$

The defined rate in terms of Jahn's mechanism is

$$R = -\frac{1}{2}\frac{d[O_3]}{dt} = K_1 k_3 \frac{[O_3]^2}{[O_2]} = k_J \frac{[O_3]^2}{[O_2]},\qquad (3\text{-}7)$$

where Jahn's constant, k_J, is the product of the equilibrium constant and rate constant,

$$k_J = K_1 k_3 = k_1 k_3/k_2.\qquad (3\text{-}8)$$

Stoichiometry provides a relation between ozone and oxygen, at any stage of reaction:

$$[O_2] = [O_2]_0 + \frac{3}{2}\left([O_3]_0 - [O_3]\right) = [O_2]_\infty - \frac{3}{2}[O_3],\qquad (3\text{-}9)$$

where $[O_2]_0$ is oxygen at zero time, $[O_2]_\infty$ is oxygen at infinite time,

$$[O_2]_\infty = [O_2]_0 + \frac{3}{2}[O_3]_0,\qquad (3\text{-}10)$$

and $[O_3]_0$ is initial ozone. With the stoichiometric relation, the differential rate expression can be expressed in terms of one variable, $[O_3]$:

$$-\frac{d[O_3]}{dt} = 2k_J \frac{[O_3]^2}{[O_2]_\infty - \frac{3}{2}[O_3]}.\qquad (3\text{-}11)$$

This equation is readily integrated to give

$$\frac{[O_2]_\infty}{[O_3]_0}\left(\frac{[O_3]_0}{[O_3]} - 1\right) - \frac{3}{2}\ln\frac{[O_3]_0}{[O_3]} = 2k_J t.\qquad (3\text{-}12)$$

It is convenient to define the ratio of final oxygen to initial ozone as A and the ratio of initial ozone to ozone at any time as x:

$$A = [O_2]_\infty/[O_3]_0,\qquad x = [O_3]_0/[O_3].\qquad (3\text{-}13)$$

With these definitions the integrated equation for Jahn's mechanism is

$$A(x-1) - \frac{3}{2}\ln x = 2\,k_J t.\qquad (3\text{-}14)$$

If one starts with dilute ozone (a few percent or less) in oxygen, data are described fairly well by this rate expression.

c. Bimolecular Mechanism

Some authors have interpreted their data in terms of a bimolecular mechanism,

$$O_3 + O_3 \rightarrow 3O_2 \qquad k_B.\qquad (3\text{-}15)$$
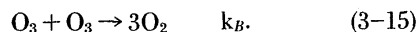
For this mechanism the differential and integral equations are the simple, standard forms:

$$-\frac{d[O_3]}{dt} = 2k_B[O_3]^2,\qquad \frac{1}{[O_3]} - \frac{1}{[O_3]_0} = 2k_B t.\qquad (3\text{-}16)$$

In terms of the quantity, x, defined above, the integrated equation is

$$[O_3]_0(x-1) = 2k_B t.\qquad (3\text{-}17)$$

If one starts with pure ozone, the expression fits the data moderately well at early times, but the calculated "constant" increases throughout the course of a given run. This drift, unexplained in the 1930's, was one of the major problems faced by workers on this reaction at that time, and it is a feature of relative efficiency of O_3 and $3/2\ O_2$ as an energy-transfer catalyst in the unimolecular decomposition of ozone.

d. Unimolecular Mechanism

The unimolecular mechanism takes the rate-determining step to be the elementary unimolecular decomposition of ozone at its low-pressure limit, followed by reaction 3 as a fast following reaction:

$$\begin{aligned} O_3 + M &\rightarrow O_2 + M, & k_1 \text{ (slow)}, \\ O_3 + O &\rightarrow O_2 + O_2, & k_3 \text{ (fast)}. \end{aligned}\qquad (3\text{-}18)$$
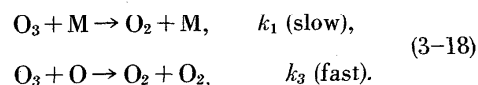
The rate in terms of ozone is

$$-\frac{d[O_3]}{dt} = 2k_1[O_3][M].$$

Actually, M is not one thing, but at least two (O_3 and O_2), and perhaps more if foreign gases, X, are added. The efficiency with which oxygen or a foreign gas, X, excites the vibrational states of ozone is different from that for ozone itself. Thus the rate expression should be written:

$$-\frac{1}{2}\frac{d[O_3]}{dt} = k_1[O_3][O_3] + k_{12}[O_3][O_2] + k_{1X}[O_3][X]$$

$$= k_1[O_3]\left\{[O_3] + \frac{k_{12}}{k_1}[O_2] + \frac{k_{1X}}{k_1}[X]\right\}$$

$$= k_1[O_3]\{[O_3] + \alpha[O_2] + \beta[X]\}\qquad (3\text{-}19)$$

where $\alpha = k_{12}/k_1$ is the relative efficiency of oxygen and ozone, and $\beta = k_{1X}/k_1$ is the relative efficiency of the foreign gas, X, and ozone. It is convenient to define the "equivalent concentration of ozone" as [M],

$$[M] = [O_3] + \alpha[O_2] + \beta[X].\qquad (3\text{-}20)$$

However, since 2 ozone molecules are not equivalent to 3 oxygen molecules, the value of [M] changes

throughout the course of reaction. The differential equation in one variable, $[O_3]$, including the stoichiometric relation and the definition of $[M]$, is

$$-\frac{d[O_3]}{dt} = 2k_1[O_3][M]$$

$$= 2k_1\left(1 - \frac{3}{2}\alpha\right)[O_3]^2 + 2k_1(\alpha[O_2]_\infty + \beta[X])[O_3].$$

(3–21)

The integrated equation is

$$\frac{1}{[M]_\infty} \ln\left\{\frac{[O_3]_0}{[O_3]}\frac{[M]}{[M]_0}\right\} = 2k_1 t,$$

(3–22)

where $[M]$ has been defined above, and the limits on $[M]$ are

$$[M]_0 = [O_3]_0 + \alpha[O_2]_0 + \beta[X]$$

$$[M]_\infty = \alpha[O_2]_\infty + \beta[X].$$

(3–23)

If a new variable y is defined as the ratio of initial M to M at any time,

$$y = [M]_0/[M],$$

(3–24)

the integrated equation takes the simple form of

$$\ln x/y = 2[M]_\infty k_1 t.$$

(3–25)

This rate expression is applicable at moderately high temperatures, perhaps 750–1100 K. At still higher temperatures, above 1500 K, reaction 1 is so much faster than reaction 3 that reaction 3 may be neglected entirely. In this case the above rate expressions still apply if the factor of two in front of k, is dropped. At low temperatures reaction 3 gives a factor of two increase over reaction 1 alone, at high temperatures reaction 3 does not occur to a significant degree, and at intermediate temperatures the rate of reaction 3 may be directly and separately observed [62].

e. Benson and Axworthy Mechanism [11]

The mechanism proposed by Jahn was applied in most of the early work on ozone decomposition in excess oxygen. A complex mechanism was proposed by Glissman and Schumacher for the decomposition of concentrated ozone [47]. This included Jahn's two reactions (3–3 and 3–4). With the passage of time the requirement of equilibrium in reaction (3–3) was removed and a steady-state condition applied to the concentration of oxygen atoms in all the mechanisms [47, 74a]. In 1957 Benson and Axworthy [11] showed that the steady-state adaptation of Jahn's mechanism could explain the results obtained both for concentrated and dilute ozone. Their formulation considers reaction 1 an

elementary unimolecular reaction at the low-pressure limit. The scheme is:

$$O_3 + M \rightarrow O_2 + O + M \qquad k_1,$$

$$O_2 + O + M \rightarrow O_3 + M \qquad k_2, \qquad (3\text{–}26)$$

$$O_3 + O \rightarrow O_2 + O_2 \qquad k_3.$$
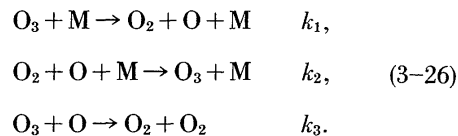
The steady-state condition applied to oxygen atoms gives

$$[O] = \frac{k_1[O_3][M]}{k_2[O_2][M] + k_3[O_3]}.$$

(3–27)

As in other mechanisms, stoichiometry gives

$$[O_2] = [O_2]_\infty - \frac{3}{2}[O_3],$$

and the definition of M is

$$[M] = [O_3] + \alpha[O_2] + \beta[X]$$

$$= \left(1 - \frac{3}{2}\alpha\right)[O_3] + \alpha[O_2]_\infty + \beta[X].$$

In terms of the defined rate R the differential equation is

$$R = -\frac{1}{2}\frac{d[O_3]}{dt} = \frac{k_1k_3[O_3]^2[M]}{k_2[M][O_2] + k_3[O_3]}.$$

(3–28)

Benson and Axworthy interpreted experimental data directly in terms of the differential equation, by constructing the functions $[O_3][M]/R$ and $[O_2][M]/[O_3]$:

$$\frac{[O_3][M]}{R} = \frac{1}{k_1} + \frac{k_2[M][O_2]}{k_1k_3[O_3]} = \frac{1}{k_1} + \frac{1}{k_J}\frac{[M][O_2]}{[O_3]}.$$

(3–29)

Between successive experimental points (actually a graphical smoothing procedure was used) the instantaneous rate, R, is computed, and a plot of experimental $[O_3][M]/R$ against experimental $[M][O_2]/[O_3]$ should be a straight line of intercept k_1^{-1} and of slope k_J^{-1}. To carry out this procedure one must first know the relative efficiencies, α and β, especially α. Benson and Axworthy [11] deduced these constants from Glissman and Schumacher's [47] experimental data and also from some data obtained by Axworthy [3] but never published. Also other experimental studies (to be discussed later) give these relative efficiencies. At this point we tabulate the relative efficiencies, α and β, for various gases as found by various workers and as used and recommended in this review, table 17. Benson and Axworthy used Glissman and Schumacher's data both to evaluate relative efficiency of M gases and as a test of mechanism. This procedure adds up to fitting a large number of param-

23

eters to the data; the confirmation of Benson and Axworthy's values by completely independent experimental methods [26, 70, 62] and systems gives strong support to this mechanism for the homogeneous thermal decomposition of ozone in the temperature range 300 to at least 1000 K, since the high temperature mechanism given above is a special case of the Benson and Axworthy mechanism.

Benson and Axworthy interpreted Glissman and Schumacher's data by the differential equation

derived from their mechanism. Their published article did not list the individual values of k_1 and k_J but only the parameters of the Arrhenius equation fitted to these quantities. From Axworthy's thesis we recomputed k_1 and k_J by this method, and the values for individual runs are listed in table 18 for k_1 and table 22 for k_J.

The differential equation from Benson and Axworthy's mechanism can be expressed in terms of one variable [O$_3$] and integrated. The differential equation is

$$-\frac{d[O_3]}{dt} = \frac{2k_1k_3[O_3]^2\{(1-3/2\alpha)[O_3]+\alpha[O_2]_\infty+\beta[X]\}}{k_2\left([O_2]_\infty-\frac{3}{2}[O_3]\right)\left\{\left(1-\frac{3}{2}\alpha\right)[O_3]+\alpha[O_2]_\infty+\beta[X]\right\}+k_3[O_3]}. \tag{3-30}$$

The integrated equation is

$$\frac{\ln\frac{[O_3]_0[M]}{[O_3][M]_0}}{2[M]_\infty t}=k_1-\frac{k_2}{k_3}\frac{\frac{[O_2]_\infty}{[O_3]_0}\left(\frac{[O_3]_0}{[O_3]}-1\right)-\frac{3}{2}\ln\frac{[O_3]_0}{[O_3]}}{2t}. \tag{3-31}$$

In terms of A, x, and y defined above, the integrated equation is

$$\frac{\ln x/y}{2[M]_\infty t}=k_1-\frac{k_2}{k_3}\frac{A(x-1)-\frac{3}{2}\ln x}{2t}. \tag{3-32}$$

The observable function on the left-hand side may be defined as f_1, and the observable function on the right-hand side may be defined as f_J, since these functions give k_1 and k_J if one has respectively the unimolecular mechanism and Jahn's mechanism. The integrated equation may be written in several different forms for different purposes. For a run with a series of observed concentrations of ozone as a function of time, a plot of f_1 against f_J gives k_1 as intercept and k_2/k_3 as slope:

$$f_1=k_1-\frac{k_2}{k_3}f_J. \tag{3-33}$$

The integrated equation may be written as

$$\frac{f_1}{k_1}+\frac{f_J}{k_J}=1. \tag{3-34}$$

Once we have an estimate of k_1 and k_J, as from Benson and Axworthy's study [11], we can test a given set of experimental conditions to see if it is clearly in the unimolecular mechanism $(f_J/k_J\ll1)$, clearly in Jahn's region $(f_1/k_1\ll1)$, or in the intermediate region where the full Benson-Axworthy mechanism must be used. One of the confusions in the older literature is that usually both mechanisms operated at once, but with different weights over the course of a run. Starting with pure ozone, one is fully within the unimolecular region at first, but as the reaction

approaches completion the Jahn mechanism makes an important contribution to the rate. Starting with ozonized oxygen, typically about 3 percent ozone, one starts the run with both unimolecular mechanism and Jahn mechanism contributing to the rate; but as the reaction progresses, the unimolecular mechanism (with its sensitivity to M gases) fades to zero, and the reaction fully follows the Jahn mechanism.

If an experimenter reported initial conditions and the reactant concentration at only one time, it would appear that we have two unknowns, k_1 and k_J, and only one datum, so that the data are useless for any quantitative reinterpretation. However, if conditions are close to the Jahn region, we can correct for the effect of the unimolecular term by using literature values of k_1 as a correction on k_J:

$$k_J=\frac{f_J}{1-f_1/k_1}, \tag{3-35}$$

where f_J and f_1 are obtained from the experimental data, k_1 is obtained from Benson and Axworthy, and the corrected Jahn constant, k_J, is then found from the experimental data. The data of Garvin [43] and table 3 of Pshezhetskii et al. [99] were corrected in this way. Similarly, data close to the unimolecular limit may be corrected for the Jahn term by the relation

$$k_1=\frac{f_1}{1-f_J/k_J}. \tag{3-36}$$

Some of Garvin's data [43] and table 1 of Pshezhetskii et al. [99] were corrected in this way.

A considerable body of the older literature [3] contains data with such experimental scatter and uncertainty that the data cannot be used to obtain
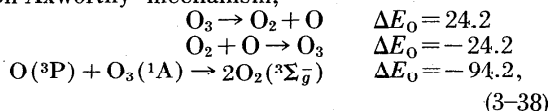
values of rate constants. However, we can test to see if the observations generally fall within the range of the present interpretation and assignment of constants or if the observations contain some quite different trends or some real unsuspected feature. A consistency test between current interpretation and older data is to write the integrated equation as

$$t = \frac{\ln x/y}{2[\mathrm{M}]_\infty k_1} + \frac{A(x-1) - \frac{3}{2}\ln x}{2k_J}. \qquad (3\text{-}37)$$

The experimental points are plotted as $x = [\mathrm{O}_3]_0/[\mathrm{O}_3]$ against time t. The currently assigned values of the constants k_1 and k_J are used in the above equation to solve for time t as a function of x.

f. Energy Chains

The energetics of the three steps in the Benson-Axworthy mechanism,

$$\begin{array}{ll} \mathrm{O}_3 \rightarrow \mathrm{O}_2 + \mathrm{O} & \Delta E_0 = 24.2 \\ \mathrm{O}_2 + \mathrm{O} \rightarrow \mathrm{O}_3 & \Delta E_0 = -24.2 \\ \mathrm{O}(^3\mathrm{P}) + \mathrm{O}_3(^1\mathrm{A}) \rightarrow 2\mathrm{O}_2(^3\Sigma_g^-) & \Delta E_0 = -94.2, \end{array}$$

$$(3\text{-}38)$$

have led many investigators to assign a large part of ΔE_3 as vibrational energy to one or both products, O_2^*. This excited vibrational species is assumed to decompose an ozone molecule:

$$\mathrm{O}_2^* + \mathrm{O}_3 \rightarrow \mathrm{O}_2 + \mathrm{O}_2 + \mathrm{O}, \qquad k_E. \qquad (3\text{-}39)$$
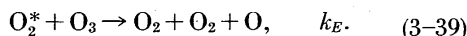
The combination of reactions E and 3 gives a chain reaction, where vibrational excitation of the product is one carrier of the chain and an oxygen atom is the other chain carrier. There has been direct spectroscopic observation of oxygen molecules in vibration levels up to $v = 17$ in both flash photolysis of ozone [78] and in its thermal decomposition [62] at moderately high temperatures, 700–900 K. It has been demonstrated by direct experiment that highly vibrationally excited nitrogen N_2^* can decompose ozone [97], and as discussed in section 1 O_2^* from $\mathrm{O}(^1\mathrm{D}) + \mathrm{O}_3$ decomposes ozone to give $\mathrm{O}(^1\mathrm{D})$. Thus it is extremely plausible that reaction E does occur. However, there are experimental studies that indicate that the "chain length" may be very short, less than 1.05 at room temperature [26], and less than 1.2 at 800 K [22].

These experimental studies and the related arguments are as follows: In the photolysis of ozone by red light (see below), reaction 2 and 3 occur, and any contribution by step E would give a quantum yield greater than two; the quantum yield extrapolated to pure ozone was precisely two with uncertainty less than 5 percent; thus the strong upper limit of 1.05 for "chain length" at room temperature. In the shock-tube study of decom-

posing ozone, Jones and Davidson [62] observed ozone disappearance with a time resolution of about 5 μs, such that at early times all reaction was from reaction 1 and at later times reaction 3 built up to give a doubling of the overall rate. If the energy chain played a predominant role, the rate when reaction 3 was fully developed would be much more than twice as great as the rate where reaction 3 was totally inoperable. The errors and uncertainties of the shock-tube experiments set a 20-percent limit on any conclusion that can be made, and thus the upper length on the energy chain at 800 K is assigned to be 1.2. Energy chains do not seem to be important in the overall kinetics of the thermal decomposition of ozone. It must be concluded that ozone deactivates an excited oxygen molecule (with $v < 17$) more rapidly than it is dissociated by it:

$$\begin{array}{ll} \mathrm{O}_2^*(v > 6) + \mathrm{O}_3 \rightarrow 2\mathrm{O}_2 + \mathrm{O}(^3\mathrm{P}), & \text{slow} \\ \mathrm{O}_2^*(v > 17) + \mathrm{O}_3 \rightarrow 2\mathrm{O}_2 + \mathrm{O}(^1\mathrm{D}). & \text{fast} \end{array}$$
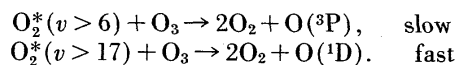
g. Photolysis in Red Light [26]

With radiation around 6000 Å, ozone weakly absorbs light to give the forbidden transition,

$$\mathrm{O}_3 + h\nu \rightarrow \mathrm{O}_2(^3\Sigma_g^-) + \mathrm{O}(^3\mathrm{P}).$$
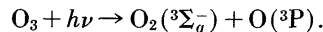
Let I represent the rate of light absorption in units of photons cm^{-3}s^{-1}. This reaction is followed by steps 2 and 3:

$$\begin{array}{ll} \mathrm{O}_2 + \mathrm{O} + \mathrm{M} \rightarrow \mathrm{O}_3 + \mathrm{M}, & k_2, \\ \mathrm{O}_3 + \mathrm{O} \rightarrow \mathrm{O}_2 + \mathrm{O}_2, & k_3. \end{array}$$
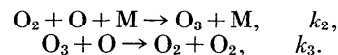
With the steady-state assumption for intermediate oxygen atoms, one obtains the rate expression for ozone disappearance,

$$-\frac{d[\mathrm{O}_3]}{dt} = \frac{2Ik_3[\mathrm{O}_3]}{k_2[\mathrm{O}_2][\mathrm{M}] + k_3[\mathrm{O}_3]}. \qquad (3\text{-}40)$$

The definition of quantum yield, Φ, is the number of molecules that react per photon absorbed:

$$\Phi = -\frac{d[\mathrm{O}_3]/dt}{I}. \qquad (3\text{-}41)$$

From the mechanism, the quantum yield is

$$\Phi = \frac{2k_3[\mathrm{O}_3]}{k_2[\mathrm{O}_2][\mathrm{M}] + k_3[\mathrm{O}_3]}. \qquad (3\text{-}42)$$

It is useful to solve this relation in terms of reciprocal quantum yield, with some rearrangement of terms, to give

$$\frac{1}{[\mathrm{O}_2]}\left(\frac{2}{\Phi} - 1\right) = \frac{k_2}{k_3}\frac{[\mathrm{M}]}{[\mathrm{O}_3]}$$

$$= \frac{k_2}{k_3} + \frac{\alpha k_2}{k_3}\frac{[\mathrm{O}_2]}{[\mathrm{O}_3]} + \frac{\beta k_2}{k_3}\frac{[\mathrm{X}]}{[\mathrm{O}_3]}. \qquad (3\text{-}43)$$

By omitting foreign gases, X, this system gives k_2/k_3 as an intercept and $\alpha k_2/k_3$ as the slope of a plot of the observable function $[O_2]^{-1}(2/\Phi-1)$ against the ratio $[O_2][O_3]$. The ratio of slope to intercept gives α the relative efficiency of oxygen to ozone in energy-transfer to ozone. The method gives the best and most direct measure of relative efficiencies of various gases in this role. By flooding ozone with a great excess of foreign gas, X, its relative efficiency, β, can also be found. Values of these relative efficiencies as energy transfer agents are given in table 17, and values of k_2/k_3 directly observed this way are listed in table 25.

3.2. Observed Data

a. Relative Efficiency of Foreign Gases

The relative efficiency of a foreign gas, M, in energy transfer to ozone can be found by relative rate measurements of either reaction 1 or reaction 2:

$$O_3 + O_3 \rightarrow O + O_3 \qquad k_1$$
$$O_3 + X \rightarrow O + X \qquad k_{1x},$$
$$O_2 + O + O_3 \rightarrow O_3 + O_3 \qquad k_2$$
$$O_2 + O + X \rightarrow O_3 + X \qquad k_{2X}. \qquad (3\text{-}44)$$

Since oxygen is the product of reaction, it is present in all runs, and its relative efficiency in either reaction 1 or reaction 2 is defined as

$$\alpha = k_1(O_2)/k_1 = k_2(O_2)/k_2. \qquad (3\text{-}45)$$

The relative efficiency of added gas, X, is defined as

$$\beta = k_{1X}/k_1 = k_{2X}/k_2. \qquad (3\text{-}46)$$

Observed values for relative efficiencies of various gases is given in table 17. Three different authors find this important factor for oxygen to lie between 0.42 and 0.44, and the value 0.44 is adopted here. Unlike the case for oxygen molecules (table 14), the relative efficiencies of X gases in the dissociation of ozone are well and reproducibly characterized. These factors for O_2 and for Ar are probably accurate to 10 percent or better. The ratio, k_{Ar}/k_{N_2}, is essentially the same at 291 K and around 800 K (last entry in table 17), and based on this fact, one assumes the relative efficiency of foreign gases for ozone not to change significantly with temperature. In subsequent tables of k_1 and k_2, the relative efficiencies of table 17 have been used to put all rate constants on the basis of equivalent ozone:

$$[M] = [O_3] + \alpha[O_2] + \beta[X]. \qquad (3\text{-}47)$$

b. Rate Constants for Reaction 1

The observed rate constants for reaction 1, k_{1X}, have been corrected for relative efficiency of foreign gases and entered as log k_1 as a function of

T and $1000/T$ in table 18. All sets of data judged to be free of large systematic errors are included. The temperature range is 343 to 910 K, although no one author covered all of this range. Axworthy [3] made a series of runs with various added gases, such as H_2O and H_2O_2, and with ozone produced in various ways; these data were never published except in the Ph. D. thesis, but they are included in table 18. One run was made at 303 K. In most later interpretations of data, we do not use Axworthy's data, although his values of k_1 agree quite well with those of other authors. The observed values of k_1 including Axworthy's point at 303 K are plotted in figure 5. The various authors are in satisfactory agreement with each other.

The data of each author in table 18 were fitted by the method of least squares to three empirical equations (1–33) to (1–35). In general, the data of any one investigation had so much scatter that the three-parameter equation gave ridiculous results to the least squares treatment. Most interpretation of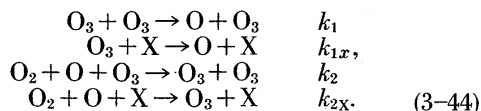 the data is based on the two-parameter Arrhenius equation, and these parameters for each author are reported as log A and E in table 19. The activation energies, E, reported by the various authors, varied between 21.4 and 25.2 kcal/mole—with no apparent trend with temperature (note that this is much better than the results on the dissociation of oxygen, k_D, table 11). All data by all authors were pooled, and the Arrhenius parameters are reported in table 20. Also each author was omitted from the total, and A and E found. The activation energies, omitting given authors, vary between 22.8 and 23.5 kcal. The interpretation of ozone kinetics by Benson and Axworthy was based on the data of Glissman and Schumacher. From table 20 we see that all data excluding Glissman and Schumacher give essentially the same Arrhenius parameters as all data by all authors including Glissman and Schumacher. However, the combined data of all authors with their wide range of temperature give significantly different results from those obtained by Benson and Axworthy from Glissman and Schumacher alone.

The observed rate constants, k_1, are so numerous that it is difficult to get all of the points on one graph. In order to display certain functions more clearly, the rate constants, k_1, are averaged in groups of approximately constant temperature in table 21 and plotted in figure 12.

The good agreement between various authors, figure 5, and the stability of the Arrhenius parameters to omission of any set of data, table 20, indicate that the rate constant function for reaction 1 is very well characterized.

c. Jahn's Rate Constant and the Ratio k_2/k_3

The rate constant, k_J, has been observed over a much more narrow temperature range than k_1. The experimental points as found for various workers are given in table 22 and plotted in figure 6.

26

FIGURE 5. *Observed values of* k_1. $O_3 + M \rightarrow O_2 + O + M$, *where* M *is equivalent ozone. Units are* $cm^3/particle$-s.

☐ Jones and Davidson [62]
■ Garvin [43], data recalculated with integrated equation
△ Pshezhetskii et al. [99]
◇ Zaslowsky et al. [131]
○ Glissman and Schumacher [47], data recalculated by method of Benson and Axworthy [11]
◆ Axworthy's room temperature point [3]
The line is given by:

$$\log k_1 = -8.783 - 4.965 \, (1000/T).$$
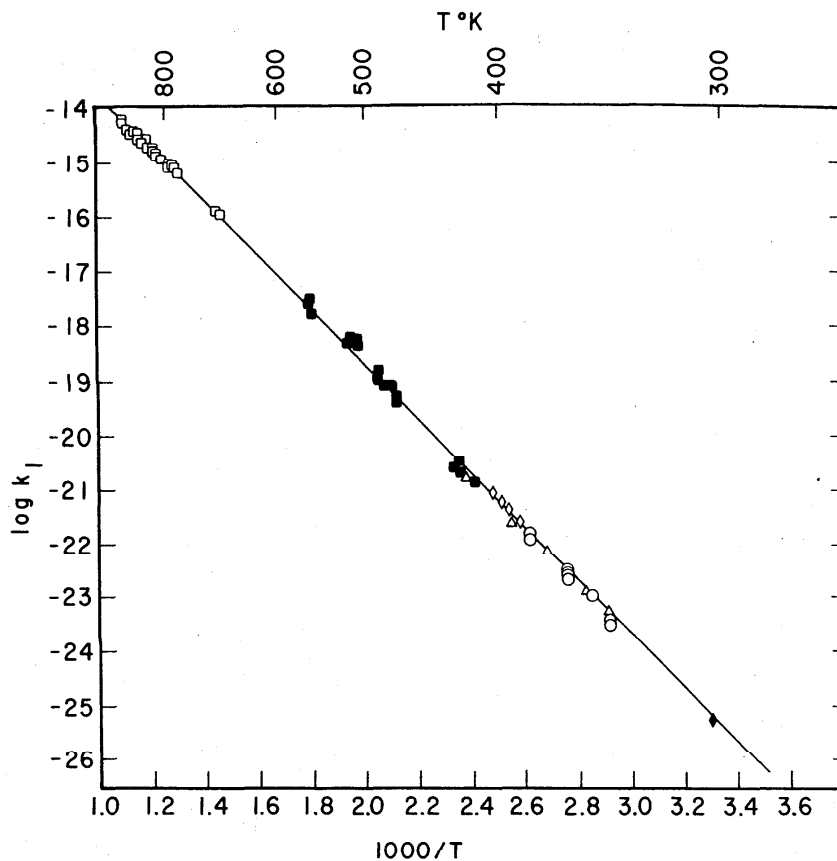
FIGURE 6. *Observed values of Jahn's constant*

$$k_J = K_1 k_3.$$

Units are s^{-1}.

Symbols are the same as in figure 5, except ● is value observed by Jahn [56] in 1906. Line calculated from $\log k_J = 14.855 - 6.471 \, (1000/T)$ (not least-squares fit to the data).
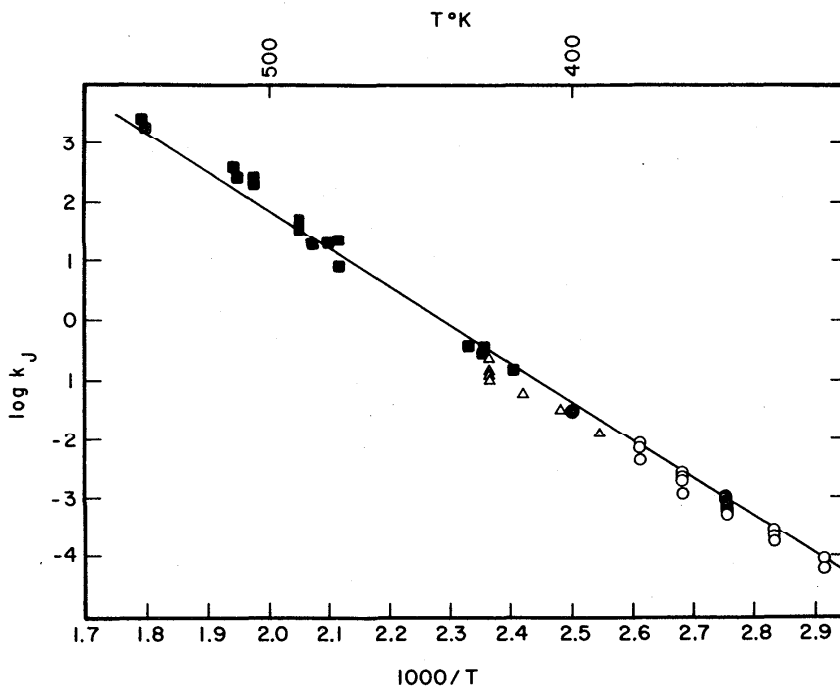
The ratio of rate constants, k_2/k_3, is directly observed in photolysis of ozone by red light, and it is obtained by interpreting detailed sets of data by the integrated equation. In the latter case values of k_2/k_3 and of k_J are obtained from the same data. Observed values of k_2/k_3 are given in table 23 and figure 7.

d. Rate Constants for Reaction 2

Many investigators have attempted to measure the rate of reaction 2 $(O + O_2 + M \rightarrow O_3 + M)$. Oxygen atoms are typically produced by an electrical discharge through oxygen. For many years results were especially irreproducible between different investigators. The side reactions that caused the trouble are discussed in section 1, 1.5c. About 1964 the nature of the difficulty was recognized, and quantitative studies have since been made, in one case over a wide temperature range and in the other case over a wide range of foreign gases, M. These results are listed in tables 24 and 25; and the data are plotted in figure 8 according to $k_2 = C_2 T^n$, and in figure 11 according to the Arrhenius equation. The data still show moderately severe scatter and agreement between different workers is only fairly good. An error of about 50 percent is indicated.

e. Rate Constants for Reaction 3

Only in the shock-tube work of Jones and Davidson [62] was it possible to measure directly the rate of reaction 3 $(O + O_3 \rightarrow 2O_2)$. In other cases one always measures the ratio of reaction 2 to reaction 3 or some other complex quantity. The directly observed rate constants, k_3, are given in table 25. The scatter of the data is such and the range of $1000/T$ is so small that these 11 observations really constitute only one point (log $k_3 = -11.9$ with a range of ± 0.3) at one temperature, about 850 K. At other temperatures we have observed values of k_2/k_3 and observed values of k_2 over the same temperature range. The data in figure 8 were fitted by least squares to the function $k_2 = C_2 T^n$. For an observed value of k_2/k_3 at a particular temperature T, we evaluate k_2 from the least-squares function at that temperature, and k_3 is calculated from k_2 (function)/$(k_2/k_3)_{observed}$. The values of k_3 deduced from kinetic data in this way are listed in table 23. These rate constants plus those directly observed, table 25, are plotted together in figure 9A. The points fall into three groups: Jones and Davidson's shock-tube points at high temperature, Glissman and Schumacher's data around 100 °C from the decomposition of ozone, and Castellano and
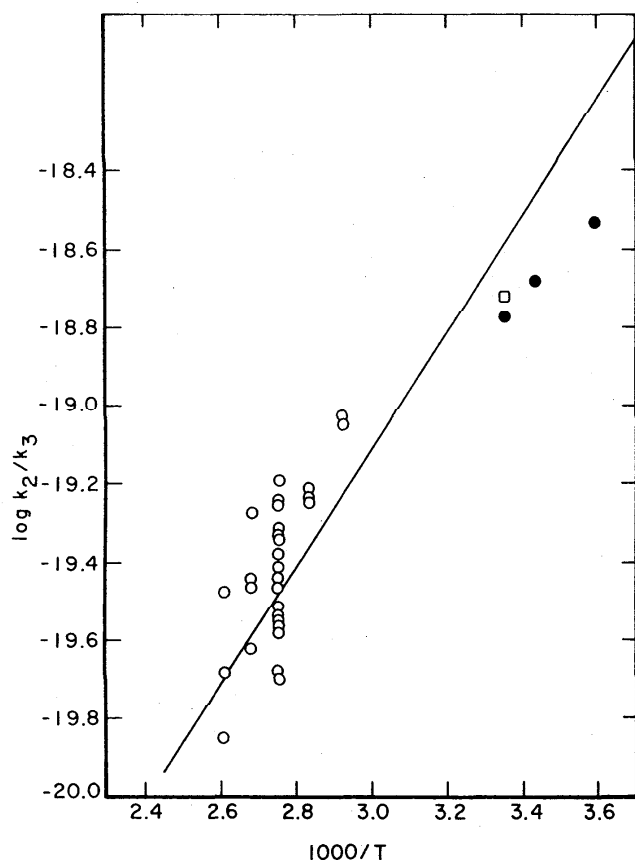
FIGURE 7. *Observed values of* k_2/k_3.

●Castellano and Schumacher [25, 26]
□ Mathias and Schiff [87]
○ Glissman and Schumacher [47]
Line not based on least-squares fit to these data but from the ratio of separately fitted k_2 and k_3.

$$\log k_2/k_3 = -23.638 + 1.506 \ (1000/T).$$

28

FIGURE 8. *Observed values of* k_2 $(cm^6/particle^2\text{-}s)$.

○Experimental points [28]
Least-squares line given by
$\log k_2 = -24.0768 - 3.4683 \log T$.
Data of Kaufman and Kelso [70]
indicated by □ are not included in
least-squares fit to the line.
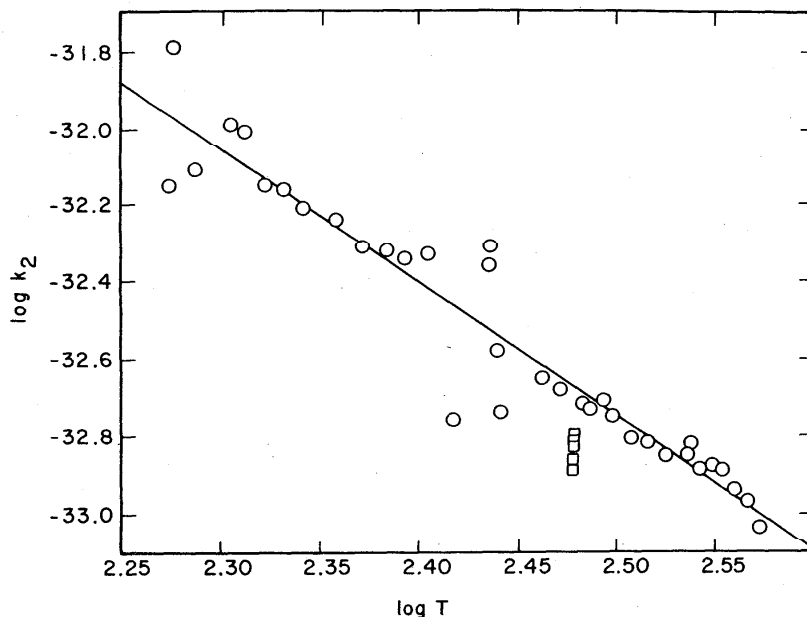
Schumacher's points at room temperature from the photolysis of ozone in red light. It is to be noted that Glissman and Schumacher's data around 373 K show just as much scatter as Jones and Davidson's shock-tube data. We believe that if Castellano and Schumacher had obtained more points, their results too would show a fairly high scatter, since the activation energy indicated by Castellano and Schumacher is far less than that indicated by all three sets of data, covering a wide temperature range. The Arrhenius parameters for k_3, as shown in figure 9A, are given in table 27. The observed value of k_3 and the value of K_3 calculated from the JANAF tables were used to obtain the rate constant, k_4, for the reverse reaction (table 26).

3.3. Interpretation of Observed Data

a. Equilibrium Constants from Kinetic Data

It should be emphasized that all figures from 5 through 9A contain only observed rate constants; these constants were deduced from the experimental data by means of the Benson-Axworthy mechanism. No use has been made of the presumed relation between rate constants and equilibrium constant,

$$K_1 = k_1/k_2$$

$$k_3 = k_J/K_1. \qquad (3\text{-}48)$$

We have refrained from assuming these relationships for two reasons: Some doubt has been expressed about the heat of formation of ozone (it may be in error by as much as 0.4 kcal), and some

doubt has been expressed as to whether the relation is valid for a unimolecular reaction at its low-pressure limit.

The JANAF value for the heat of formation of ozone is based on two calorimetric experiments [50, 63] on the overall reaction,

$$O_3(g) \rightarrow 3/2\, O_2(g).$$
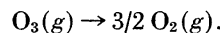
The paper [50] by Guenther, Wassmuth, and Schryver (1932) contains extensive error analysis and detailed description of the equipment; they report data from which one calculates [5]

$$\Delta_f H^\circ_{298} = 33.89 \pm 0.36 \text{ kcal/mole}.$$

A previous paper [63] by Kailan and Jahn (1910), which reports less experimental detail and gives less basis for estimation of error, gives data from which one estimates

$$\Delta_f H^\circ_{298} = 34.3 \pm 0.6 \text{ kcal/mole}.$$

The JANAF tables accept the average of these two values with an overall error limit,

$$\Delta_f H^\circ_{298} = 34.1 \pm 0.4 \text{ kcal/mole}.$$

In this review the JANAF value is used, but we feel that the value, 33.9 of Guenther, Wassmuth, and Schryver is to be preferred.

Let us review the arguments why some people fear that $K_1 = k_1/k_2$ might not be valid in the present case. At total chemical equilibrium between O_2,

---

[5] The estimates of error in the next three expressions were made by the authors of the JANAF tables.

29
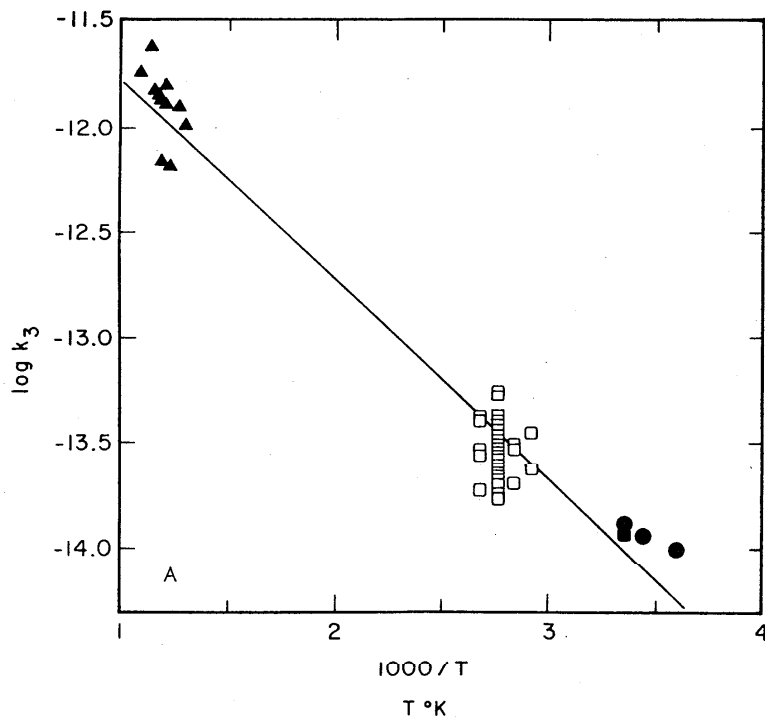
FIGURE 9.   (A) *Observed values of* k_3.

▲ Directly observed by Jones and David-
son [62]. Computed from k_2/k_3.
● Castellano and Schumacher [26]
■ Mathias and Schiff [87]
☐ Glissman and Schumacher [47]
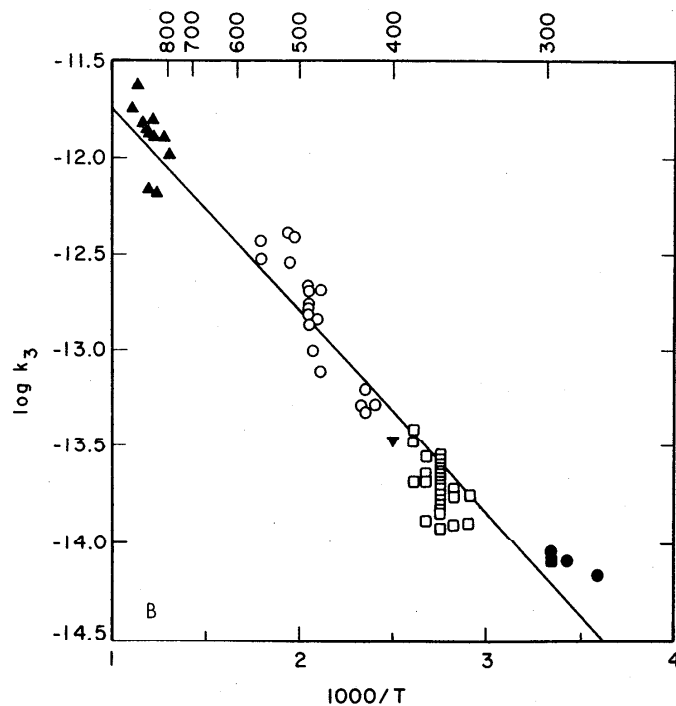
FIGURE 9.   (B) *Observed values of*
k_3 *($cm^3/particle$-s) including ex-
tended values from* k_J/K_1.

▲ Directly observed by Jones and Davidson
[62]. Computed from k_2/k_3, and k_2.
● Castellano and Schumacher [26]
■ Mathias and Schiff [87]
Computed from k_J/K_1.
☐ Glissman and Schumacher [47]
○ Garvin [43]
▼ Jahn [56]
Line calculated from least-squares fit to
the data. $\log k_3 = -10.697 - 1.047\ (1000/T)$.

O, and O_3, all states of reactants, products, and
intermediate collision complexes have the equi-
librium distribution characterized by the tempera-
ture T. The rate constant, k_1, for example, is an
average of molecular rate constants (elementary
chemical physical rate constants) over the definite

equilibrium distribution function. If there are no
products of reaction, the forward reaction will
proceed under conditions where reactants and
products are not at equilibrium. If the reactants
have a distribution over states essentially the same
as at equilibrium, then any average taken over this

30

distribution function should be essentially the same as an average taken at true chemical equilibrium. In particular the average of the molecular rate constants that give k_1 at equilibrium would give the same average value of k_1 under conditions of unbalanced chemical reaction. If the reactants have a nonequilibrium distribution over molecular states, then the averaging of molecular transition probabilities that gives k_1 would not be expected to be the same as at equilibrium. For a unimolecular reaction at its low-pressure limit, the reactants have a profoundly nonequilibrium distribution over vibrational states, and this change in distribution function gives an average rate constant lower than the equilibrium value, easily a factor of 1000. The reactant of reaction 1 is O_3 with a strong nonequilibrium distribution over vibrational states. The reactants of reaction 2 are O and O_2 with an essentially equilibrium distribution over translational states. With O_3 having a nonequilibrium distribution function and with O_2 and O having an equilibrium distribution over their states, one may fear that k_2 will have its equilibrium value, k_1 will have its nonequilibrium value, and $K_1 = k_1/k_2$ would fail (see, however, section 5).

For ozone kinetics we have precisely observed values of k_1 over a wide temperature range and the data are well described by an Arrhenius function,

$$k_1(f) = A_1 \exp\left(-E_1/RT\right),$$

where A_1 and E_1 have been fitted to experimental data, table 20. Also we have fairly precise values of k_2 over a more restricted temperature range. Each value of observed k_2 divided by the functional k_1 calculated for the same temperature gives a strictly kinetic estimate of the equilibrium constant,

$$K_1' = k_1 \text{ (function)}/k_2 \text{ (observed)}. \qquad (3\text{--}49)$$

This ratio is entered for each observed k_2 in table 24A to give a set of K' from 188 to 373 K. Another method of estimating the equilibrium constant by a strictly kinetic method is from observed values of k_J divided by functional (fig. 9A) k_3:

$$K_1'' = k_J \text{ (observed)}/k_3 \text{ (function)}. \qquad (3\text{--}50)$$

This ratio is given for each observed k_J in table 22. The thermodynamic equilibrium constant K_1 is given in table 16, and is plotted as the smooth curve in figure 10. Points for the kinetic-constant ratio K_1' are plotted circles or as a triangle in figure 10, and points for K_1'' are plotted as squares. The kinetic constants K' and K'' overlap each other quite well. The equilibrium constants deduced from kinetics generally lie slightly below the thermodynamic equilibrium constant. Agreement between the kinetic K and thermodynamic K would be improved if the heat of formation of ozone is reduced a few tenths of a kilocalorie. The dis-

crepancy between K' and K at low temperature depends critically on the activation energy assigned to k_1. The points in table 24A and the circles in figure 10 were calculated, using 23.06 kcal as the activation energy for reaction 1. If this activation energy is decreased to about 22.7 or 22.8, the kinetic K' and thermodynamic K come into agreement within the scatter of the kinetic data. It must be admitted that the scatter in the kinetic data is such that no strong case can be made for changing the heat of formation of ozone, and figure 10 cannot be interpreted as giving a measurable demonstration of failure of $K_1 = k_1/k_2$.

b. Extended Values of k_1 and k_3

Since the relation, $K_1 = k_1/k_2$, appears to be at least as valid as the observed function, k_1, this relation can be used to extend the temperature range of the rate constant, k_1. The extended set of these rate constants is

$$k_1 \text{ (extended) is } k_1 \text{ (obs) and } k_2 \text{ (obs)} K_1 \text{(thermo).}$$

$$(3\text{--}51)$$

The values of k_1 (extended) as found from k_2 are given as the last column in table 24A. The full data of k_1 (extended) are shown in figure 12 with the least-squares line.

Likewise the function, k_3, can be extended as follows by adding the terms, k_J/K_1, to the observed values of k_3:

$$k_3 \text{ (extended) is } k_3 \text{ (obs) and } k_J/K_1 \text{ (thermo).} \qquad (3\text{--}52)$$

The additional values of k_3 as deduced from k_J are given as the last column in table 22. The observed values of k_3, the values obtained from red-light photolysis, $k_2/(k_2/k_3)$, and the values extended from k_J are plotted in figure 9B with the least-squares line.

The rate constant functions, k_1, k_1 (extended), k_J, k_2/k_3, k_2, and k_3 were each fitted to the three functions, $A \exp\left(-E/RT\right)$, $BT^m \exp\left(-E'/RT\right)$, and CT^n. The parameters, A, E, B, m, E', C, and n for each of these six functions are listed in table 27. Even with the extended data for k_1, the three-parameter function gives physically unreasonable parameters, and the parameters are unstable with respect to omission or inclusion of small sets of data. For the other rate constants, note particularly k_J, the data are totally unable to support the three-parameter function. In some cases the empirical function C gave about as good a fit to the scattered data as the Arrhenius equation. However, the general picture is that the data, including k_2, are best described by the two-parameter Arrhenius equation. Unlike the case with the dissociation of oxygen, there is nothing about the data that gives compelling evidence for equation B.
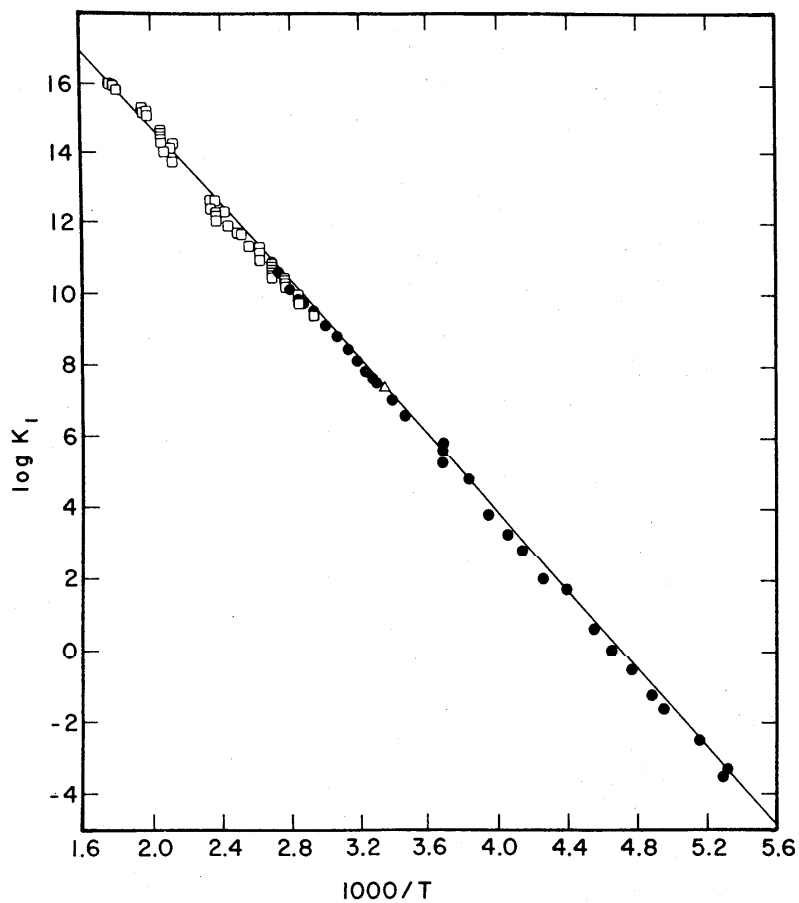
FIGURE 10. *Comparison of equilibrium constant calculated from kinetic data and that found from thermodynamics.*

●$K' = k_1/k_2$ with k_2 from reference [28]
△K' with k_2 from Kaufman and Kelso [70]
□$K'' = k_1/k_3$
Line is K from JANAF Thermodynamic Tables.
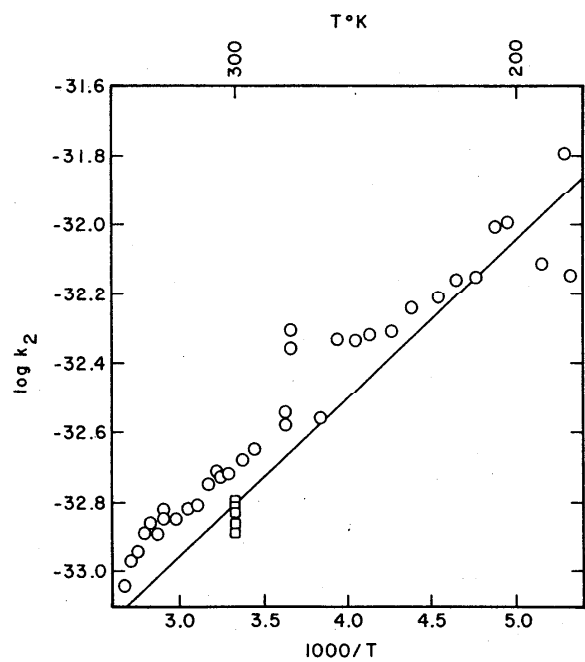
FIGURE 11. *Observed values of k_2 with line calculated from $k_2 = k_1/K_1$ (compare Fig. 8).*
log $k_2 = -34.335 + 0.459$ $(1000/T)$.

32
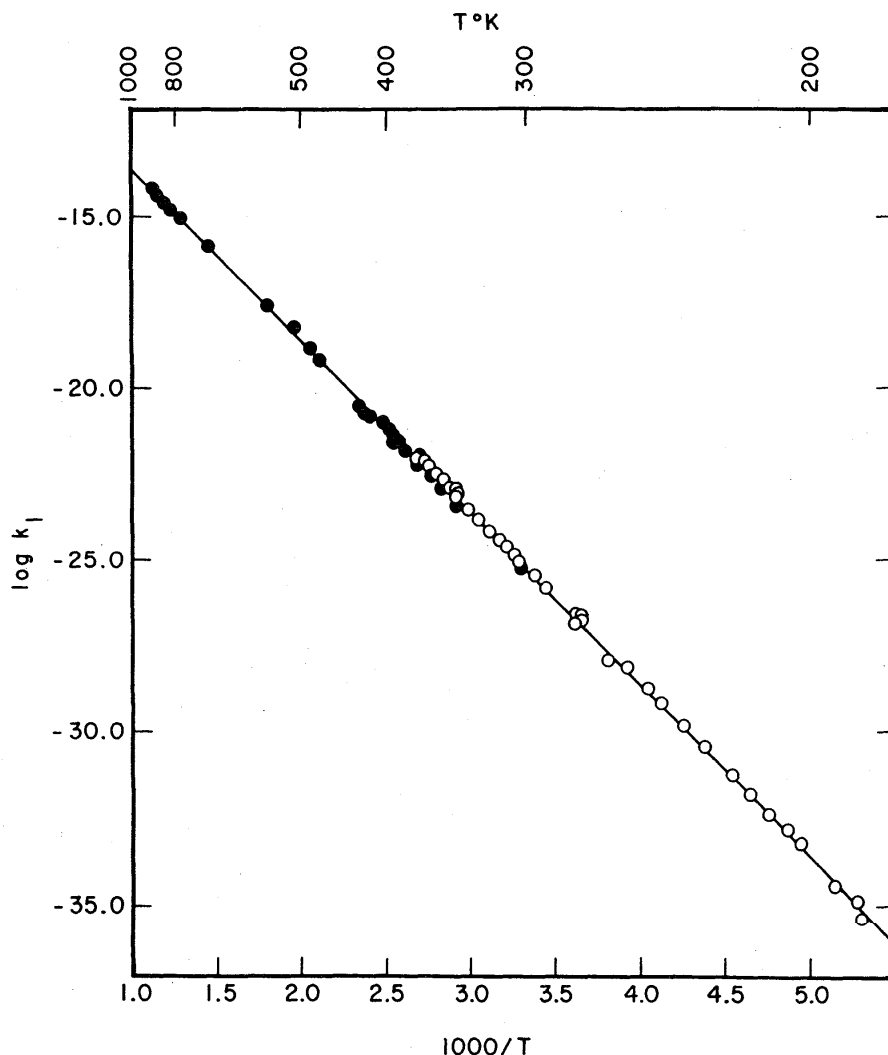
FIGURE 12. *The extended function* k_1.

Observed values of k_1 averaged in groups, ● ; and values of k_1 calculated from reverse reaction and equilibrium constant, $k_1 = k_2 K_1$, ○. The line is given by
$$\log k_1 = -8.783 - 4.965 \ (1000/T)$$
$$k_1 = 1.65 \times 10^{-9} \ \exp \ (-22.72/RT) \ \text{cm}^3/\text{particle-s}.$$

c. Self-Consistent Set of Elementary Rate Constants

This reviewer has at his disposal substantially more quantitative data than that available to Benson and Axworthy about 10 years ago. Some quantitative differences in finally recommended rate factors will appear, and yet the same qualitative conclusions are reached: (1) The mechanism is adequately given by that of Benson and Axworthy; (2) the functions, k_1, k_2, k_3, k_J, and K_1 are adequately described by the Arrhenius equation, $A \exp \ (-E/RT)$; and (3) we should demand self-consistency between the rate constants and the equilibrium constant:

$$K_1 = k_1/k_2 = k_J/k_3. \tag{3-53}$$

The various observed rate constants and rate constant ratios, k_1, k_2, k_2/k_3, k_J, k_3, cover different ranges of temperature and represent the work of various sets of investigators. The least-squares parameters fitted to the individual observed functions are not completely self-consistent, and it is desirable to find a self-consistent set for the recommended rate factors. Out of the six observable quan-

33

tities, k_1, k_2, k_3, k_2/k_3, k_J, and K_1, only three are independent. Benson and Axworthy took k_1, k_J, and K_1 as their independent set, and derived k_2 and k_3. With the quantitative data now available, k_J covers a relatively narrow temperature range and parameters based on it have a high error of estimate. We take as our three independent sets of data: (1) the extended k_1 (figure 12), (2) the equilibrium constant K_1 (table 16), and (3) the extended k_3 (figure 9B). The least-squares parameters for the Arrhenius equation of these functions are given in table 28, and the lines in figures 9B and 12 are based on these parameters. The function k_2 was calculated from $k_2 = k_1/K_1$, and the observed data are compared to this function in figure 11. The function follows Thrush's [28] trend with temperature, and it falls between the somewhat different room-temperature values as given by Thrush [28] and by Kaufman [70]. If the observed values of k_2 are regarded as having random errors of ±25 percent, there is satisfactory agreement between the recommended function, $k_2 = k_1/K_1$, and observed k_2. For extrapolation to other temperatures, we recommend $k_2 = k_1/K_1$, not the observed k_2 function itself. The function, k_J, was calculated from $k_J = K_1 k_3$, and this is the function plotted through the data points in figure 6. The line plotted through the data of k_2/k_3 in figure 7 is based on the recommended values of k_3 and k_2.

The recommended values for the elementary rate constants in the decomposition of ozone are listed in table 28 and repeated in the summary, section 6.

TABLE 16. *Equilibrium constant K_1 for the reaction* $O_3 = O_2 + O$ *(particles/cm^3) from JANAF tables*

T	$1000/T$	$\log K_1$
200	5.000	− 1.548
300	3.333	7.484
400	2.500	11.921
500	2.000	14.658
600	1.667	16.546
700	1.429	17.830
800	1.250	18.788
900	1.111	19.529

Approximate equations for calculation of K_1.

$$\log K_1 = 25.5524 - 5.4243 \ (1000/T)$$
$$\log K_1 = 24.2129 - 5.3520 \ (1000/T) + 0.4357 \log T.$$

TABLE 17. *Relative efficiencies for various foreign gases in activating ozone at its low-pressure limit*

M	T	k_M/k_{O_3} obs.	k_M/k_{O_3} used here	References
O_3		1.00	1.00	
O_2	300	0.42	0.44	[a] [70]
	291	.44		[26]
	343 − 383	.44		[47], [11]
He	300	.28	.34	[70]
	291	.34		[26]
	343 − 383	.34		[47], [11]
Ar	300	.26	.25	[70]
	291	.25		[26]
N_2	300	.36	.39	[70]
	291	.39		[26]
	343 − 383	[a] .41		[47], [11]
CO_2	300	(.96)	.96	[70]
	291	.96		[26]
	343 − 383	1.06		[47], [11]
N_2O	300	0.96		[70]
CF_4		1.02		[70]
SF_6		2.17		[70]
H_2O		3.84		[70]
		k_{Ar}/k_{N_2}		
	291	0.64		[26]
	300	.71		[70]
	769 − 863	.65		[62]

[a] Assuming $k(CO_2)/k(O_3)$ is 0.96.

TABLE 18. *Observed values of* k_1 *(cm³/particle-s), corrected to equivalent ozone*

T	1000/T	log k_1	M	Ref.	T	1000/T	log k_1	M	Ref.
769.	1.300	−15.19	Ar	[62].	403.	2.480	−21.05		
778.	1.286	−15.09			403.	2.480	−21.04		
779.	1.284	−15.05			403.	2.480	−21.06		
787.	1.270	−15.00			416.	2.404	−20.85		[a][43].
792.	1.262	−15.09			425.	2.353	−20.69		
812.	1.230	−14.93			425.	2.353	−20.49		
824.	1.213	−14.81			429.	2.331	−20.60		
825.	1.211	−14.85			473.	2.114	−19.26		
827.	1.209	−14.76			473.	2.114	−19.36		
828.	1.208	−14.76			477.	2.096	−19.09		
840.	1.190	−14.72			483.	2.070	−19.08		
840.	1.190	−14.67			488.	2.049	−18.83		
841.	1.188	−14.70			488.	2.049	−18.89		
846.	1.181	−14.54			488.	2.049	−18.96		
871.	1.148	−14.41			488.	2.049	−18.84		
876.	1.140	−14.43			507.	1.972	−18.24		
881.	1.133	−14.44			507.	1.972	−18.35		
890.	1.122	−14.35			514.	1.946	−18.26		
910.	1.098	−14.24			516.	1.938	−18.31		
910.	1.098	−14.18			557.	1.795	−17.77		
689.	1.452	−15.94	N₂		559.	1.789	−17.52		
694.	1.440	−15.89			559.	1.789	−17.52		
788.	1.269	−15.04			343.	2.915	−23.47		[47].
831.	1.202	−14.71			343.	2.915	−23.41		
837.	1.193	−14.72			353.	2.833	−22.96		
855.	1.169	−14.60			353.	2.833	−22.96		
863.	1.158	−14.56			353.	2.833	−22.96		
344.	2.910	−23.26		[99]. Table 1.	363.	2.755	−22.68		
354.	2.825	−22.90			363.	2.755	−22.68		
373.	2.680	−22.27			363.	2.755	−22.58		
392.	2.550	−21.60			363.	2.755	−22.57		
420.	2.380	−20.80			363.	2.755	−22.55		
388.	2.580	−21.58		[131].	363.	2.755	−22.55		
388.	2.580	−21.58			363.	2.755	−22.55		
393.	2.542	−21.36			363.	2.755	−22.55		
393.	2.542	−21.37			363.	2.755	−22.54		
393.	2.542	−21.34			363.	2.755	−22.54		
393.	2.542	−21.37			363.	2.755	−22.52		
393.	2.542	−21.34			363.	2.755	−22.52		
393.	2.542	−21.36			363.	2.755	−22.52		
393.	2.542	−21.35			363.	2.755	−22.52		
393.	2.542	−21.36			363.	2.755	−22.51		
393.	2.542	−21.35			363.	2.755	−22.49		
398.	2.512	−21.22			363.	2.755	−22.49		
398.	2.512	−21.20			363.	2.755	−22.48		

[a] As reinterpreted by use of integrated equation.

TABLE 18. *Observed values of* k_1 *(cm^3/particle-s), corrected to equivalent ozone* — Continued

T	$1000/T$	$\log k_1$	M	Ref.		T	$1000/T$	$\log k_1$		
363.	2.755	−22.47				344.	2.907	−23.00		
373.	2.681	−22.19				344.	2.907	−23.08		
373.	2.681	−22.19				344.	2.907	−23.17		
373.	2.681	−22.15				352.	2.841	−23.04		
373.	2.681	−22.14				362.	2.762	−22.57		
373.	2.681	−22.10				362.	2.762	−22.60		
383.	2.611	−21.89				363.	2.755	[b] −22.43		
383.	2.611	−21.80				363.	2.755	−22.48		
383.	2.611	−21.80				363.	2.755	[c] −22.48		
353.	2.833	−22.96				363.	2.755	−22.44		
353.	2.833	−22.96				363.	2.755	−22.55		
353.	2.833	−22.96				363.	2.755	−22.52		
363.	2.755	−22.55				363.	2.755	−22.51		
363.	2.755	−22.54				363.	2.755	−22.43		
363.	2.755	−22.54				363.	2.755	−22.17		
363.	2.755	−22.52				364.	2.747	[c] −22.06		
373.	2.681	−22.19				364.	2.747	[c] −22.47		
373.	2.681	−22.14				364.	2.747	[c] −22.48		
373.	2.681	−22.14				364.	2.747	[c] −22.35		
353.	2.833	−23.00				364.	2.747	−22.51		
353.	2.833	−22.96				364.	2.747	−22.51		
363.	2.755	−22.57				364.	2.747	−22.49		
363.	2.755	−22.55				373.	2.681	−22.00		
363.	2.755	−22.55				373.	2.681	−22.14		
353.	2.833	−23.00				374.	2.674	−22.09		
							374.	2.674	−21.92		
353.	2.833	−22.96								
363.	2.755	−22.55								
363.	2.755	−22.55								
363.	2.755	−22.55								
303.	3.300	−25.26		[3].						

[b] Added H_2O_2.
[c] Added H_2O.

TABLE 19. *Least-squares fit of* k_1 *to Arrhenius equation for the various authors*

References	T Range K	M	Intercept log A_1	E_1 kcal/mole
Jones and Davidson [62]	769–910	Ar	−8.99	21.8
Jones and Davidson [62]	689–863	N_2	−9.02	21.8
Garvin [43]	416–559	O_2	−7.66	25.1
Pshezhetskii et al. [99]	344–420	O_3	−9.70	21.4
Zaslowsky et al. [131]	388–403	O_3	−8.21	23.6
Glissman and Schumacher [47]	343–383	O_3	−8.02	24.1
	353–373	N_2	−7.98	24.2
	353–363	He	−7.60	24.8
	353–363	CO_2	−7.36	25.2
Axworthy [3]	303–374	O_3	−8.68	22.9

$\log k_1 = \log A_1 - E_1/2.303\ RT$.

A is A_M converted to equivalent ozone.

TABLE 20. *Least-squares fit of* k_1 *to Arrhenius equation for all data excluding authors one by one*

All data excluding references	T range	Intercept log A_1	E_1 kcal/mole
Jones and Davidson [62]	303–559	−8.39	23.5
Garvin [43]	303–910	−8.70	22.9
Pshezhetskii et al. [93]	303–910	−8.67	23.0
Zaslowsky et al. [131]	303–910	−8.67	23.0
Glissman and Schumacher [47]	303–910	−8.73	22.8
Axworthy [3]	343–910	−8.64	23.1
All data	303–910	−8.68	23.0

TABLE 21. *Observed values of* k_1 *averaged in groups for plotting in figure 12*

Authors	1000/T	log k_1	Authors	1000/T	log k_1
Jones and Davidson [62]	1.11	−14.21	Zaslowsky et al [131] − Con.	2.54	−21.35
	1.135	−14.40		2.58	−21.58
	1.185	−14.63			
	1.22	−14.85	Pshezhetskii et al. [99]	2.38	−20.80
	1.28	−15.10		2.55	−21.60
	1.445	−15.92		2.68	−22.27
				2.82	−22.90
Garvin [43]	1.79	−17.64		2.91	−23.26
	1.955	−18.30			
	2.05	−18.90	Glissman and Shumacher [47]	2.61	−21.85
	2.10	−19.22		2.68	−22.15
	2.34	−20.59		2.76	−22.58
	2.40	−20.85		2.83	−22.96
				2.92	−23.44
Zaslowsky et al. [131]	2.48	−21.05			
	2.51	−21.20	Axworthy [3]	3.30	−25.26

TABLE 22. *Observed values of* k_J, s^{-1} *and other quantities deduced from* k_J

T	1000/T	log k_J	log K_1''	M	log k_3 (calc)	Ref.	T	1000/T	log k_J	log K_1''	M	log k_3 (calc)	Ref.
416.	2.404	−0.80	12.31		−13.29	[a] [43]	363.	2.755	−3.10	10.35		−13.68	
425.	2.353	−.55	12.51		−13.32		363.	2.755	−3.08	10.37		−13.66	
425.	2.353	−.44	12.62		−13.20		363.	2.755	−3.07	10.38		−13.65	
429.	2.331	−.40	12.64		−13.28		363.	2.755	−3.06	10.39		−13.64	
473.	2.114	.95	13.79		−13.11		363.	2.755	−3.03	10.42		−13.61	
473.	2.114	1.38	14.22		−12.68		363.	2.755	−3.02	10.43		−13.60	
477.	2.096	1.32	14.14		−12.84		363.	2.755	−3.02	10.43		−13.60	
483.	2.070	1.30	14.09		−13.00		363.	2.755	−3.00	10.45		−13.58	
488.	2.049	1.56	14.33		−12.86		363.	2.755	−3.00	10.45		−13.58	
488.	2.049	1.61	14.38		−12.81		363.	2.755	−3.00	10.45		−13.58	
488.	2.049	1.64	14.41		−12.78		363.	2.755	−2.96	10.49		−13.54	
488.	2.049	1.66	14.43		−12.76		373.	2.681	−2.89	10.49		−13.88	
488.	2.049	1.73	14.50		−12.69		373.	2.681	−2.70	10.68		−13.68	
488.	2.049	1.73	14.50		−12.69		373.	2.681	−2.66	10.72		−13.64	
507.	1.972	2.34	15.04		−12.50		373.	2.681	−2.57	10.81		−13.56	
507.	1.972	2.43	15.13		−12.41		373.	2.681	−2.57	10.81		−13.56	
514.	1.946	2.44	15.12		−12.54		383.	2.611	−2.32	10.99		−13.47	
516.	1.938	2.63	15.30		−12.39		383.	2.611	−2.11	11.20		−13.68	
557.	1.795	3.28	15.81		−12.52		383.	2.611	−2.04	11.27		−13.40	
559.	1.789	3.41	15.94		−12.42		353.	2.833	−3.62	9.90	N₂		
559.	1.789	3.41	15.94		−12.42		353.	2.833	−3.59	9.93			
393.	2.545	−1.88	11.37		−13.60	[99]	353.	2.833	−3.57	9.95			
403.	2.481	−1.48	11.70		−13.55		363.	2.755	−3.18	10.27			
413.	2.421	−1.17	11.96		−13.56		363.	2.755	−3.14	10.31			
423.	2.364	−0.96	12.11		−13.66		363.	2.755	−3.08	10.37			
423.	2.364	−.91	12.16		−13.62		363.	2.755	−3.02	10.43			
423.	2.364	−.89	12.18		−13.60		373.	2.681	−2.70	10.68			
423.	2.364	−.89	12.18		−13.60		373.	2.681	−2.66	10.72			
423.	2.364	−.83	12.24		−13.54		373.	2.681	−2.59	10.79			
433.	2.309	−.60	12.42		−13.60		353.	2.833	−3.60	9.92	He		
343.	2.915	−4.17	9.43		−13.75	[47]	353.	2.833	−3.55	9.97			
343.	2.915	−4.03	9.57		−13.89		363.	2.755	−3.14	10.31			
353.	2.833	−3.74	9.78		−13.90		363.	2.755	3.00	10.45			
353.	2.833	−3.59	9.93		−13.75		363.	2.755	−3.00	10.45			
353.	2.833	−3.55	9.97		−13.71		353.	2.833	−3.52	10.00	CO₂		
363.	2.755	−3.33	10.12		13.91		353.	2.833	−3.51	10.01			
363.	2.755	−3.24	10.21		−13.82		363.	2.755	−3.10	10.35			
363.	2.755	−3.24	10.21		−13.82		363.	2.755	−3.09	10.36			
363.	2.755	−3.21	10.24		−13.79		363.	2.755	−3.06	10.39			
363.	2.755	−3.20	10.25		−13.78		373.	2.681	−2.60	10.78		−13.58	[28]
363.	2.755	−3.19	10.26		−13.77		373.	2.681	−2.51	10.87		−13.50	
363.	2.755	−3.18	10.27		−13.76		400.	2.500	−1.50	11.70		−13.47	[56]
363.	2.755	−3.17	10.28		−13.75								

[a] Reinterpreted by use of integrated equation.
$K_1'' = k_J$(observed)/k_3(function).
log k_3(function) = − 10.8215 − 0.9526 (1000/T)
k_3(calc) = k_J(observed)/K_1(thermodynamic).

38

TABLE 23. *Observed values of* k_2/k_3, *$cm^3/particle$, and value of* k_3 *deduced from this ratio and observed* k_2 *(where ranges of temperature overlap). The ratio* k_2/k_3 *is corrected to equivalent ozone*

T	$1000/T$	$\log k_2/k_3$	M	$\log k_3$	Ref.	T	$1000/T$	$\log k_2/k_3$	M	$\log k_3$	Ref.
278.	3.595	−18.53		−14.02	[26]	373.	2.681	−19.27		−13.73	
291.	3.434	−18.68		−13.94		373.	2.681	−19.62		−13.38	
298.	3.353	−18.77		−13.89		373.	2.681	−19.44		−13.56	
298.	3.353	−19.09			[87]	373.	2.681	−19.46		−13.54	
298.	3.353	−18.72		−13.94		373.	2.681	−19.62		−13.38	
343.	2.915	−19.24		−13.63	[47]	383.	2.611	−19.47			
343.	2.915	−19.42		−13.45		383.	2.611	−19.68			
353.	2.833	−19.21		−13.70		383.	2.611	−19.85			
353.	2.833	−19.38		−13.53		353.	2.833	−19.38	N_2		
353.	2.833	−19.39		−13.52		353.	2.833	−19.41			
363.	2.755	−19.57		−13.39		353.	2.833	−19.35			
363.	2.755	−19.34		−13.62		363.	2.755	−19.47			
363.	2.755	−19.38		−13.58		363.	2.755	−19.35			
363.	2.755	−19.51		−13.45		363.	2.755	−19.52			
363.	2.755	−19.46		−13.50		363.	2.755	−19.39			
363.	2.755	−19.41		−13.55		373.	2.681	19.43			
363.	2.755	−19.58		−13.38		373.	2.681	−19.48			
363.	2.755	−19.70		−13.26		373.	2.681	−19.58			
363.	2.755	−19.68		−13.28		353.	2.833	−19.42	He		
363.	2.755	−19.34		−13.62		353.	2.833	−19.38			
363.	2.755	−19.31		−13.65		363.	2.755	−19.42			
363.	2.755	−19.25		−13.71		363.	2.755	−19.55			
363.	2.755	−19.44		−13.52		363.	2.755	−19.57	CO_2		
363.	2.755	−19.24		−13.72		353.	2.833	−19.46			
363.	2.755	−19.33		−13.63		353.	2.833	−19.48			
363.	2.755	−19.19		−13.77		363.	2.755	−19.46			
363.	2.755	−19.46		−13.50		363.	2.755	−19.48			
363.	2.755	−19.55		−13.41		363.	2.755	−19.47			
363.	2.755	−19.54		−13.42							
363.	2.755	−19.44		−13.52							

TABLE 24A. *Observed values of* k_2, $cm^6/particle^2$ *s, in the presence of Ar corrected to equivalent ozone and other quantities derived from* k_2.

T	$1000/T$	log k_2 (obs)	log K_1'	log k_1 (calc)	Ref.
188.	5.319	−32.15	−3.30	−35.41	[28]
189.	5.291	−31.79	−3.52	−34.90	
194.	5.155	−32.11	−2.51	−34.49	
202.	4.950	−31.99	−1.60	−33.26	
205.	4.878	−32.01	−1.22	−32.90	
210.	4.762	−32.15	−0.49	−32.41	
215.	4.651	−32.16	0.08	−31.82	
220.	4.545	−32.21	0.66	−31.30	
228.	4.386	−32.24	1.49	−30.47	
235.	4.255	−32.31	2.22	−29.84	
242.	4.132	−32.32	2.85	−29.18	
247.	4.048	−32.34	3.30	−28.75	
254.	3.937	−32.33	3.85	−28.14	
262.	3.817	−32.76	4.88	−27.92	
273.	3.663	−32.36	5.26	−26.69	
273.	3.663	−32.31	5.21	−26.64	
275.	3.636	−32.58	5.61	−26.76	
276.	3.623	−32.74	5.84	−26.85	
290.	3.448	−32.65	6.63	−25.82	
296.	3.378	−32.68	7.01	−25.47	
304.	3.289	−32.72	7.50	−25.03	
307.	3.257	−32.73	7.67	−24.86	
311.	3.215	−32.71	7.87	−24.62	
315.	3.175	−32.75	8.11	−24.44	
321.	3.115	−32.81	8.47	−24.18	
328.	3.049	−32.82	8.81	−23.83	
335.	2.985	−32.85	9.16	−23.51	
343.	2.915	−32.85	9.52	−23.13	
344.	2.907	−32.82	9.53	−23.06	
348.	2.874	−32.89	9.76	−22.95	
353.	2.833	−32.86	9.94	−22.70	
358.	2.793	−32.89	10.17	−22.51	
363.	2.755	−32.94	10.41	−22.36	
368.	2.717	−32.97	10.63	−22.18	
373.	2.681	−33.04	10.89	−22.06	

$K_1' = k_1$ (function)/k_2 (observed).

log k_1 (function) $= -8.6430 - 5.0394$ (1000/T).

k_1 (calc) $= k_2$ (observed) K_1 (thermodynamic).

TABLE 24B. *Observed values of* k_2, $cm^6/particle^2$-s, *in the presence of various foreign gases*

T	$1000/T$	$\log T$	$\log k_2$ (obs)	$\log k_2$ (eq O_3)	M	Ref.
300.	3.333	2.477	−33.36	−32.89	He	[70]
300.	3.333	2.477	−33.40	−32.83	Ar	
300.	3.333	2.477	−33.19	−32.83	O_2	
300.	3.333	2.477	−33.25	−32.86	N_2	
300.	3.333	2.477	−32.82	−32.80	CO_2	
300.	3.333	2.477	−32.82	−32.80	N_2O	
300.	3.333	2.477	−32.80	−32.81	CF_4	
300.	3.333	2.477	−32.47	−32.81	SF_6	
300.	3.333	2.477	−32.22	−32.80	H_2O	

TABLE 25. *Observed values of* k_3 cm^3 s^{-1}

T K	$1000/T$	M	$\log k_3$	Ref.
769	1.300	Ar	−11.98	[62]
812	1.230		−12.19	
827	1.209		−11.89	
840	1.190		−12.16	
846	1.181		−11.85	
876	1.140		−11.62	
910	1.098		−11.74	
788	1.269	N_2	−11.90	[62]
831	1.202		−11.80	
837	1.193		−11.87	
863	1.158		−11.82	

TABLE 26. *Equilibrium constant* K_3 *for the reaction* $O + O_3 \overset{k_3}{\underset{k_4}{\rightleftarrows}} O_2 + O_2$. *From JANAF tables and the calculated function for the reverse reaction* k_4

T	$1000/T$	$\log K_3$	Ref.
3500.	0.286	5.96	[57]
4000.	.250	5.21	
4500.	.222	4.63	
5000.	.200	4.16	
5500.	.182	3.78	
6000.	.167	3.47	

$\log K_3 = -0.0254 + 20.941 \ (1000/T)$.
$\log k_3 = -10.697 - 1.047 \ (1000/T)$.
$\log k_4 = -10.672 - 21.988 \ (1000/T)$.

TABLE 27. *Summary of least-squares parameters for ozone kinetics*

Equation	Parameter	k_1	k_1 (ex)	k_J	k_2/k_3	k_2	k_3
A	$\log A$	−8.68	−8.78	15.25	−22.52	−34.00	−10.82
	E, kcal	23.0	22.7	30.5	−5.1	−1.8	4.4
B	$\log B$	2.86	−10.1	−67.2	−37.4	−25.4	−26.4
	m	−3.61	0.44	26.9	5.0	3.0	4.9
	E'	26.8	22.4	7.9	−8.4	−0.25	−0.44
C	$\log C$	−77.6	−90.4	−96.0	0.49	−24.1	−25.1
	n	21.6	26.3	36.3	−7.8	−3.47	4.48

Equations:

A $\quad k = A \exp(-E/RT)$
B $\quad k = B \ T^m \exp(-E'/RT)$
C $\quad k = C \ T^n$

k_1(ex) = k_1(obs) and $k_2 K_1$.
$k_3 = k_3$(obs) and $k_2/(k_2/k_3)$.

41

TABLE 28. *Recommended values of constants*
(200–900 K)[a]

Self-consistency between k_1, k_2, k_3, k_J, and K_1 in terms of Arrhenius equations.

	E, kcal/mole
$log\ k_1 = -8.783 - 4.965\ (1000/T)$	22.72
based on all observed k_1 and $k_2 K_1$.	
$log\ K_1 = 25.552 - 5.424\ (1000/T)$	24.82
based on JANAF tables.	
$log\ k_2 = log\ k_1 - log\ K_1$	
$= -34.335 + 0.459\ (1000/T)$	-2.10
$log\ k_3 = -10.697 - 1.047\ (1000/T)$	4.79
based on observed k_3, k_J/K_1, and	
$k_2/(k_2/k_3)$.	
$log\ k_J = log\ K_1 + log\ k_3$	
$= 14.855 - 6.471\ (1000/T)$	29.60
$log\ k_4 = -10.672 - 21.988\ (1000/T)$	100.6
based on observed k_3 and K_3 from	
JANAF tables.	

$k_1 = 1.65 \times 10^{-9}\ exp\ (-22.72/RT)$ cm^3/particle-s
$k_2 = 4.63 \times 10^{-35}\ exp\ (2.10/RT)$ cm^6/particle^2-s
$k_3 = 2.00 \times 10^{-11}\ exp\ (-4.79/RT)$ cm^3/particle-s

$k_J = 7.16 \times 10^{14}\ exp\ (-29.60/RT)$ s^{-1}
$K_1 = 3.56 \times 10^{25}\ exp\ (-24.82/RT)$ particle/cm^3
$k_4 = 2.12 \times 10^{-11}\ exp\ (-100.6/RT)$ cm^3/particle-s

[a] The reactions are:
  1. $O_3 + M \rightarrow O + O_2 + M$
  2. $O + O_2 + M \rightarrow O_3 + M$
  3. $O + O_3 \rightarrow O_2 + O_2$
  4. $O_2 + O_2 \rightarrow O + O_3$

K_1 is the equilibrium constant for reactions 1 and 2.

k_J is the Jahn mechanism rate constant for ozone decomposition in excess oxygen, see eq (3–8).

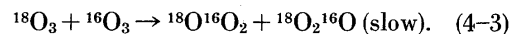# 4. Isotopic Exchange Between Oxygen Species

Molecular oxygen is readily obtained highly enriched in the isotope of mass number 18. Exchange reactions can be followed by analysis with mass spectrometers. Unperturbed molecular oxygen can be stored indefinitely at room temperature without measurable exchange:

$$^{16}O_2 + ^{18}O_2 \rightarrow ^{16}O^{18}O + ^{16}O^{18}O \text{ (slow)}. \quad (4-1)$$
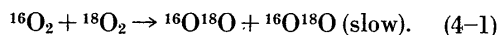
Similarly, direct exchange between molecular ozone and molecular oxygen is slow:

$$^{18}O_2 + ^{16}O_3 \rightarrow ^{18}O^{18}O^{16}O + ^{16}O_2 \text{ (slow)}, \quad (4-2)$$
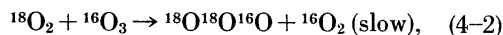
and direct exchange between molecular ozone with itself is slow:

$$^{18}O_3 + ^{16}O_3 \rightarrow ^{18}O^{16}O_2 + ^{18}O_2^{16}O \text{ (slow)}. \quad (4-3)$$

However, the exchange between oxygen molecules occurs very rapidly if oxygen atoms are produced in or added to the system. The elementary exchange reaction appears to be

$$O + O_2 \xrightarrow{k_5} O_2 + O, \quad (4-4)$$
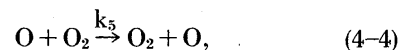
which is measurable by virtue of exchange of isotopic species:

$$^{16}O + {}^{18}O_2 \rightarrow {}^{16}O^{18}O + {}^{18}O \left. \right\}$$
$$^{18}O + {}^{16}O_2 \rightarrow {}^{16}O^{18}O + {}^{16}O \left. \right\} \text{ chain} \quad (4-5)$$

net $^{18}O_2 + {}^{16}O_2 \rightarrow 2\ {}^{16}O^{18}O.$
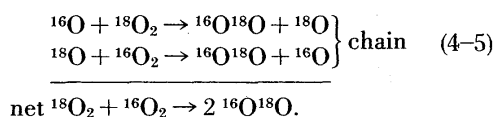
When ozone was photolyzed in the presence of $^{18}O_2$ and $^{16}O_2$, the quantum yield for exchange between the oxygen species was 125 at room temperature [61]. Results of four different investigations giving quantitative values of k_5 are summarized in table 29.

The value of the rate constant is

$$k_5 = 1.0 \times 10^{-12} \text{ cm}^3/\text{particle-s}$$

at 273 K, which is a moderately large bimolecular rate constant, and little or no activation energy is indicated for this reaction. In any system of O, O_2, and O_3, several fast reactions will occur simultaneously; the most rapid reactions at low temperature are:

$$O + O_2 \xrightarrow{k_5} O_2 + O \quad (4-6)$$

$$O + O_2 + M \xrightarrow{k_2} O_3 + M$$

$$O + O_3 \xrightarrow{k_3} O_2 + O_2.$$
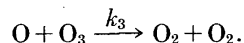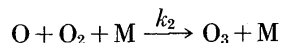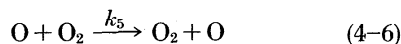
The ratio of rate 5 to rate 2, at room temperature, depends only on the concentration of gas M:

$$\frac{\text{Rate } 5}{\text{Rate } 2} = \frac{k_5}{k_2[\text{M}]} \quad (4-7)$$

and this ratio is plotted as a function of total pressure in figure 13. The exchange rate is faster than ozone formation at all pressures below 40 atm. Between 0.02 and 0.2 atm the exchange reaction occurs 1000 to 100 times as often as the formation of ozone. The ratio of rate 5 to rate 3 depends on temperature and the ratio of ozone to oxygen:

$$\frac{\text{Rate } 5}{\text{Rate } 3} = \frac{k_5[\text{O}_2]}{k_3[\text{O}_3]}. \quad (4-8)$$

This ratio of rates is plotted in figure 14 as an Arrhenius plot for various values of the ratio $[O_3]/[O_2]$. Under most conditions rate 5 is faster than rate 3. At room temperature rate 5 exceeds rate 3 if the ozone is less than 99 percent.

TABLE 29. *Observed values of isotopic exchange reactions in oxygen species*

$$O + O_2 \xrightarrow{k_5} O_2 + O$$

T	$\log k_5$ (cm³/particle-s)	References
272	-11.8	Ogg and Sutphen [93, 94].
273	-11.77	Brennen and Niki [18].
298–402	$-11.19 - 239/T$	Jaffe and Klein [55a].
300	-12.0	Herron and Klein [53].

273, adopted value, $\log k_5$, -12.0.
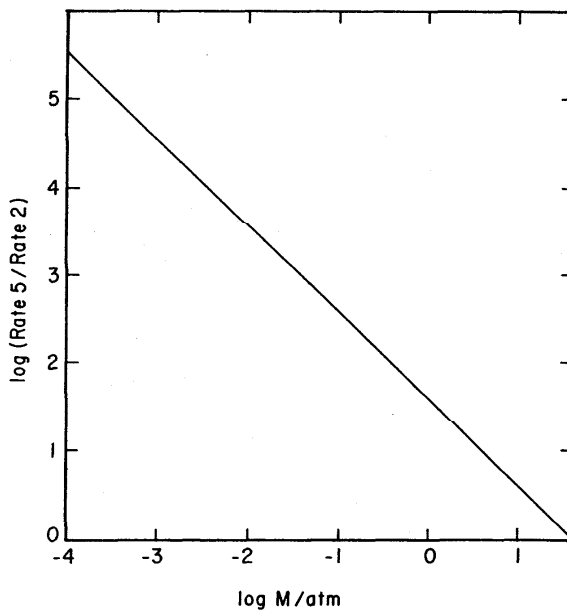
FIGURE 13. *Relative rate of oxygen exchange* $(O + O_2 \xrightarrow{5} O_2 + O)$ *to ozone formation* $(O + O_2 + M \xrightarrow{2} O_3 + M)$ *as a function of equivalent ozone* M *pressure in atmospheres; room temperature, but these ratios are not expected to vary rapidly with temperature.*
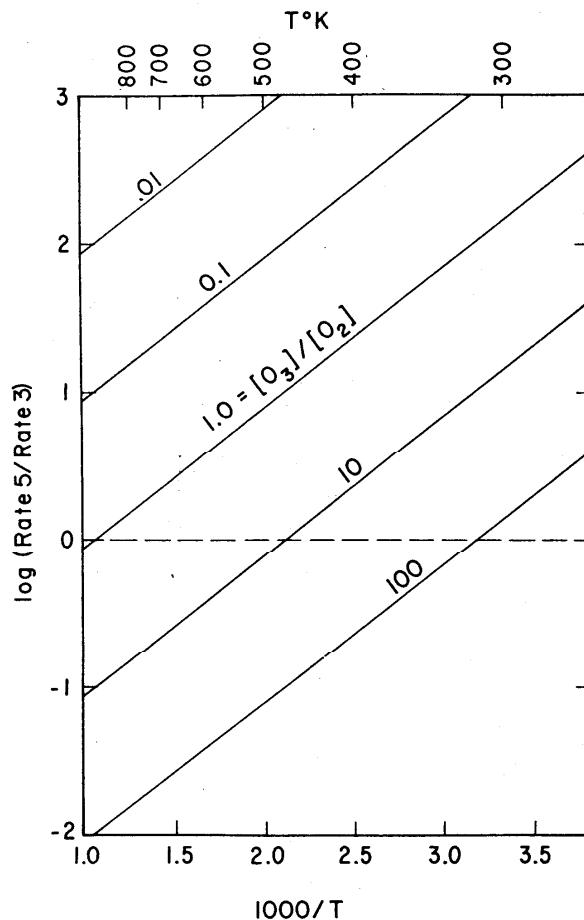
43

FIGURE 14. *Relative rate of oxygen exchange* $(O+O_2 \xrightarrow{5} O_2+O)$ *to oxygen atom reaction with ozone* $(O+O_3 \xrightarrow{3} O_2+O_2)$ *as function of the ratio of ozone to oxygen* $[O_3]/[O_2]$ *and temperature (on the assumption that* k_5 *does not change with temperature).*

5. Discussion

5.1. Why Does $K_1 = k_1/k_2$ at the Low-Pressure Limit of a Unimolecular Reaction?

At the low-pressure limit of a unimolecular reaction, the reactant has an extraordinarily nonequilibrium distribution over vibrational state, which gives large measurable consequences (easily a factor of 1000 in observed rate). At the low-pressure limit of a bimolecular association the reactants still have an essentially equilibrium distribution over states. At the molecular level, the elementary chemical dissociation is the flying apart of an excited polyatomic molecule; for a bimolecular association it is the stabilization by collision of an excited molecule. One may well ask, how can the average of a molecular transition function over a nonequilibrium distribution function possibly be equal to the average of an energy transfer function over an essentially equilibrium distribution function? In terms of ozone kinetics, one asks, how can K_1 possibly equal k_1/k_2 at the nonequilibrium, low-pressure limit of the unimolecular reaction?

The activation energy for the dissociation of O_2 is less than the bond dissociation energy. Also, the activation energy of the decomposition of ozone is less than the bond dissociation energy. This effect can be formally explained in terms of a rate-constant expression that has the form

$$k = BT^m \exp\ (-D/RT), \qquad (5-1)$$

where D is the dissociation energy and m is some constant. The activation energy, as given by eq (1-38), is

$$E_A = D + mRT. \qquad (5-2)$$

If m is negative, the observed activation energy is less than the bond dissociation energy. For low-pressure dissociations, mRT represents the thermal excitation of the internal coordinates of the molecule above the zero-point vibrational energy. The average energy of a harmonic oscillator above the zero-point energy is

$$\epsilon = \frac{h\nu}{e^{h\nu/kT} - 1} \qquad (5-3)$$

44

The energy term mRT is a classical-mechanical, upper-limit estimate of the quantum mechanical average energy as given by eq (5-3). For O_2 at 5000 K the average vibrational energy of the molecule is 8 kcal, and at 10,000 K the average vibrational energy of the molecule is 18 kcal. Thus the empirical value of $m = -1$ as deduced in section 2 is largely ascribable to average vibrational excitation of the O_2 molecule (compare relation 2-6). For ozone at 300 K, the three vibrational energies are:

Frequency (cm^{-1})	Average energy (kcal)
705	0.08
1043	.02
1110	.02
	Total......0.12

The bond dissociation energy of ozone at absolute zero is 24.2 kcal/mole; the minimum activation energy in terms of the oscillators is thus 24.1 kcal/mole; but the observed activation energy is 22.7 kcal/mole. If we invoke three degrees of rotational energy of reactant with only two degrees of rotational energy of dissociating fragments, another $\frac{1}{2}RT$ or 0.3 kcal can be found. However, it remains a fact that the observed activation energy for the ozone dissociation is substantially less than can be explained by the existing simple theories (Rice, Ramsperger, Kassel, Marcus, etc.).

Thus we have two interesting facts to discuss: (1) Why do the ratios of nonequilibrium rate constants give the correct equilibrium constant, and (2) Why is the activation energy for ozone so much less than the bond dissociation energy?

a. Mathematical Models

General aspects of this question have been discussed recently by Widom [121a] and by Rice [101a]. In terms of general arguments Rice concluded that if unambiguous reaction rate constants can be measured experimentally, then the quotient of the experimentally determined constants will give the equilibrium constant. Widom illustrated and enlarged on this theorem with a detailed treatment of a very simple example, a reversible isomerization. The theory of Rice is logical and persuasive, but not rigorous. The example given by Widom is rigorous; but the case is special, forward and reverse reactions being first order; and one is not convinced as to its generality.

The experimental data for both the decomposition of oxygen and for the decomposition of ozone indicate that the ratio of forward to reverse rate constant agree very well with the chemical equilibrium constant. These examples represent extreme conditions. At the high temperature of observation, the vibrational relaxation time of O_2 approaches the

dissociation relaxation time actually observed. The rate constant, k_1, for ozone represents the low-pressure (second-order) limit of a unimolecular decomposition, and k_2 represents a bimolecular recombination at its low-pressure (third-order) limit. The extended theory of Rice and of Widom predicts that even for these extreme cases the ratio of observed rate constants should give the thermodynamic equilibrium constant. In this review we have been careful to keep separate what experiments actually show and what theory actually predicts. In the present instance there is satisfactory agreement between theory and experiment on this score.

b. Physical Model as Derived From Rate of Exchange

The reaction of hydrogen atom, H, with hydrogen molecule, H_2, occurs over an energy barrier, the H_3 collision complex [59]. The interaction of atomic oxygen with molecular oxygen does not occur over a potential barrier but rather over a potential-energy well, namely, ozone. The exchange reaction 5 is probably of the "compound nucleus" type with an intermediate complex lasting about 10^{-11} s, as opposed to the H_3 complex which lasts only for a period of about one vibration:

$$O + O_2 \xrightarrow{d} O_3^*$$

$$O_3^* \xrightarrow{c} O_2 + O \qquad (5\text{-}4)$$

$$O_3^* + M \xrightarrow{b} O_3 + M.$$
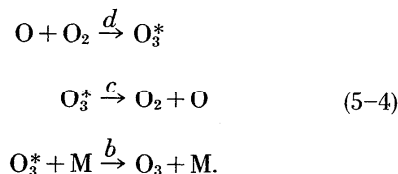
With this simplified scheme the rate constants for reactions 5 and 2 are identified:

$$k_5 = d/2$$
$$k_2 = b(d/c). \qquad (5\text{-}5)$$

(The factor 1/2 comes from the equal probability of excited $^{16}O^{16}O^{18}O$ breaking up as $^{16}O + {}^{16}O^{18}O$ and $^{18}O + {}^{16}O^{16}O$.)

The ratio of rate 5 to rate 2 is given by figure 13, and it is generally much larger than one. The principle of microscopic reversibility states that at equilibrium every molecular process and its exact reverse occurs at the same average rate. Conversely, if a molecular process and its exact reverse occur at the same average rate, the reactants and products are at equilibrium. If the molecular process d occurs at approximately the same rate as its inverse c (b is a rare event, figure 13), then the highly excited vibrational states of ozone (O_3^* above the critical energy) are in equilibrium with O_2 and O and therefore in a distribution with respect to ozone the same as that at chemical equilibrium. The population distribution among many of the low-lying vibrational states of ozone must be that

corresponding to equilibrium. If ozone was at equilibrium with all of its vibrational states up to the critical energy, then the rate of reaction 1 would necessarily have its high-pressure limiting value since $O_2 + O$ sets up an equilibrium distribution of O_3^* above the critical energy. Thus the nonequilibrium distribution that gives rise to the "fall-off" with pressure of a unimolecular reaction must apply primarily to states just below the critical energy. For such a band of states, activation to the high-density states above the critical energy is faster than deactivation to the low-density states well below the critical energy. The "rate determining step" in ozone decomposition is activation up to a band of states a few kilocalories per mole below the critical energy (hence the activation energy of 22.7 kcal whereas the bond energy is 24.2 kcal). Within this band further activation to dense upper states and dissociation to O_2 and O are faster than deactivation to relatively nondense lower vibrational states. For the bimolecular association, the reactants O and O_2 associate and fly apart many times before they are deactivated below the critical energy, and even that is not enough since re-dissociation is more rapid than further deactivation. The "rate determining step" is further deactivation to get across the "nonequilibrium band" of states.

Thus, the observed rate of exchange gives a clear, qualitative, physical picture of why the activation energy is less than the bond-dissociation energy and why the ratio of rate constants at the low-pressure, nonequilibrium limit of unimolecular reactions, still gives the equilibrium constant.

6. Summary

Thermal, homogeneous reactions of O_3, O_2, and O are well accounted for by a set of seven elementary chemical reactions:

D. $O_2 + M \rightarrow O + O + M$
R. $O + O + M \rightarrow O_2 + M$
1. $O_3 + M \rightarrow O + O_2 + M$
2. $O + O_2 + M \rightarrow O_3 + M$
3. $O + O_3 \rightarrow O_2 + O_2$
4. $O_2 + O_2 \rightarrow O + O_3$
5. $O + O_2 \rightarrow O_2 + O$ (exchange)

The experimental data obtained by many different investigations have been combined to obtain rate constants as a function of temperature for each of the first six elementary reactions and to obtain the rate constant of reaction 5 at room temperature. The recommended rate constants for the seven elementary reactions are (where energies in the exponent are kilocalories/mole):

$k_D(O_2) = 4.57 \times 10^{-5} T^{-1} \exp(-118.7/RT)$
$$\text{cm}^3/\text{particle-s}$$

$k_R(O_2) = 3.80 \times 10^{-30} T^{-1} \exp(-0.34/RT)$
$$\text{cm}^6/\text{particle}^2\text{-s}$$

$k_D(O_2)/k_D(\text{Ar}) = 10.8$ (and $k_R(O_2)/k_R(\text{Ar})$ 10.8)

T: 300 to 15,000 °K for Ar as M
   1000 to 8000 °K for O_2 as M

$k_1(O_3) = 1.65 \times 10^{-9} \exp(-22.72/RT)$
$$\text{cm}^3/\text{particle-s}$$

$k_2(O_3) = 4.63 \times 10^{-35} \exp(2.10/RT)$
$$\text{cm}^6/\text{particle}^2\text{-s}$$

$k_3 = 2.00 \times 10^{-11} \exp(-4.79/RT)$
$$\text{cm}^3/\text{particle-s}$$

$k_4 = 2.12 \times 10^{-11} \exp(-100.6/RT)$
$$\text{cm}^3/\text{particle-s}$$

$$k_5 = 1.7 \times 10^{-12} \text{ cm}^3/\text{particle-s}$$

T: 200 to 1000 °K

Relative efficiencies of various M gases for reactions 1 and 2 are given in table 17.

As an aid to the reader in forming his own estimate of the magnitude of error in these functions, we have presented graphs of actual experimental data for the first five elementary rate constants, together with a curve representing the recommended function:

k_D figures 1A and 1B
k_R figure 4
k_1 figures 5 and 12
k_2 figure 11
k_3 figure 9B

Over the actual range of observations we present the following estimates [6] of the uncertainty in the logarithm of k:

log $k_D \pm 0.3$
log $k_R \pm 0.3$
log $k_1 \pm 0.1$
log $k_2 \pm 0.2$
log $k_3 \pm 0.2$

---

[6] These error estimates are subjective and personal. Consideration is given to the scatter of points for given authors (see the figures in this report), the agreement between different authors, the stability of the overall picture to inclusion or omission of any one author, possible systematic errors especially under extreme conditions, and conformation of the experimental data to gas-phase reaction-rate theory. Within the temperature ranges of the experimental data, we feel that a 95 percent confidence can be placed on the rate constants plus or minus the error interval given here.

7. References

[1] O. L. Anderson, Shock-Tube Measurement of Oxygen Dissociation Rates in Argon, United Aircraft Corporation Research Laboratories, Report R–1828–1 (1961).

[2] J. S. Arnold, R. J. Browne, and E. A. Ogryzlo, The red emission bands of molecular oxygen, Photochem. and Photobiol. **4**, 963 (1965).

[3] A. E. Axworthy, Jr., Collisional Processes in Gas Phase Kinetics, Ph. D. Dissertation, University of Southern California (1959).

[4] A. E. Axworthy, Jr. and S. W. Benson, Mechanism of Gas Phase Decomposition of Ozone, Thermal and Photochemical Reactions, Ozone Chemistry and Technology, No. 21 in series published by Am. Chem. Soc., 388 (1959).

[5] L. W. Bader and E. A. Ogryzlo, Reactions of $O_2(^1\Delta_g)$ and $O_2(^1\Sigma_g^+)$, Discussions Faraday Soc. **37**, 46 (1964).

[6] V. D. Baiamonte, D. R. Snelling, and E. J. Bair, Vibrational energy of ozone during photolytic explosion, J. Chem. Phys. **44**, 673 (1966).

[7] N. Basco, The reaction of cyanogen radicals with oxygen, Proc. Roy. Soc. (London), **282**, 302 (1965).

[8] N. Basco and R. G. W. Norrish, Vibrational disequilibrium in reactions between atoms and molecules, Can. J. Chem. **38**, 1769 (1960).

[9] N. Basco and R. G. W. Norrish, The production of vibrationally excited hydroxyl radicals under isothermal conditions by flash photolysis, Proc. Roy. Soc. (London), **A260**, 293 (1961).

[10] S. W. Benson, On the existence of energy chains in ozone decomposition, J. Chem. Phys. **34**, 939 (1960).

[11] S. W. Benson and A. E. Axworthy, Jr., Mechanism of the gas phase, thermal decomposition of ozone, J. Chem. Phys. **26**, 1718 (1957).

[12] S. W. Benson and A. E. Axworthy, Reconsideration of the rate constants from the thermal decomposition of ozone, J. Chem. Phys. **42**, 2614 (1965).

[13] S. W. Benson and W. B. DeMore, Gas Kinetics, Ann. Rev. Phys. Chem. **16**, 397 (1965).

[14] S. W. Benson and T. Fueno, Mechanism of atomic recombination by consecutive vibrational deactivations, J. Chem. Phys. **36**, 1597 (1962).

[15] U. Beretta and H. J. Schumacher, Die Photokinetik des Ozons. (I). Der Zerfall des Ozons im ultravioletten Licht, Z. Physik. Chem. **B17**, 417 (1932).

[16] C. M. Birdsall, A. C. Jenkins, J. S. Dipoalo, J. A. Beattie, and C. M. Apt, Compressibilities of ozone, oxygen, and ozone-oxygen mixtures and the thermodynamic quantities for pure ozone, J. Chem. Phys. **23**, 441 (1955).

[17] F. E. Blacet, T. C. Hall, and P. A. Leighton, The photochemistry of nitrogen dioxide at 3130 and 4050 Å, J. Am. Chem. Soc. **84**, 4011 (1962).

[18] W. Brennen and H. Niki, On the exchange reaction $^{16}O_2$ and $^{18}O_2$, J. Chem. Phys. **42**, 3725 (1965).

[19] P. Brix and G. Herzberg, The dissociation energy of oxygen, J. Chem. Phys. **21**, 2240 (1953).

[20] H. P. Broida, H. I. Schiff, and T. M. Sugden, Some atomic reactions by absorption spectroscopy, Nature, **185**, 759 (1960).

[21] R. L. Brown, Effects of impurities on the production of oxygen atoms by a microwave discharge, J. Phys. Chem. **71**, 2492 (1967).

[22] S. R. Byron, Measurement of the rate of dissociation of oxygen, J. Chem. Phys. **30**, 1380 (1959).

[23] M. Camac and A. Vaughan, O_2 dissociation rates in O_2-Ar mixtures, J. Chem. Phys. **34**, 460 (1961).

[24] E. S. Campbell and C. Nudelman, Reaction Kinetics, Thermodynamics, and Transport Properties in the Ozone-Oxygen System, AFOSR TN–60–502, NYU (1960).

[25] E. Castellano and H. J. Schumacher, Photochemical decomposition of ozone in yellow-red light and the mechanism of its thermal decomposition, J. Chem. Phys. **36**, 2238 (1962).

[26] E. Castellano and H. J. Schumacher, Die Kinetik des photochemischen Zerfalles von Ozon in rot-gelbem Licht, Zeit. Physik. Chem. **34**, 198 (1962).

[27] J. P. Chesick and G. B. Kistiakowsky, Gaseous detonations. X. Study of reaction zones, J. Chem. Phys. **28**, 956 (1958).

[28] M. A. A. Clyne, D. J. McKenney, and B. A. Thrush, Rate of combination of oxygen atoms with oxygen molecules, Trans. Faraday Soc. **61**, 2701 (1965).

[29] M. A. A. Clyne, B. A. Thrush, and R. P. Wayne, Some reactions of ozone in discharge-flow experiments, Nature **199**, 1057 (1963).

[30] M. A. A. Clyne and B. A. Thrush, Trans. Faraday Soc. **58**, 511 (1962).

[31] M. A. A. Clyne, B. A. Thrush, and R. P. Wayne, The formation and reactions of metastable oxygen (Σ_g^+) molecules, Photochem. and Photobiol. **4**, 957 (1965).

[32] M. A. A. Clyne and B. A. Thrush, Rates of elementary processes in the chain reaction between hydrogen and oxygen. I. Reactions of oxygen atoms, Proc. Roy. Soc. (London) **275**, 544 (1963).

[33] M. A. A. Clyne and B. A. Thrush, Isotopic exchange in the $O + NO_2$ reaction, J. Chem. Phys. **38**, 1252 (1963).

[34] S. T. Demetriades and M. Farber, Theoretical study of recombination kinetics of atomic oxygen, J. Am. Rocket Soc. **29**, 528 (1957).

[35] W. B. DeMore and O. F. Raper, Primary processes in ozone photolysis, J. Chem. Phys. **44**, 1780 (1966).

[36] J. C. Devins, "Mechanism of ozone formation in the silent electric discharge, J. Electrochem. Soc. **103**, 460 (1956).

[37] P. G. Dickens, R. D. Gould, J. W. Linnett, and A. Richmond, Recombination of oxygen atoms in the gas phase, Nature **187**, 686 (1960).

[38] J. P. Doering and B. H. Mahan, Photolysis of nitrous oxide. I. 1236 A, J. Chem. Phys. **34**, 1617 (1961).

[39] J. P. Doering and B. H. Mahan, Photolysis of nitrous oxide. II. 1470 and 1830 A, J. Chem. Phys. **36**, 1682 (1962).

[40] Jerome Eckerman, The Measurement of the Rate of Dissociation of Oxygen at High Temperatures, U.S. Naval Ordnance Laboratory Report 6724, White Oak, Maryland (1961).

[41] L. Elias, E. A. Ogryzlo, and H. I. Schiff, The study of electrically discharged O_2 by means of isothermal calorimetric detector, Can. J. Chem. **37**, 1680 (1959).

[42] R. V. Fitzsimmons and E. J. Bair, Distribution and relaxation of vibrationally excited oxygen in flash photolysis of ozone, J. Chem. Phys. **40**, 451 (1964).

[43] D. Garvin, The oxidation of carbon monoxide in the presence of ozone, J. Am. Chem. Soc. **76**, 1523 (1954).

[43a] N. A. Generalov and S. A. Losevn, Vibrational excitation and molecular dissociation of O_2 and CO_2 in a shock wave, J. Quant. Spectry Radiative Transfer **6**, 101 (1966).

[44] E. K. Gill and K. J. Laidler, Reactions involving electronically excited oxygen, Can. J. Chem. **36**, 79 (1958).

[45] E. K. Gill and K. J. Laidler, The vibration and decomposition of the ozone molecule, Trans. Faraday Soc., **55**, 753 (1959).

[46] H. S. Glick and W. H. Wurster, Shock tube study of dissociation relaxation in oxygen, J. Chem. Phys. **27**, 1224 (1957).

[47] A. Glissman and H. J. Schumacher, Der thermische Ozonzerfall, Z. Physik. Chem. **21B**, 323 (1933). Data recalculated for this review by use of Benson and Axworthy mechanism.

[48] J. A. Golden and A. L. Myerson, Recombination of atomic oxygen observed by means of the flash spectroscopy of molecular oxygen in the vacuum ultraviolet, J. Chem. Phys. **28**, 978 (1958); Planetary Space Sci. **3**, 175 (1961).

[49] V. I. Gorgoraki, G. K. Boreskov, and L. A. Kasatkina, Catalytic properties of NiO in the reaction of homomolecular exchange of oxygen, Kinetics and Catalysis **7**, 239 (1966).

47

[50] P. Günther, E. Wassmuth, and L. A. Schryver, Die Bildungswärme des Ozons, Z. Phys. Chem. **158**, 297 (1932).

[51] P. Harteck and U. Kopsch, Gasreaktionen mit atomarem Sauerstoff, Z. Physik. Chem. **B12**, 327 (1931).

[52] L. J. Heidt, The photolysis of dry ozone at 208, 254, 280, and 313 mμ. II. Reaction kinetics, J. Am. Chem. Soc. **57**, 1710 (1935).

[53] J. T. Herron and F. S. Klein, Mass spectrometric study of the isotopic exchange rate of oxygen atoms with O_2, J. Chem. Phys. **40**, 2731 (1964).

[54] J. T. Herron and H. I. Schiff, A mass spectrometric study of normal oxygen and oxygen subjected to electrical discharge, Can. J. Chem. **36**, 1159 (1958).

[55] G. Herzberg, Spectra of Diatomic Molecules 2nd ed (D. van Nostrand Co., Inc., New York, N.Y., 1950).

[55a] S. Jaffe and F. S. Klein, Isotopic exhange reactions of atomic oxygen produced in the photolysis of NO_2 at 3660 Å, Trans. Faraday Soc. **62**, 3135 (1966).

[56] S. Jahn, Beitrage zur Kenntnis des Ozons, Z. Anorg. Chem. **48**, 260 (1906).

[57] JANAF Thermochemical Data, The Dow Chemical Co., Midland, Michigan (1961).

[58] H. S. Johnston, Four mechanisms involving nitrogen pentoxide, J. Am. Chem. Soc. **73**, 4542 (1951).

[59] H. S. Johnston, Gas Phase Reaction Rate Theory (The Ronald Press Co., New York, N.Y., 1966).

[60] (a) H. S. Johnston and J. R. White, Statistical interpretation of unimolecular reaction rates, J. Chem. Phys. **22**, 1969 (1954); (b) H. S. Johnston, High concentration limit of unimolecular reaction kinetics, J. Chem. Phys. **20**, 1103 (1952).

[61] W. H. Johnston and C. J. O'Shea, The homomolecular exchange of oxygen, J. Chem. Phys. **21**, 2080 (1953).

[62] W. M. Jones and N. Davidson, The thermal decomposition of ozone in a shock tube, J. Am. Chem. Soc., **84**, 2868 (1962).

[63] Anton Kailan and Stephan Jahn, Über die Wärmetönung des Ozonzerfalls, Z. Anorg. Chem. **68**, 243 (1910).

[64] F. Kaufman, Aeronomic Reactions Involving Hydrogen, A Review of Recent Laboratory Studies, Ann. Geophys. **20**, 106 (1964).

[65] F. Kaufman, The air afterglow and its use in the study of some reactions of atomic oxygen, Proc. Roy. Soc. (London) **A247**, 123 (1958).

[66] F. Kaufman, Air afterglow and kinetics of some reactions of atomic oxygen, J. Chem. Phys. **28**, 352 (1958).

[67] F. Kaufman, Reactions of oxygen atoms, Progr. Reaction Kinetics, **1**, 1 (1961).

[68] F. Kaufman and J. R. Kelso, Catalytic effects in the dissociation of oxygen in microwave discharges, J. Chem. Phys. **32**, 301 (1960).

[68a] F. Kaufman, personal communication.

[69] F. Kaufman and J. R. Kelso, The Homogeneous Recombination of Atomic Oxygen, Chemical Reactions in the Lower and Upper Atmosphere, p. 255 (Interscience, New York, 1961).

[70] F. Kaufman and J. R. Kelso, Rate Constant of the Reaction $O + 2O_2 \rightarrow O_2$, Discussions Faraday Soc. **37**, 26 (1964); M effect in the gas-phase recombination of O with O_2, J. Chem. Phys. **46**, 4541 (1967).

[71] J. H. Kiefer and R. W. Lutz, Recombination of oxygen atoms at high temperatures as measured by shock-tube densitometry, J. Chem. Phys. **42**, 1709 (1965).

[72] F. S. Klein and J. T. Herron, Mass-spectrometric study of the reactions of O atoms with NO and NO_2, J. Chem. Phys. **41**, 1285 (1964).

[73] C. B. Kretschmer and H. L. Petersen, Recombination kinetics of atomic oxygen at room temperature, J. Chem. Phys. **33**, 948 (1960).

[74] S. Krongelb and M. W. P. Strandberg, Use of paramagnetic-resonance techniques in the study of atomic oxygen recombinations, J. Chem. Phys. **31**, 1196 (1959).

[74a] K. J. Laidler, Chemical Kinetics, p. 224. (McGraw-Hill Book Co., New York, N.Y., 1950).

[75] E. N. Lassettre, Collision cross-section studies on molecular gases and the dissociation of oxygen and water, Radiation Res. Supplement 7, 530 (1959).

[76] J. W. Linnett and D. G. H. Marsden, Effect of surfaces on rate of recombination of oxygen atoms, Proc. Roy. Soc. (London) **A234**, 489–504 (1956); J. C. Greaves and J. W. Linnett, Trans. Faraday Soc. **55**, 1346 (1959).

[77] S. A. Losev and N. A. Generalov, A study of the excitation of vibrations and dissociation of oxygen molecules at high temperatures, Soviet Phys.—Doklady **6**, 1081 (1962).

[78] W. D. McGrath and R. G. W. Norrish, Production of vibrationally excited oxygen molecules in the flash Photolysis of ozone, Nature **180**, 1272 (1957).

[79] W. D. McGrath and R. G. W. Norrish, The flash photolysis of ozone, Proc. Roy. Soc. (London) **A242**, 265 (1957).

[80] W. D. McGrath and R. G. W. Norrish, Influence of water on the photolytic decomposition of ozone, Nature **182**, 235 (1958).

[81] W. D. McGrath and R. G. W. Norrish, The study of energy transfer and energy distributions in fast chemical reactions by flash photolysis and kinetic spectroscopy, Z. Physik. Chem. **15**, 245 (1958).

[82] W. D. McGrath and R. G. W. Norrish, Studies of the reactions of excited oxygen atoms and molecules produced in the flash photolysis of ozone, Proc. Roy. Soc. (London) **A254**, 317 (1960).

[83] D. J. McKenney and K. J. Laidler, Elementary processes in the decomposition of ozone, Can. J. Chem. **40**, 539 (1962).

[84] B. H. Mahan, Photolysis of carbon dioxide, J. Chem. Phys. **33**, 959 (1960).

[85] R. E. March, S. G. Furnival, and H. I. Schiff, The production of electronically excited oxygen molecules and their reactions with ozone, Photochem. and Photobiol. **4**, 971 (1965).

[86] T. C. Marshall, Studies of atomic recombination of nitrogen, hydrogen, and oxygen by paramagnetic resonance, Phys. Fluids **5**, 743 (1962).

[87] A. Mathias and H. I. Schiff, Discussions Faraday Soc. **37**, 38 (1964); Role of excited molecules in a stream of electronically discharged oxygen, J. Chem. Phys. **40**, 3118 (1964).

[88] D. L. Matthews, Interferometric measurement in the shock tube of the dissociation rate of oxygen, Phys. Fluids, **2**, 170 (1959).

[89] (a) R. L. Mills and H. S. Johnston, Decomposition of nitrous pentoxide in the presence of nitric oxide, J. Am. Chem. Soc. **73**, 938 (1951); (b) H. S. Johnston and R. L. Perrine, Decomposition of nitrogen pentoxide in the presence of nitric oxide. Details at low pressure, J. Am. Chem. Soc. **73**, 4782 (1951); (c) ibid., Decomposition of nitrogen pentoxide. III. Effect of foreign gases, **75**, 1567 (1953); (d) H. F. Cordes and H. S. Johnston, Thermal decomposition of nitryl chloride. Second order unimolecular rate study, J. Am. Chem. Soc. **76**, 4264 (1954).

[90] J. E. Morgan and H. I. Schiff, Recombination of oxygen atoms in the presence of inert gases, J. Chem. Phys. **38**, 1495 (1963).

[91] R. G. W. Norrish and R. P. Wayne, The photolysis of ozone by ultraviolet radiation. I. The photolysis of pure, dry ozone, Proc. Roy. Soc. (London) **A288**, 200 (1965).

[92] R. G. W. Norrish and R. P. Wayne, The photolysis of ozone by ultraviolet radiation. II. The photolysis of ozone mixed with certain hydrogen-containing substances, Proc. Roy. Soc. (London) **A288**, 361 (1965).

[93] R. A. Ogg, Jr., and W. T. Sutphen, Ozone catalysis of isotope exchange between molecular oxygen species, J. Chem. Phys. **21**, 2078 (1953).

[94] R. A. Ogg, Jr., and W. T. Sutphen, Reactions of atomic oxygen with molecular oxygen, Discussions Faraday Soc. **17**, 47 (1954).

[95] E. A. Orgyzlo and H. I. Schiff, The reaction of oxygen atoms with NO, Can. J. Chem. **37**, 1690 (1959).

[96] E. P. Perman and R. H. Greaves, Effect of surfaces on rate of decomposition of ozone, Proc. Roy. Soc. (London) **A80**, 353 (1908).

[97] L. F. Phillips and H. I. Schiff, Mass spectrometric studies of atom reactions. I. Reactions in atomic nitrogen-ozone system, J. Chem. Phys. **36**, 1509 (1962).

48

[98] L. F. Phillips and H. I. Schiff, Vibrationally excited O_2 molecules from the reactions of O atoms with NO_2 and with O_3, J. Chem. Phys. **37**, 924 (1962).

[99] S. Ya. Pshezhetskii, N. M. Morozov, S. A. Kamenetskaya, V. N. Siryatskaya, and E. I. Gribova, Kinetics of the Thermal Decomposition of Ozone, Russ. J. Phys. Chem. **33**, 402 (1959).

[100] O. F. Raper and N. B. DeMore, Reaction of $O(^1D)$ with CO, J. Chem. Phys. **40**, 1053 (1964).

[101] R. R. Reeves, G. Mannella, and P. Harteck, Rate of recombination of oxygen atoms, J. Chem. Phys. **32**, 632 (1960).

[101a] O. K. Rice, On the relation between equilibrium constant and the non-equilibrium rate constants of direct and reverse reactions, J. Phys. Chem. **65**, 1972 (1961).

[102] J. P. Rink, Relative efficiencies of inert third bodies in dissociating oxygen, J. Chem. Phys. **36**, 572 (1962).

[103] J. P. Rink, H. T. Knight, and R. E. Duff, Shock-tube determination of dissociation rates of oxygen, J. Chem. Phys. **34**, 1942 (1961).

[104] Mowbray Ritchie, The thermal decomposition of ozone, Proc. Roy. Soc. (London) **A146**, 848 (1934).

[105] Y. L. Sandler and D. D. Durigon, The desorption and isotopic exchange of oxygen at a silver surface, J. Phys. Chem. **69**, 4201 (1965).

[106] M. C. Sauer, Jr., and L. M. Dorfman, Pulse radiolysis of gases, J. Am. Chem. Soc. **86**, 4218 (1964).

[107] M. C. Sauer, Jr., and L. M. Dorfman, Pulse radiolysis of gaseous argon-oxygen solutions. Rate constant for the ozone formation reaction, J. Am. Chem. Soc. **87**, 3801 (1965).

[108] C. J. Schexnayder, Jr., and J. S. Evans, Measurement of the Dissociation Rate of Molecular Oxygen, NASA Technical Report R–108 (1961).

[109] H. I. Schiff, Reactions involving nitrogen and oxygen, Ann. Geophys. **20**, 115 (1964).

[110] G. J. Schulz and J. T. Dowell, Excitation of vibrational and electronic levels in O_2 by electron impact, Phys. Rev. **128**, 174 (1962).

[111] H. J. Schumacher, Die Photokinetik des Ozons. I. Der zerfall in rotem Licht, Physik. Chem. **B17**, 405 (1932).

[112] H. J. Schumacher, The mechanism of the photochemical decomposition of ozone, J. Am. Chem. Soc. **52**, 2377 (1930).

[113] H. J. Schumacher and G. Sprenger, Der thermische Ozonzerfall, Z. Phys. Chem. **B6**, 446 (1929).

[114] Felix Smith, Participation of Vibration in exchange reactions, J. Chem. Phys. **31**, 1352 (1959).

[115] J. O. Sullivan and P. Warneck, Reactions of ^1D oxygen atoms. III. *Ozone formation in the 1470 Å photolysis of O_2, J. Chem. Phys. **46**, 953 (1967).

[116] W. T. Sutphen, Kinetic Study of the Thermal Decomposition of Ozone, Ph. D. Dissertation, Stanford University, 1955.

[117] E. A. th. Verdurmen, Mechanism of oxygen isotopic exchange in mixtures of carbon monoxide and oxygen in a quartz vessel, J. Phys. Chem. **71**, 678 (1966).

[118] E. A. th. Verdurmen and C. A. Bank, Chemical kinetics of oxygen exchange between CO and O_2, J. Inorg. Nucl. Chem. **25**, 1521 (1963).

[119] Peter Warneck, Reactions of ^1D oxygen atoms in the photolysis of carbon dioxide, Discussions Faraday Soc. **37**, 57 (1964).

[120] F. Weigert, Über chemische Lichtwirkungen. VII. Die Ozonzersetzung im ultravioletten Licht, Z. Physik. Chem. **80**, 78 (1912).

[121] F. Weigert and H. Böhm, Photochemische Reaktionen in Gemischen von Ozon und Wasserstoff, Z. Physik. Chem. **90**, 189 (1915).

[121a] B. Widom, Molecular transitions and chemical reaction rates, Science **148**, 1555 (1965).

[122] Grace Wieder and R. A. Marcus, Dissociation and isomerization of vibrationally excited species. II. Unimolecular reaction rate theory and its applications, J. Chem. Phys. **37**, 1835 (1962).

[123] J. Wilson, A shock-tube measurement of the recombination rate of oxygen, J. Fluid Mech. **15**, 497 (1963); Ph. D. Dissertation, Cornell University, 1962.

[124] Henry Wise and C. M. Ablow, Diffusion and heterogeneous reaction. IV. Effects of gas-phase reaction and convective flow, J. Chem. Phys. **35**, 10 (1961).

[125] K. L. Wray, Kinetics of O_2 dissociation and recombination, Tenth Symposium on Combustion, 523 (1965); Shock-tube study of the coupling of the O_2-Ar rates of dissociation and vibrational relaxation, J. Chem. Phys. **37**, 1254 (1962); Shock-tube study of the recombination of O atoms by Ar catalysts at high temperatures, J. Chem. Phys. **38**, 1518 (1963).

[126] O. R. Wulf, The dissociation of ozone and the mechanism of its thermal decomposition, J. Am. Chem. Soc. **54**, 156 (1932).

[127] O. R. Wulf and R. C. Tolman, The thermal decomposition of ozone. I. The homogeneity, order, specific rate, and dependence of rate on total pressure, J. Am. Chem. Soc. **49**, 1183 (1927).

[128] O. R. Wulf and R. C. Tolman, The thermal decomposition of ozone. III. The temperature coefficient of reaction rate, J. Am. Chem. Soc. **49**, 1650 (1927).

[129] H. Yamazaki and R. J. Cvetanovic, Isotopic exchange of the excited oxygen atoms with CO_2^{18} and their collisional deactivation, J. Chem. Phys. **40**, 582 (1964).

[130] R. A. Young, R. L. Sharpless, and R. Stringham, Additional observations of chemiluminescence in mixtures of atomic oxygen and nitrogen, J. Chem. Phys. **41**, 1497 (1964).

[131] J. A. Zaslowsky, H. B. Urbach, F. Leighton, R. J. Wnuk, and J. A. Wojtowicz, The kinetics of the homogeneous gas phase thermal decomposition of ozone, J. Am. Chem. Soc. **82**, 2682 (1960).